

AD_____

Award Number: DAMD17-01-1-0012

TITLE: Endothelial Vehicles as a Novel Anti-Angiogenic Gene
Therapy in Cancer of Prostate

PRINCIPAL INVESTIGATOR: Waleed Arafat, M.D.

CONTRACTING ORGANIZATION: The University of Alabama at Birmingham
Birmingham, Alabama 35294-0111

REPORT DATE: October 2003

TYPE OF REPORT: Annual Summary

PREPARED FOR: U.S. Army Medical Research and Materiel Command
Fort Detrick, Maryland 21702-5012

DISTRIBUTION STATEMENT: Approved for Public Release;
Distribution Unlimited

The views, opinions and/or findings contained in this report are those of the author(s) and should not be construed as an official Department of the Army position, policy or decision unless so designated by other documentation.

REPORT DOCUMENTATION PAGEForm Approved
OMB No. 074-0188

Public reporting burden for this collection of information is estimated to average 1 hour per response, including the time for reviewing instructions, searching existing data sources, gathering and maintaining the data needed, and completing and reviewing this collection of information. Send comments regarding this burden estimate or any other aspect of this collection of information, including suggestions for reducing this burden to Washington Headquarters Services, Directorate for Information Operations and Reports, 1215 Jefferson Davis Highway, Suite 1204, Arlington, VA 22202-4302, and to the Office of Management and Budget, Paperwork Reduction Project (0704-0188), Washington, DC 20503

1. AGENCY USE ONLY
(Leave blank)**2. REPORT DATE**
October 2003**3. REPORT TYPE AND DATES COVERED**
Annual Summary (24 Sep 2001 - 23 Sep 2003)**4. TITLE AND SUBTITLE**
Endothelial Vehicles as a Novel Anti-Angiogenic Gene Therapy in Cancer of Prostate**5. FUNDING NUMBERS**
DAMD17-01-1-0012**6. AUTHOR(S)**
Waleed Arafat, M.D.

20040130 026

7. PERFORMING ORGANIZATION NAME(S) AND ADDRESS(ES)
The University of Alabama at Birmingham
Birmingham, Alabama 35294-0111**E-Mail:** waleed.arafat@ccc.uab.edu**8. PERFORMING ORGANIZATION
REPORT NUMBER****9. SPONSORING / MONITORING
AGENCY NAME(S) AND ADDRESS(ES)**
U.S. Army Medical Research and Materiel Command
Fort Detrick, Maryland 21702-5012**10. SPONSORING / MONITORING
AGENCY REPORT NUMBER****11. SUPPLEMENTARY NOTES**
Original contains color plates: All DTIC reproductions will be in black and white.**12a. DISTRIBUTION / AVAILABILITY STATEMENT**
Approved for Public Release; Distribution Unlimited**12b. DISTRIBUTION CODE****13. ABSTRACT (Maximum 200 Words)**

Tumor angiogenesis is the common pathophysiological factor of both primary tumors and distant metastases. Therefore, the ablation of the antiogenesis may have a key role to stop tumor progression. In this regard, we and others have shown that, when given systemically, normal endothelial progenitors (EPs) circulate and localize into areas of active angiogenesis. In the proposal, we will evaluate the employment of these EPs as cellular vehicles for gene delivery into primary and metastatic carcinoma of the prostate. To this end, we will apply EPs genetically modified ex vivo with a toxin gene for cell-mediated molecular chemotherapy. Thus, if localization occurs in the areas of tumor angiogenesis as proposed, expression of the toxin gene inside the EPs could induce death in these toxin-expressing cells and their neighbors, thus abrogating angiogenesis, and therefore potentially inducing regression of the tumor thereafter by vascular deprivation.

14. SUBJECT TERMS
Cellular vehicle vector**15. NUMBER OF PAGES**
54**16. PRICE CODE****17. SECURITY CLASSIFICATION
OF REPORT**
Unclassified**18. SECURITY CLASSIFICATION
OF THIS PAGE**
Unclassified**19. SECURITY CLASSIFICATION
OF ABSTRACT**
Unclassified**20. LIMITATION OF ABSTRACT**
Unlimited

Table of Contents

Cover.....	Page 1
SF 298.....	Page 2
Table of Contents.....	Page 3
Introduction.....	Page 4
Body.....	Page 4-12
Key Research Accomplishments.....	Page 13
Reportable Outcomes.....	Page 13
Conclusions.....	Page 14
References.....	N/A
Appendices.....	Page 14

Title: Endothelial progenitors as a novel anti-angiogenic gene therapy in cancer of prostate

INTRODUCTION

A novel vector approach based on cellular vehicles was proposed. The employment of cellular vehicles offered several theoretical advantages over available viral and non-viral vector approaches for the implementation of cancer gene therapy approaches. On this basis work sought to establish basic feasibilities with this approach to rationalize full development of cellular vehicles for application to gene therapy for cancer of the prostate.

BODY

Task 1: To characterize the ability of the endothelial progenitors to into areas of prostate tumor angiogenesis after in vivo intravascular administration (months 0-10).

- *To isolate EPs from human and mouse origin and characterize their phenotype as relates to angiogenesis (months 0-4)*
- *To characterize angiogenesis in prostate primary and metastatic xenograft tumors established in an animal model (months 5-7).*
- *To mark the EPs, infuse them in vivo, and detect them in areas of angiogenesis with different tracking methods (months 8-10).*

Technical issues related to acquisition of adequate numbers of endothelial progenitors limited direct application of this approach. On this basis, we explored the usefulness of mesenchymal progenitor cells (MPC) as alternative cellular vehicles. Studies supportive of the application are as follows:

Characterization of isolated human MPC.

The practical realization of cells as vehicles for gene therapy requires both a favorable combination of native properties of a chosen cell population, as well as the ability to be effectively loaded by genes, or other therapeutics, and to deliver such a payload to target sites. The theoretical considerations of utilizing MPC as such a cellular vector were predicated primarily by their availability, propagating properties, and simple culturing conditions. On this basis, our intention was to test several properties of MPC related to their potential application as delivery vehicles for gene therapy. First, we tested the ability of human MPC to be maintained in culture and their ability to propagate in quantities required for *in vivo* applications. Human MPC were isolated according a protocol described elsewhere [75, 76] and plated at a density of $6-7 \times 10^3$ cell/cm² in medium supplemented with 10% FBS. Human MPC cultures after 2 passages *in vitro* contained a mainly homogeneous population of cells as assessed by cell morphology, with predominant fibroblast-shaped cells. Different cultures also included various percentages of large flat cells and star-shaped cells (Fig1A). Several MPC isolations were accomplished according to described protocol and primary cultures were monitored for a number of passages (Fig1C). The doubling time was calculated for each passage of individual cultures under described culture conditions and varied from 3 to 6 days. Some MPC cultures were monitored far as long as 12 passages without significant changes in

propagating properties (Fig1B). To confirm that the population of isolated human bone marrow cells contained mesenchymal progenitor or stem cells, we tested ability of primary cultures on passage 2-3 to undergo osteogenic, adipogenic and chondrogenic differentiation after applying corresponding conditioned media (Fig 2A-D). The differentiation potential of each individual culture varied, from have either all three tested lineages being represented or to being predominantly skewed towards osteogenic or adipogenic differentiation. Nevertheless, most of the tested cultures demonstrated good propagation and differentiation abilities, confirming the concept that this adherent cell population in fact contains progenitor cells and has sufficient propagation properties that can be exploited for their application as cell vehicles.

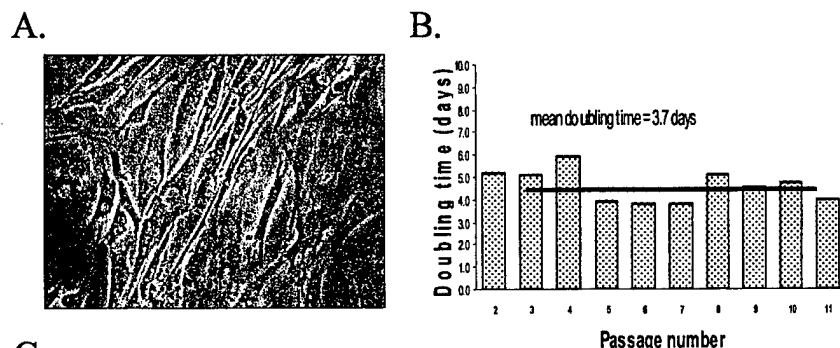


Figure 1. A) Representative phase-contrast photomicrograph of human MPC culture. Typical cell phenotypes were observed: most cells were spindle-shaped, whereas large flat cells, and star-shaped cells were present at lower numbers.

B) Expansion of MPC in culture. Primary culture from a single BM donor was followed up to 12 passages, doubling times for each passage and mean doubling time (MDT) for all passages in observation was calculated as described in Materials and Methods.

C) Mean doubling time for different MPC cultures.

C.

MPC clone	# Passages cultured	Mean doubling time (days)
MPC	12	3.7
MPC-C2	12	3.0
MPC-C18	3	6.7
MPC-C19	5	5.4
MPC-U1	12	4.6
MPC-U2	4	4.4
MPC-U4	5	6.0
MPC-U5	6	3.5
MPC-U6	5	3.8

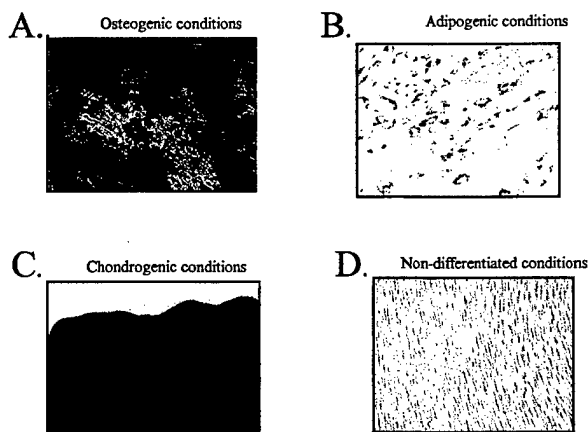


Figure 2. Assay for differentiation ability of MPC. Primary MPC cultures at passage 2-5 were subjected *in vitro* to conditions stimulating osteogenic, adipogenic and chondrogenic differentiation followed by appropriate staining.

A) MPC cultured in osteogenic media for 21 days. The accumulation of mineral deposits was detected by staining with Alizarin Red.

B) MPC culture incubated in adipogenic media for 7 days. Fat droplets in the cells were stained with Oil Red.

C) MPC culture incubated under chondrogenic conditions for 14 days. Cells formed a pellet, which stains blue with Alcian Blue.

D) MPC culture incubated in non-differentiating media, stained with Alizarin Red. No mineral deposits were observed.

Task 2: To determine the capacity of the endothelial progenitors to effect the expression of transgene-encoded molecules into areas of prostate tumor angiogenesis (months 11-16).

- *To genetically modify EPs with herpes virus and genetically adenovirus (months 11-13).*
- *To detect the magnitude, distribution and time course of gene expression (months 14-16).*

Having established the utility of MPC as candidate cellular vehicles, we next explored the ability to "genetically load" the cells with anti-cancer payloads.

Infection efficiency of MPC with adenoviral vector encoding reporter genes.

Our next step was to test the ability of MPC to be efficiently transduced and then express the genetic payload. An effective method of gene transfer is infection with Ad vectors. Previous studies have documented that MPC could be transduced *in vitro* by Ad vectors although efficiency of transduction did not exceed 20%. For our studies, Ad vectors contained reporter genes *E. coli* LacZ or eGFP were used at escalating MOI. Forty-eight hours post infection, MPC and HeLa cells expressing LacZ were stained with X-gal and transduction efficiency was assessed by microscopic scoring. Cells expressing eGFP were detected by flow cytometry. MPC cultures consistently demonstrated lower efficiency of transduction compared to HeLa cells, ranging from of 10-20% at an MOI of 100 vp/cell (Fig 3A). At the highest MOI tested (5000 vp/cell), when almost 100 % of HeLa cells were transduced; however, MPC transduction was only 40% as detected by flow cytometry (Fig 3B). These results are consistent with previous observations by others reporting that MPC are relatively refractive to Ad transduction.

The observed relative resistance of MPC cultures to Ad transduction could be due to low expression of adenoviral attachment (CAR) and/or internalization receptors ($\alpha v \beta$ integrins). We tested the expression profile of adenoviral receptors on MPC by flow cytometry compared to HeLa (high CAR, relatively low integrins) and RD (low CAR, 4, MPC populations have very low, if any, expression of CAR but high expression of both of the integrins tested. Thus, the pattern of expression of adenoviral receptors on MPC resembles that of RD cells and corresponds to a low CAR, high integrin phenotype. These data suggest that CAR-independent transfer is required to improve the level of Ad-mediated transgene expression by MPC cultures. These considerations prompted our evaluation of the genetically modified adenoviruses for genetic transfer to MPC.

Increase in gene expression by MPC transduced with modified adenoviral vectors.

It has been shown that significant augmentation of transduction efficiency can be successfully achieved by exploiting Ad vectors with genetically modified tropism. We have designed and characterized an adenoviral vector with the RGD-4C peptide incorporated in the HI loop of the fiber knob (AdRGD) as well as a vector having the Ads knob replaced with the knob of adenovirus of serotype 3 (Ad5/3). These structural modifications confer expanded tropism to the adenoviruses, enabling CAR-independent mechanisms of infection via binding to either cellular integrins of still unknown Ad' receptor. In addition, these vectors have shown a remarkable improvement of gene transfer efficiency in cell lines normally refractory to CAR-dependent infection. We used genetically modified Ads encoding the luciferase gene, AdRGDluc and Ad5/3luc, in which the expression of luciferase is driven by the CMV promoter, to evaluate the transduction of several primary MPC cultures. Improvement in transduction efficiency was evaluated by direct comparison with an unmodified control Ad5 vector, AdCMVluc. The application of AdRGD to MPC repeatedly resulted in a 10-fold augmentation of gene transfer

compared with AdCMVluc (Fig 5). Ad5/31uc also showed an improvement in gene transfer, although with more varied results on different primary MPC cultures (data not shown). Thus, these results indicate that an adenoviral vector retargeted to cellular integrins provides a means to overcome the CAR deficiency in MPC and allows the achievement of an enhanced level of gene transfer in this cell population.

MPC expression of toxic gene HSV-TK rendering susceptibility to the cytotoxic effect of GCV.

With the demonstration that MPC could be genetically loaded in vitro we proceeded to confirm the ability of MPC to express a therapeutic anticancer genes. For this study we utilized HSV Thymidine Kinase gene as a payload, expression of which causes cell toxic effect after addition of a prodrug ganciclovir (GCV). This therapeutic payload was chosen with a future intent to employ MPC as vehicles delivering cytotoxicity to tumor sites in an animal model relevant to ovarian cancer. In this analysis, MPC and SKOV3.ip1 cells, a human ovarian cancer cell line, taken as a parallel control, were transduced with AdCMV-TK and AdRGD-TK at different MOI (5, 50, 100, 500 pfu/cell). Forty-eight hours post-infection cells the prodrug GCV was added to the media at different concentrations (0, 10, 100, 1000 μ M), and 5 days later the number of remaining viable cells was determined by an NITS assay. Data were plotted as percentage of viable cells against prodrug concentration (Fig 6). A similar killing effect on MPC and SKOV3.ip1 cells was observed after AdCMV-TK transduction (Fig 6A, C). For example, infection at MOI of 50 pfu/cell resulted in 50% cell killing of both cell types after applying 10 μ M GCV to the culture media. In contrast, a dramatic enhancement of the toxic effect exerted by the prodrug was observed when AdRGD-TK was used for MPC transduction (Fig6B, D). AdRGD-TK initiated a killing effect at a lower MOI and a lower GCV concentrations compared with AdCMV-TK (Fig6.B). This finding validated the aforementioned advantage of RGD-containing tropism modified Ad vectors in introducing genes into MPC. Results of this experiment also suggest that transient expression of the HSV-TK delivered by adenoviral vectors will allow achievement of sufficient level of suicide gene expression suitable for a cellular vehicle strategy.

Bystander effect of AdCMV-TK transduced MPC on SKOV3.ip1 tumor cells

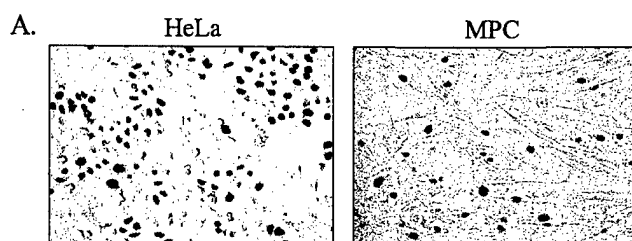
A key advantage embodied in molecular chemotherapy strategy to kill cancer cells is based on the bystander effect, whereby killing of untransduced neighboring cells can be induced by a toxic drug metabolite present in the transduced cell. We therefore investigated whether HSV-TK expressing MPC could accomplish such a bystander effect on the SKOV3.ip1 tumor cells in vitro. AdCMV-TK or AdRGD-TK transduced MPC were mixed in various ratios with untransduced MPC or SKOV3.ip1 cells. An MOI of 50 pfu/cell for transduction of cell populations and GCV concentration of 10 μ M were chosen as the lowest viral and prodrug dose showing a killing effect in the previous experiment (Fig 6). Moreover, this MOI/GCV concentration combination provided a differential killing effect between AdCMV-TK and AdRGD-TK transduced MPC, resulting in prominent killing in AdRGD-TK transduced cells. Our mixing experiment demonstrated that Ad RGD-TK transduced MPC had an enhanced killing effect on nontransduced MPC populations (Fig7A) and on SKOV3.ip1 cell populations as compared to AdCMV-TK transduced MPC (Fig7B). Moreover, an appreciable bystander effect was documented for AdRGD-TK transduced MPC, as addition of only 10% of TK- expressed MPC resulted in total cell viability of 50%. AdCMV-TK transduced MPC did not show noticeable bystander effect in this experimental settings likely due to inefficient transduction of MPC by unmodified Ad vector resulting in insufficient number of TK-producer cells in the mixture. These mixing experiments establish that MPC possess the physiological capacity to accomplish a bystander effect using the HSV-TK/GCV enzyme/prodrug approach.

MPC as cellular vehicles delivering replication competent adenovirus.

The application of conditionally replicative adenoviruses (CRAds) for oncolysis of tumor cells is a promising approach for cancer gene therapy. We therefore considered the possibility of using MPC to deliver such virus as a therapeutic payload. For this approach to be successful, MPC must be able to support adenoviral replication and produce *de novo* viral particles after viral infection. We first determined if replication-competent adenovirus could cause cytopathic effect on MPC culture, an indication of ability of MPC to support a productive adenoviral infection. For this study MPC and HeLa cells, as permissive cell line, were infected with replication-competent Ad51uc3 at escalating MOI and cytopathic effect was evaluated by crystal violet staining. Three days post infection HeLa cells were completely killed at 100 and 10 MOI and early cytopathic effects were observed at 1 MOI. At this time point, MPC remained intact at all viral doses. However, after 7 days post infection MPC showed cytopathic effect of adenovirus at the highest MOI tested (Fig8), which indicates that the cycle of adenoviral replication in MPC is not inhibited completely, but may have different kinetics.

To investigate the kinetics of adenoviral replication in MPC we infected the cells with Ad51uc3 and Ads/31h1c3 at MOI of 1 pfu/cell and monitored the infection for 11 days. Real-Time PCR was used to measure the amount of viral DNA in cells and culture media over time (Fig913,C). We also used the detection of the viral hexon protein in culture media as an indication of viral replication (Fig9A). HeLa cells were included in the experiment as a cell line supporting a high level of adenoviral replication. In all MPC cultures tested (two of four shown) we observed an increase of viral DNA copy number over time in cell lysates as well as in media samples. Quantitatively, copy numbers of viral DNA produced by MPC was 10-100 times lower compared to HeLa cells. Ads/3 did not have an infectivity advantage versus Ads in HeLa cells as judged by quantitation of viral DNA and viral protein production, while two out of the four of MPC cultures showed increased amount of viral DNA and viral protein after infection with Ads/3. This effect of replication-competent Ads/3 on MPC cultures corresponds with the earlier observation with Ads/3 non-replication viruses resulting in differential efficiencies of gene transfer on different primary MPC cultures. Testing the culture media of infected cultures for the presence of viral hexon confirmed the observations obtained with viral DNA. The amount of viral protein increased with progression of infection for all cell cultures. In HeLa cells, hexon concentration in media increased 14-fold and peaked at 5 days after infection. Hexon measurement in infected MPC cultures resulted in an increase of only 2-3 fold after 7 days post infection. These investigated parameters of viral replication such as viral cytolitic effect; levels of viral DNA and viral protein can represent an indirect indication of *de novo* viral replication.

To prove that MPC are able to complete the whole cycle of viral replication and produce the next generation of viral particles, we took cell lysates of MPC cultures infected with escalated doses of Ad51uc3 and applied 10-fold dilutions of those lysates to the Ad permissive cell line HeLa. As shown in Fig10, the positive control representing lysates of infected HeLa cells resulted in a second round of infection of HeLa cells. Lysates of infected MPC also caused a cytopathic effect on HeLa cells indicating the presence of a second round of viral infection. Thus, these data indicate that MPC are able to maintain *de novo* viral replication and can therefore potentially serve as a vehicle to deliver not only gene products but also virus *in vivo*.



B.

	% GFP positive cells gated		
MOI (vp/cell)	0	500	5000
HeLa	1	76	98
MPC	1.5	22	40

Figure 3. Transduction of MPC with recombinant Ad5 vectors.

A) MPC and HeLa cells (4×10^5) were transduced with an Ad vector encoding the *E. coli* LacZ gene at MOI of 500 vp/cell. Forty-eight hours post infection cells were fixed and stained with X-gal.

B) MPC and HeLa cells were transduced with an Ad vector encoding GFP reporter at MOI of 500 or 5000 vp/cell. Forty-eight hours post infection cells were treated with versen and the percentage of GFP-positive cells was determined by flow-cytometry. Data shown as % of gated (GFP-positive) cells at corresponding MOI.

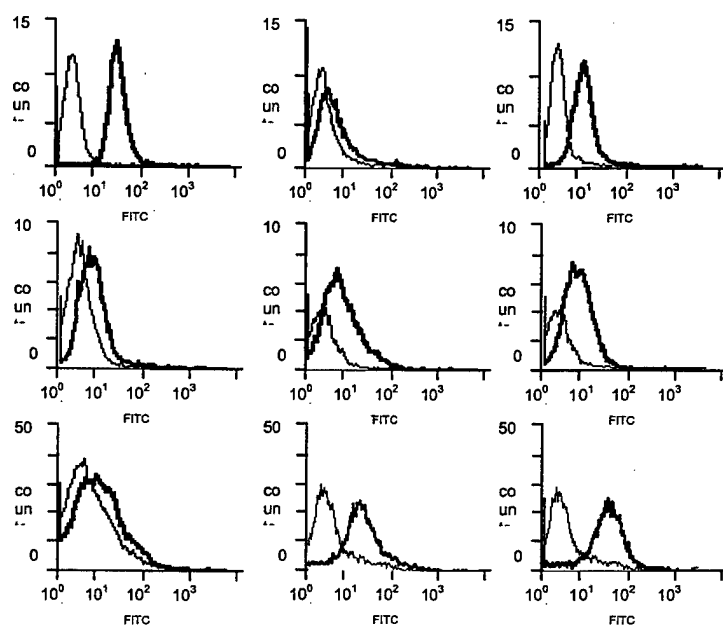


Figure 4. Cell surface expression of adenoviral attachment (CAR) and internalization ($\alpha_v\beta_3$, $\alpha_v\beta_5$) receptors. After treatment with the indicated primary antibody and FITC-conjugated secondary antibody, cells were analyzed by flow cytometry. Histograms show fluorescence intensity data for HeLa (A), RD (B) and MPC (C) cells. HeLa and RD cultures were taken as positive control for CAR and integrins expression, respectively.

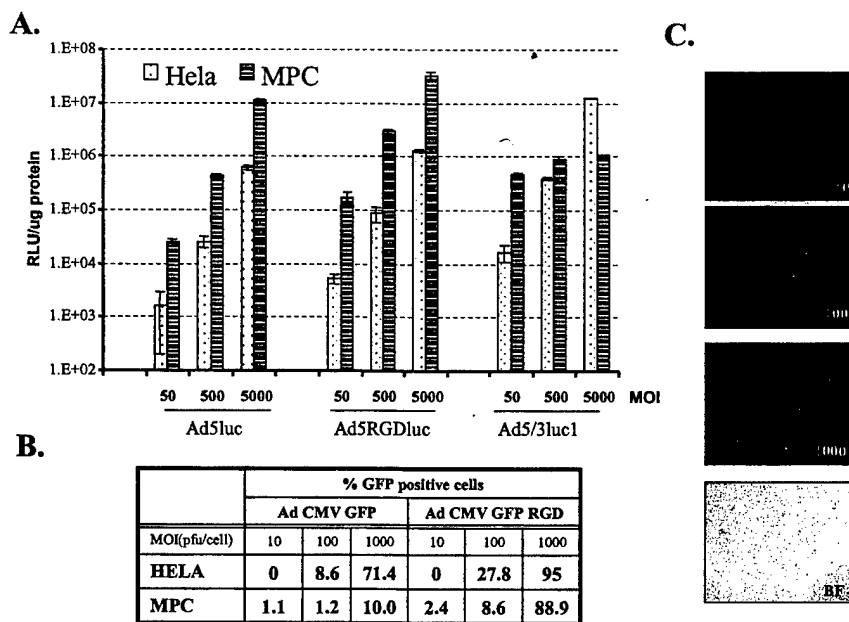


Figure 5. Enhanced transduction efficiency of MPC with adenoviral vectors having genetically modified fiber. Comparison of the gene transfer efficiencies was performed employing non-replicative Ad5 vectors: Ad5luc, Ad5RGDluc and Ad5/3Luc1 encoding the luciferase gene (A) or Ad CMV GFP and Ad CMV GFP RGD (B, C). Human MPC and HeLa cells were infected at designated MOI (pfu/cell) and analyzed for luciferase expression after 48 hr (A). Data shown as relative light units (RLU)/ μ g of total cellular protein. All experiments were done in triplicate. Error bars show standard deviation. MPC transduced with GFP-encoding vectors were analyzed for GFP expression by flowcytometry (B) or microscopically (C). Microphotographs represent MPC culture transduced with Ad CMV GFP RGD at MOI designated on pictures (10, 100, 1000 pfu/cell). Microphotograph of bright field of corresponding MPC culture labeled BF.

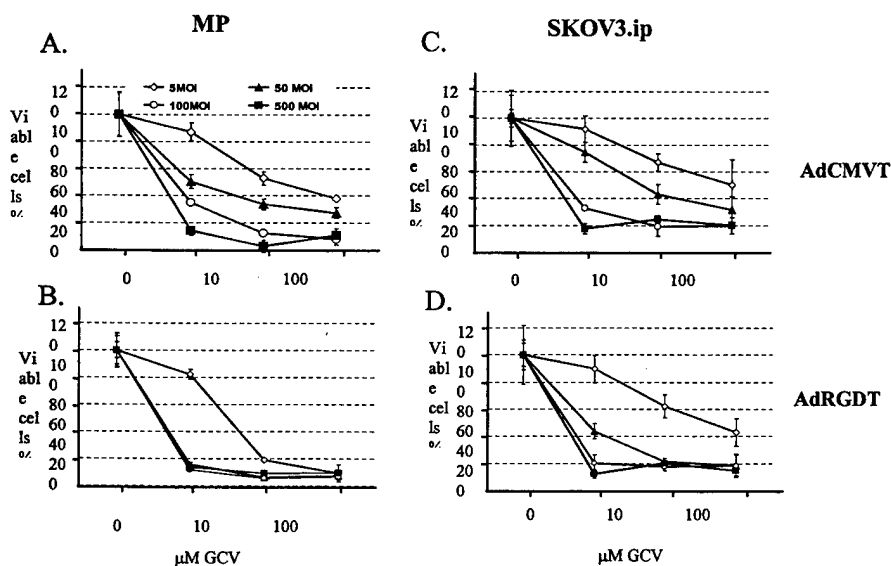


Figure 6. Viability of MPC transduced with AdCMV TK or AdRGDTK after GCV treatment. MPC or SKOV3.ip1 cells were plated on 96-well plates at a density of 3000 cell/well and transduced with AdCMV TK or AdRGDTK at MOI of 5, 50, 100, 500 pfu/cell for 2 hr. After infection GCV was added at a final concentration of 0, 10, 100, 1000 μ M. Cell viability was determined after 5 days of incubation by MTS assay. Data expressed as % of viable cells versus corresponding GCV concentration. All experiments were done in triplicate. Error bar is standard deviation.

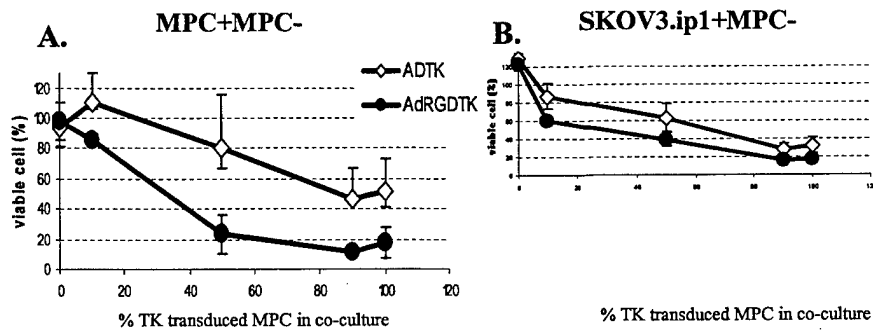


Figure 7. Bystander effect exhibited *in vitro* by AdTK and AdRGDTK transduced MPC when mixed at various ratios with uninfected MPC (A) and SKOV3.ip1 (B). MPC were first transduced with AdTK or AdRGDTK. Twenty-four hours after transduction MPC-TK were mixed in different ratios with untransduced cells (MPC or SKOV3ip1) and plated on 96 well plates. Twenty-four hours after plating cell mixture, half of the cells were treated with 10 μ M GCV. Five days later cell killing was measured by MTS assay. Data are presented as a percentage of viable cells in GCV-treated wells. All experiments were done in triplicate. Error bars represent standard deviation.

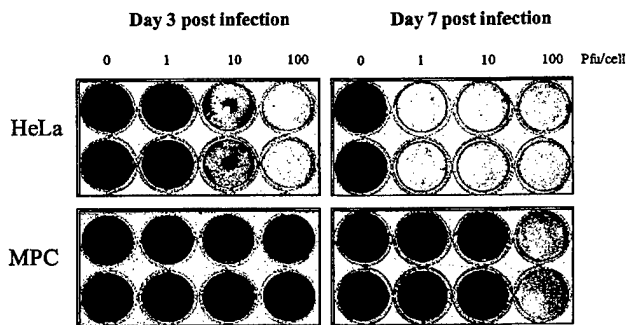


Figure 8. Cytopathic effect of replication competent adenovirus (Ad5luc3) on MPC and HeLa cells. HeLa cells and MPC were plated on 6-well plates with plating density of 5×10^5 cell/well and infected in duplicates with Ad5luc3 at designated MOI. Viral cytopathic effect has been estimated by crystal violet staining on day 3 and day 7 after infection.

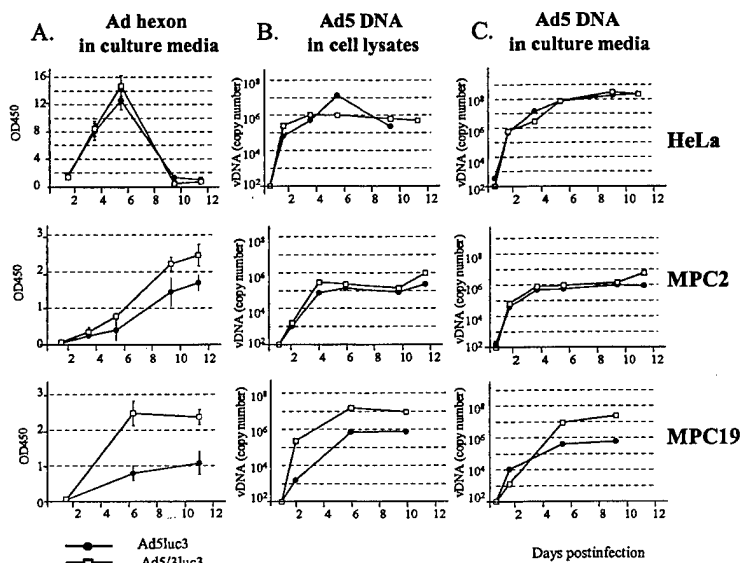


Figure 9. Kinetic of Ad production by MPC. HeLa and two primary cultures of MPC (MPC2, MPC19) were infected with replication-competent Ad5luc3 and Ad5/3Luc3 viruses at an MOI of 1 pfu/cell. Virus-containing medium was collected at 1, 3, 5, 7, 9 days after infection. Viral production was estimated as

- accumulation of viral protein in culture medium by immunoenzyme assay with detection of Ad hexon. Data presented as OD450 of 100 μ l of culture media.
- Accumulation of viral DNA in Ad-infected cells.
- Accumulation of viral DNA in culture medium measured by quantitative PCR. Data are presented as Ad vDNA copy number relative to actin DNA copy number.

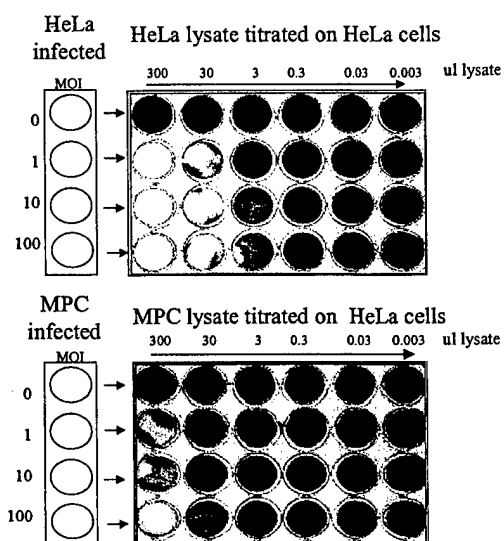
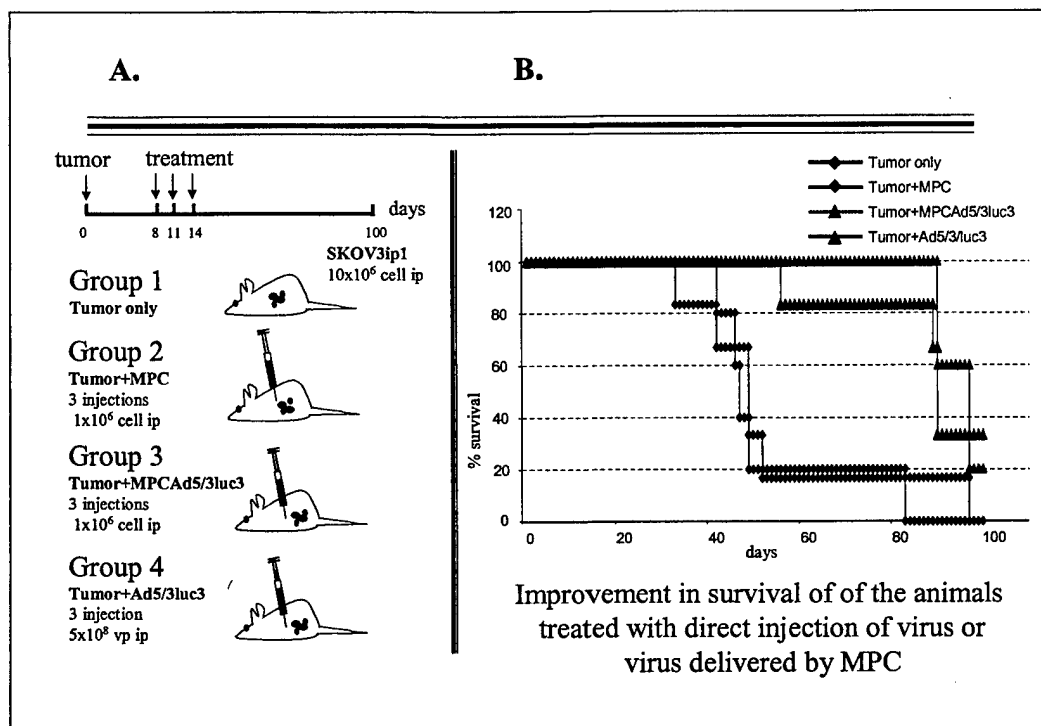


Figure 10. Production of Ad particles by MPC. HeLa cells (A) and MPC (B) were plated at 6-well plates with plating density of 5×10^5 cells/well and infected with Ad5luc3 at an MOI of 1, 10, 100 pfu/cell. After 3 days cells in individual wells were lysed and serial dilutions of lysates were applied onto HeLa cells. Cytopathic effect of produced virus on HeLa cells is shown by crystal violet staining on day 3.

Task 3: To evaluate the therapeutic capacity of EPs as cellular vehicles expressing toxin genes to mediate the abrogation of areas of prostate tumor angiogenesis (months 17-24).

- To evaluate the delivery of the genetically modified EPs containing a toxin gene into areas of angiogenesis and its therapeutic effect (months 17-20).
- To test the value of different administration schedules of cell therapy (months 21-24).

We next explored the capacity of the genetically loaded MPC to be employed as cellular vehicles in the context of a cancer gene therapy approach. For these studies MPC loaded with CRAd agent (replicative Ad) were delivered to SCID mice implanted with human tumor xenografts. We employed initially an IP delivery model for locoregional disease. We reasoned that success in this context would rationalize employment of MPC in a systemic delivery context in murine models of disseminated prostate cancer. The treatment regime is depicted (Fig 11A) as well as the outcomes of survival analysis (Fig 11B). Of note, CRAd loaded MPC yielded the greatest survival advantage in the tested groups. These studies validate our overall concept that cellular vehicles can be employed as a means to accomplish gene therapy for cancer.



KEY RESEARCH ACCOMPLISHMENTS:

- Demonstration that mesenchymal progenitor cells (MPCs) could function as a stem cell substitute for endothelial progenitors (EPs) in context of the original cell vehicle concept.
- Demonstration that MPC could be transduced with adenoviral vectors to thereby contain an anti-cancer agent.
- MPC can be infected ex vivo with replication competent adenoviruses and support viral replication.
- Level of viral production by MPC is sufficient for killing tumor cells in mixing culture *in vitro*.
- MPC can function as cell vehicles chaperoning delivery of oncolytic adenovirus to tumor sites.
- Virotherapy using MPC-based delivery of oncolytic Ad in an animal model of ovarian cancer provided an improvement in survival of experimental animals.
- MPC represent valid candidates as cellular vehicles delivering viruses and this approach provides a rational strategy for cancer gene therapy.

REPORTABLE OUTCOMES:

1. Arafat WO, Buchsbaum DJ, Gomez-Navarro J, Tawil SA, Olsen C, Xiang J, El-Akad H, Salama AM, Badib AO, Stackhouse MA, Curiel DT. An adenovirus encoding proapoptotic

Bax synergistically radiosensitizes malignant glioma. *Int J Radiat Oncol Biol Phys.* 2003 Mar 15;55(4):1037-50.

2. Kaliberov SA, Buchsbaum DJ, Gillespie GY, Curiel DT, Arafat WO, Carpenter M, Stackhouse MA. Adenovirus-mediated transfer of BAX driven by the vascular endothelial growth factor promoter induces apoptosis in lung cancer cells. *Mol Ther.* 2002 Aug;6(2):190-8.
3. Arafat WO, Buchsbaum DJ, Kaliberov S, Li F, Zhu ZB, Curiel DT. A novel radiation/tissue-specific promoter for gene therapy of brain tumors. *Int J Radiat Oncol Biol Phys.* 2003 Oct 1;57(2 Suppl):S146. No abstract available.
4. Pereboeva L, Komarova S, Mikheeva G, Krasnykh V, Curiel DT. Approaches to utilize mesenchymal progenitor cells as cellular vehicles. *Stem Cells.* 2003;21(4):389-404.

CONCLUSION:

We have shown that primary cell cultures of MPC can be efficiently transduced ex vivo by using adenoviral vectors. We have demonstrated that low transduction efficiency of primary cell cultures with Ad vectors due to adenoviral receptor deficiency can be successfully overcome by exploiting adenoviral vectors with modified CAR-independent entry mechanism. Thus, cells intended to be exploited as vehicles can be efficiently loaded ex vivo with reporter or therapeutic genes. Further, we have shown that MPC can be loaded with replicative adenoviruses (CRAd) for virotherapy and that such CRAd-loaded MPC can "home" to tumor and accomplish a therapeutic effect in murine models of cancer. These utilities suggest the feasibility of employing MPCs for implementation of prostate cancer gene therapy/virotherapy.

APPENDICES:

1. Arafat WO, Buchsbaum DJ, Gomez-Navarro J, Tawil SA, Olsen C, Xiang J, El-Akad H, Salama AM, Badib AO, Stackhouse MA, Curiel DT. An adenovirus encoding proapoptotic Bax synergistically radiosensitizes malignant glioma. *Int J Radiat Oncol Biol Phys.* 2003 Mar 15;55(4):1037-50.
2. Kaliberov SA, Buchsbaum DJ, Gillespie GY, Curiel DT, Arafat WO, Carpenter M, Stackhouse MA. Adenovirus-mediated transfer of BAX driven by the vascular endothelial growth factor promoter induces apoptosis in lung cancer cells. *Mol Ther.* 2002 Aug;6(2):190-8.
3. Arafat WO, Buchsbaum DJ, Kaliberov S, Li F, Zhu ZB, Curiel DT. A novel radiation/tissue-specific promoter for gene therapy of brain tumors. *Int J Radiat Oncol Biol Phys.* 2003 Oct 1;57(2 Suppl):S146. No abstract available.
4. Pereboeva L, Komarova S, Mikheeva G, Krasnykh V, Curiel DT. Approaches to utilize mesenchymal progenitor cells as cellular vehicles. *Stem Cells.* 2003;21(4):389-404.

BIOLOGY CONTRIBUTION

AN ADENOVIRUS ENCODING PROAPOPTOTIC BAX SYNERGISTICALLY RADIOSENSITIZES MALIGNANT GLIOMA

WALEED O. ARAFAT, M.D., PH.D.,^{*,†} DONALD J. BUCHSBAUM, PH.D.,[‡] JESÚS GÓMEZ-NAVARRO, M.D.,^{*}
 SARAH A. TAWIL, B.S.,^{*} CHRISTINE OLSEN, B.S.,[‡] JIALING XIANG, PH.D.,^{*} HAZEM EL-AKAD, M.D.,[†]
 ANWAR M. SALAMA, M.D.,[†] AHMED O. BADIB, M.D.,[†] MURRAY A. STACKHOUSE, PH.D.,[‡] AND
 DAVID T. CUIEL, M.D.^{*}

^{*}Human Gene Therapy and [†]Radiation Oncology, University of Alabama at Birmingham, Birmingham, AL; [‡]Clinical Oncology Department, Alexandria University, Alexandria, Egypt

Purpose: We explore the utility of the adenovirus-mediated delivery of proapoptotic Bax for enhancing the cytotoxicity of radiotherapy (RT) in RT-refractory glioma cells.

Methods and Materials: Cell lines D54 MG and U87 MG (p53 wild-type), and U251 MG and U373 MG (p53 mutant), and patient-derived astrocytes were evaluated. Cells were irradiated and infected with an inducible adenovirus encoding Bax. Cell proliferation, colony formation assay, quantification of early apoptotic alteration in the plasma membrane by fluorescence-activated cell sorter using annexin V, and nuclear staining with H33258 were used to evaluate apoptosis. The capacity of the combined treatment to induce regression of subcutaneous D54 MG tumors was tested in nude mice. A dose of 5 Gy was administered every other day, four times, for a total dose of 20 Gy. One day after each irradiation, tumors were injected with 1×10^9 plaque-forming units (PFU).

Results: Apoptotic death was enhanced by the combination of Ad/Bax and RT. In D54 MG, levels of apoptosis after RT alone, Ad/Bax alone, or the combination were, respectively, 12.3%, 32.1%, and 78.5%. In contrast, treatment of astrocytes did not significantly induce apoptosis. A colony-formation assay showed a 2-log inhibition with respect to controls after combined treatment, irrespective of the endogenous levels of p53. The other apoptosis assays also showed the defining characteristics of apoptosis in the combination group. Remarkably, combined treatment induced regression of tumors in mice.

Conclusion: Ad/Bax synergistically radiosensitizes glioma, with a seemingly favorable therapeutic index.
 © 2003 Elsevier Science Inc.

Gene therapy, Apoptosis, Radiosensitization, Glioma, Bax.

INTRODUCTION

Malignant glioblastoma, a poorly differentiated brain tumor, is typically refractory to conventional treatment. Radiotherapy, with or without surgery, is the cornerstone of the treatment plan for this tumor, which mostly invades and infiltrates locoregionally without disseminating out of the brain. Unfortunately, the disease recurs after initial treatment in most cases, and the survival rate is very poor. Thus, most patients die within 6 months of diagnosis (1). Although different strategies have been explored to sensitize glioblastoma to radiation, none has achieved a significant improvement in survival (2–4).

With the advances in the understanding of the molecular biology of cancer, and particularly of brain tumors, it has become well recognized that tumorigenesis and development of radioresistance are both related to change in tumor environment by hypoxia and acidosis and the dysregulation of certain genes, including not only oncogenes and tumor suppressor genes, but also other genes involved in a variety of cell signaling pathways (5–7).

In this regard, most notable has been the realization that tumors result not only from excessive proliferation, but also from an excessive or inappropriate cell survival—in other words, from a lack of programmed cell

Reprint requests to: David T. Cuiel, M.D., Director, Division of Human Gene Therapy, University of Alabama at Birmingham, 502 Biomedical Research Building II, 901 19th Street South, Birmingham, AL 35294. Tel: (205) 934-8627; Fax: (205) 975-7476; E-mail: david.cuiel@ccc.uab.edu

Supported by NIH Grants R01 CA72532, R01 CA68245, R01 CA74242, and DAMD17-01-1-0012, by DOD Grant PC001082, and by a grant from the Egyptian Ministry of High Education (W.O.A.).

Acknowledgments—We thank Andrew O. Westfall, M.S., for the biostatistical analysis and Dr. Saeed Elnowiem for critical reading.

Present addresses: J.G.N.: Pfizer, Groton, CT; M.A.S.: Southern Research Institute, Birmingham, AL; J.X.: University of Chicago, Chicago, IL; and S.A.T.: Centre de Biochimie, Parc Valrose, Nice, France.

Received Sep 6, 2000, and in revised form Nov 11, 2002.
 Accepted for publication Nov 18, 2002.

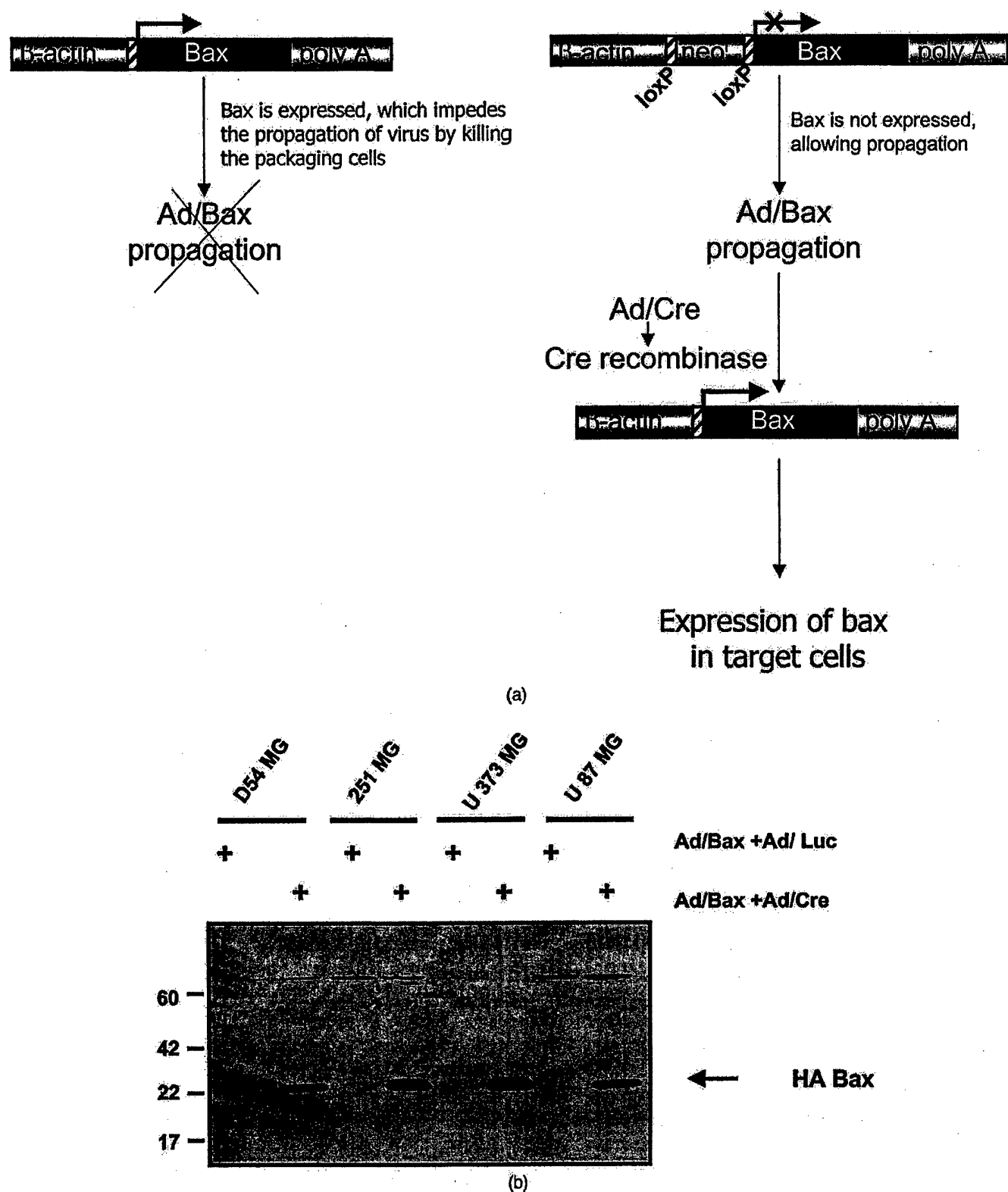


Fig. 1. (a) Schematic of the inducible recombinant Ad/Bax construct. HA-tagged *bax* cDNA was inserted in the *Swal* site of pDEloxP vector. In the presence of Cre recombinase, excision of the *loxP*-*neo*^r-*loxP* cassette allows appropriate transcription/translation of the *bax* gene. (b) Immunoblot analysis of Bax expression in four glioma cell lines infected with 100 MOI of Ad/Bax + Ad/Luc, or Ad/Bax + Ad/Cre, as indicated. The proteins (10 µg per lane) were separated on a 12% SDS-PAGE gel, followed by immunoblot with an anti-HA antibody.

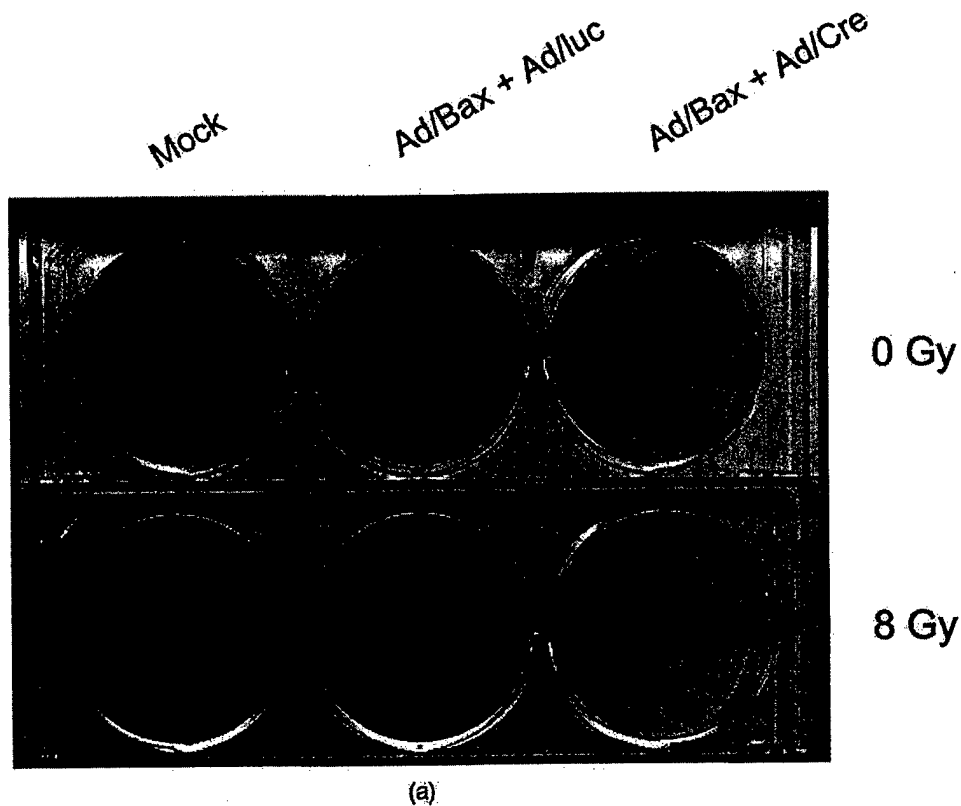


Fig. 2. (a) D54 MG glioma cells were plated in a 6-well plate with 2×10^5 cells/well and irradiated with 0 or 8 Gy. After 24 h, cells were infected with Ad/Bax and Ad/Cre or irrelevant virus, or left uninfected. Five days later, cells were stained for viability using crystal violet. The experiments were repeated 4 times; a representative example is shown. (b) Quantitation of apoptosis in D54 MG glioma cells treated with 100 MOI of Ad/Bax and Ad/Cre and radiation. D54 MG cells, 2.5×10^5 /well, were seeded into 6-well plates and irradiated with 8 Gy of ^{60}Co irradiation, or mock irradiated, 12 h after plating. Twenty-four hours after irradiation, cells were infected with Ad/Bax and Ad/Cre in a 4:1 ratio with MOI of 80/20, for 2.5 h. Control adenovirus encoding the cytosine deaminase gene (Ad/CD) was mixed with Ad/Cre in the same MOI ratios. Adenovirus mixtures were removed, the plates were rinsed once with phosphate-buffered saline (PBS), growth medium was added, and the cells were incubated at 37°C . Four days later, cells were harvested, stained with annexin V and PI, and analyzed by flow cytometry. The data were collected into four windows representing unstained cells, PI stained cells, annexin V-fluorescein isothiocyanate (FITC) stained cells, and annexin V-FITC plus PI stained cells. The plotted values come from one representative experiment repeated three times. The data show levels of annexin V-FITC stained cells and annexin V-FITC and PI stained cells. (c) Induction of apoptosis in D54 MG cells treated with Ad/Bax + Ad/Cre and radiation. Cells were trypsinized, transferred to a microscope slide using a Cytospin centrifuge at 200 g, fixed in 95% ethanol, stained with Hoechst 33258, and viewed using UV microscopy at $400\times$ magnification. Upper left panel: untreated D54 MG cells. Upper right panel: D54 MG cells infected with Ad/Bax and Ad/Cre at a ratio of 80/20, stained at 48 h to 72 h postirradiation. Note the large number of small apoptotic bodies. Bottom left panel: D54 MG cells at 72 h after exposure to 8 Gy of ^{60}Co irradiation. Bottom right panel: D54 MG cells exposed to 8 Gy of irradiation, infected with Ad/Bax and Ad/Cre at a MOI ratio of 80/20 24 h later, and stained 72 h postirradiation. Again, note the large number of small apoptotic bodies.

death (8). Apoptosis is a gene-directed cellular program that, when disturbed, contributes to malignancy and to resistance to anticancer treatments. Several genes that control apoptosis have been discovered, and among these *p53* has been well studied. Despite the promising pre-clinical results obtained by administering exogenous *p53* in the treatment of brain cancer (9–16), the preliminary clinical data suggest a very limited effect, perhaps due to the poor intratumoral gene delivery and to variable functional status of *p53* within the tumor (17). The recognition of these limitations and the discovery of other potent proapoptotic genes have prompted the evaluation of alternative genetic interventions.

Bax was discovered through its ability to bind to the *bcl-2* protein, and was soon recognized to counter this protein's death-suppressing activity (18, 19). Interestingly, Bax itself does not cause cell death; in fact, its proapoptotic effect is exerted only after a concomitant death signal, such as deprivation of a growth factor, or radiotherapy (8). Of note, the induction of apoptosis by Bax is, in some experimental conditions, independent of other important upstream and downstream components of the apoptosis pathway, such as *p53* and the caspases (20). This independence from other apoptotic mediators may be an important advantage for the eventual therapeutic exploitation of Bax, most notably in the context of het-

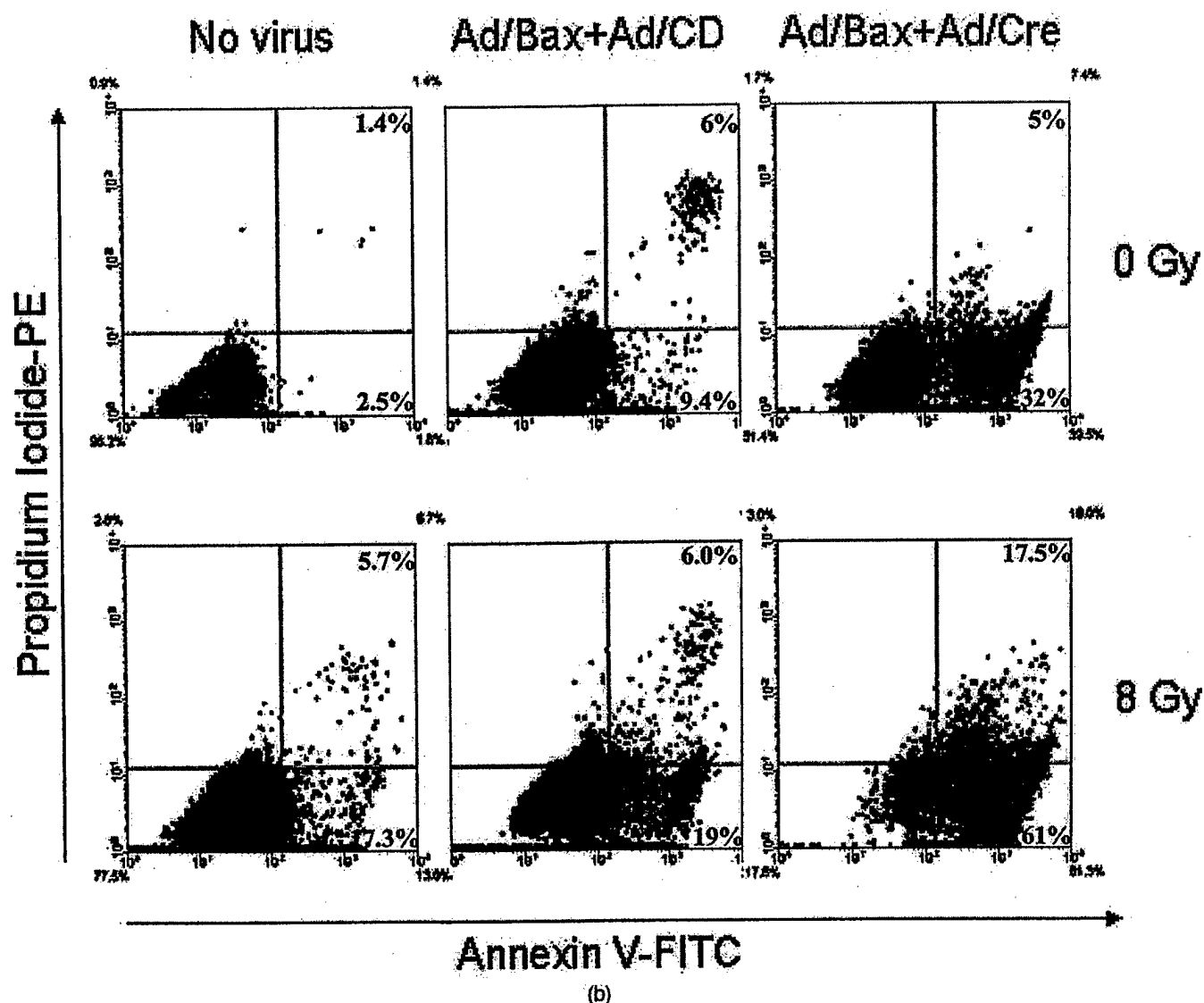


Fig. 2. (Cont'd)

erogeneous tumors that may or may not express other regulators of apoptosis needed for apoptosis induction under normal growth conditions.

It is well established that induction of apoptosis is an important mechanism that contributes to the cytotoxicity of radiotherapy, and its presence predicts the sensitivity to and outcome of radiation. It has been shown that exogenous Bax-mediated induction of apoptosis sensitizes breast cancer cells to radiation (21, 22). Recently, we have shown that adenovirus-mediated gene transfer of Bax induces apoptosis and sensitizes ovarian cancer cells to the effect of radiation (23). More importantly, it has been shown that the inability of p53 to induce the activity of Bax is associated with the development of radioresistance in malignant gliomas (24). Based on the aforementioned observations, we hypothesized that Bax gene delivery into malignant gliomas would sensitize the tumor to the cytotoxic effects of radiotherapy.

To this end, an efficient means to transfer the Bax gene into the tumor is critical. Recombinant adenoviruses have shown the required attributes of efficiency and stability *in vivo*, and have been employed in numerous clinical trials. Thus, we further hypothesized that a recombinant adenovirus encoding proapoptotic *bax* could deliver the gene effectively to brain tumors and could thus sensitize them to the cytotoxic effects of radiotherapy.

METHODS AND MATERIALS

Cell culture

The human glioblastoma cell lines D54 MG, U373 MG, U87 MG, and U251 MG and human astrocytes (a kind gift from Dr. Yancey Gillespie, University of Alabama at Birmingham) were maintained in Dulbecco's modified Eagle's medium/F12, supplemented with 10% fetal calf serum, L-glutamine (200 μ g/mL), 100 U/mL

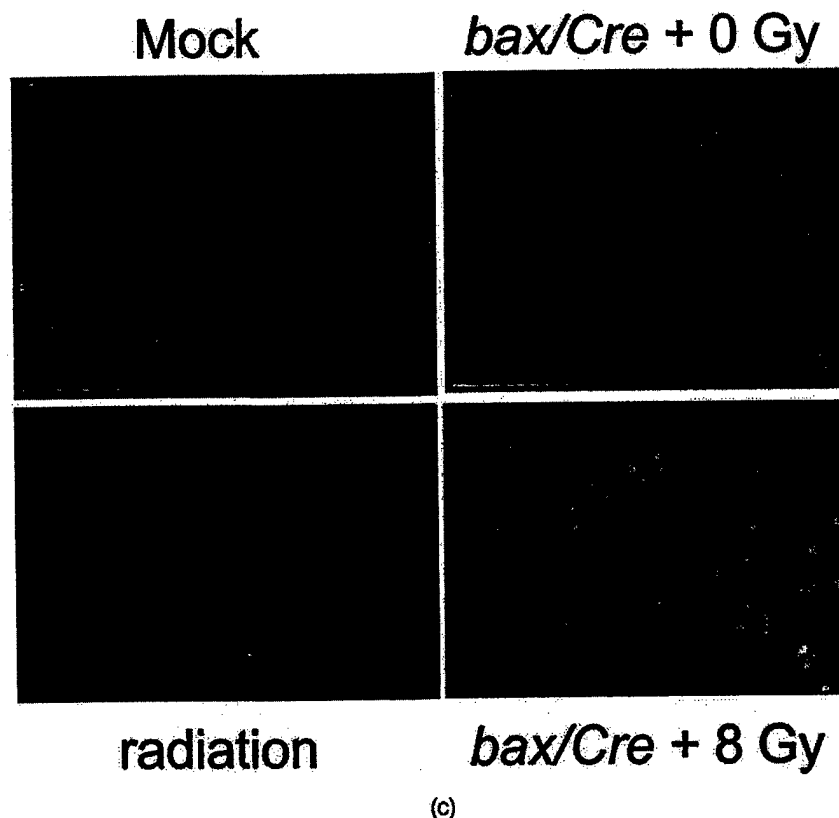


Fig. 2. (Cont'd)

penicillin, and 100 $\mu\text{g/mL}$ streptomycin, at 37°C in a 100% humidified 5% CO_2 atmosphere. The human embryonic kidney cell line 293 was obtained from the American Type Culture Collection (ATCC, Rockville, MD) and was grown in the same media used for glioma cell lines.

Production of recombinant adenoviruses

A recombinant adenoviral vector containing the human *bax* cDNA (Ad/Bax) was generated, as previously described (25, 26). For induction of Bax protein, cells were coinfecting with Ad/Bax and the inducing adenovirus Ad/Cre (a kind gift from I. Saito, University of Tokyo, Japan), a recombinant adenoviral vector encoding Cre recombinase. This enzyme cuts specifically at loxP sites, releases a stuffing loxP-delimited sequence, and thus reestablishes the contact between *bax* and its promoter, allowing active induction of expression of Bax. Equal amounts in plaque-forming units (PFU) of the following recombinant adenoviruses were used as a transduction control in different experiments: Ad/Luc, encoding the luciferase reporter gene (a kind gift of Robert D. Gerard, University of Leuven, Leuven, Belgium); Ad/GFP, encoding the reporter green fluorescent protein; Ad/lacZ, encoding the *Escherichia coli* β -galactosidase gene (provided by De-chu Tang, University of Alabama at Birmingham, Birmingham, AL); or Ad/CD, encoding bacterial cytosine deaminase. Viruses were propagated in 293

cells, purified by centrifugation in CsCl gradients, and plaque-titrated in 293 cells following standard protocols (27).

Cell proliferation assay

To evaluate the cytotoxicity of radiation, Bax overexpression, and the combination thereof, 2×10^5 D54 MG cells were plated per well in 6-well plates (Falcon, Franklin Lakes, NJ) for crystal violet staining or 1×10^5 per well in 12-well plates for cell counting, respectively. The next day, cells were irradiated with doses ranging from 0 to 8 Gy; 24 h later cells were infected with a multiplicity of infection (MOI) of 100 PFU per cell of either Ad/Bax or Ad/Bax and Ad/Luc, or Ad/Bax and Ad/Cre at 80 PFU/cell and 20 PFU/cell of each virus, respectively. Control cells were left uninfected. Five days later, cell viability was measured by crystal violet staining or by counting with trypan blue exclusion for quantification. A quantitative measurement of the crystal violet staining was obtained with an Epi Chemi II Darkroom densitometer and LabWorks software (UVP, Upland, CA).

Colony-formation assay

To evaluate radiosensitization by Bax, 2×10^5 D54 MG cells were plated in 6-well plates. Eight hours later, cells were irradiated using a ^{60}Co therapy unit (Picker, Cleveland, OH) at a dose of 80 cGy/min; 24 h later the

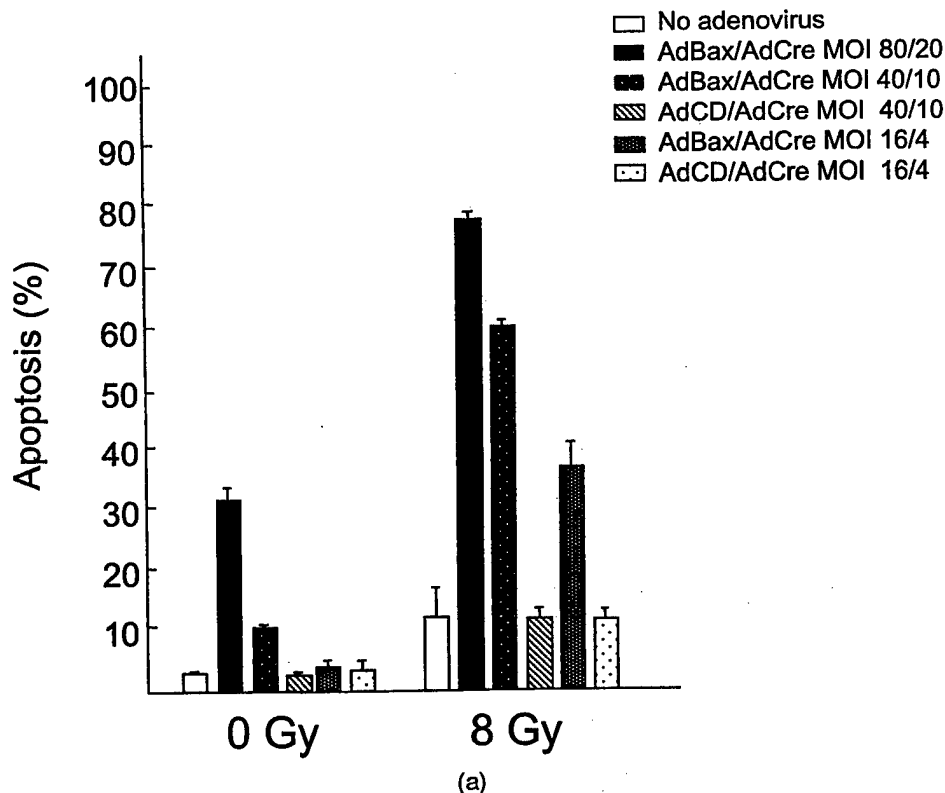


Fig. 3. (a) Quantitation of apoptosis in D54 MG glioma cells treated with various MOIs of Ad/Bax and Ad/Cre plus radiation. D54 MG cells (2.5×10^5 /well) were plated into 6-well plates and irradiated with 8 Gy of ^{60}Co irradiation or mock irradiated 12 h after plating. Twenty-four hours after irradiation, cells were infected with Ad/Bax and Ad/Cre in a 4:1 ratio with MOIs of 16/4, 40/10, and 80/20 for 2.5 h. Control adenovirus encoding the cytosine deaminase gene (Ad/CD) was mixed with Ad/Cre in the same MOI ratios. Adenovirus mixtures were removed, the plates were rinsed once with PBS, growth medium was added, and the cells were incubated at 37°C. Four days later, cells were harvested, stained with annexin V and PI, and analyzed by flow cytometry. The data were collected into four windows representing unstained cells, PI stained cells, annexin V-FITC stained cells, and annexin V-FITC plus PI stained cells. The results of a representative experiment are shown. All determinations were done in triplicate. (b) D54 MG cells were plated, irradiated with 0, 2, 4, or 8 Gy, and then infected with Ad/Bax and Ad/Cre or irrelevant virus, or left uninfected. After 96 h, flow cytometry analysis was done as described above.

cells were infected using the same MOI as above with Ad/Bax and Ad/Luc, Ad/Bax and Ad/Cre, or left uninfected. Two hours after infection, 200 to 5000 of the treated cells were plated in T-25 flasks (Falcon) and returned to the incubator for colony formation. Fourteen days later, the colonies were fixed in ethanol and stained with 1% crystal violet. Colonies that contained more than 50 cells were counted. Survival was calculated as the average number of colonies counted divided by the number of cells plated times the plating efficiency (PE), where PE was the fraction of colonies counted divided by cells plated without radiation. The clonogenic survival data were generated using Fit v2.4 software (kindly provided by Dr. N. Albright, University of California at San Francisco, San Francisco, CA).

Apoptosis assays

Apoptosis was evaluated by determining cell viability, nuclear morphology, and by a quantitative test that measures an early apoptotic plasma membrane alteration. For visualization

of nuclear morphology, cells were stained with the intercalating DNA dye H33258 (Sigma, St. Louis, MO), and observed under an ultraviolet (UV) light microscope. An early apoptotic alteration in the plasma membrane, in the form of translocation of phosphatidylserine (PS) from the inside of the plasma membrane to the outside, was also quantified by a fluorescence-activated cell sorter using the Annexin-V-FLUOS Staining Kit (Boehringer Mannheim, Indianapolis, IN), according to the manufacturer's recommendations. The proportion of cells stained by propidium iodide (PI), annexin V, or both, was determined using a Beckman Coulter flow cytometer (Fullerton, CA). Cells that were PI negative and annexin V positive were considered apoptotic; cells that were PI positive and annexin V negative were considered necrotic.

Immunoblot analysis

Glioma cells were lysed with a Nonidet P-40 (NP-40) buffer containing 0.3% NP-40, 142 mM KCl, 5 mM MgCl_2 , 2 mM ethylenediaminetetraacetic acid (EDTA), 20 mM HEPES pH 7.4, and a cocktail of protease inhibitors (aprotinin, leupeptin,

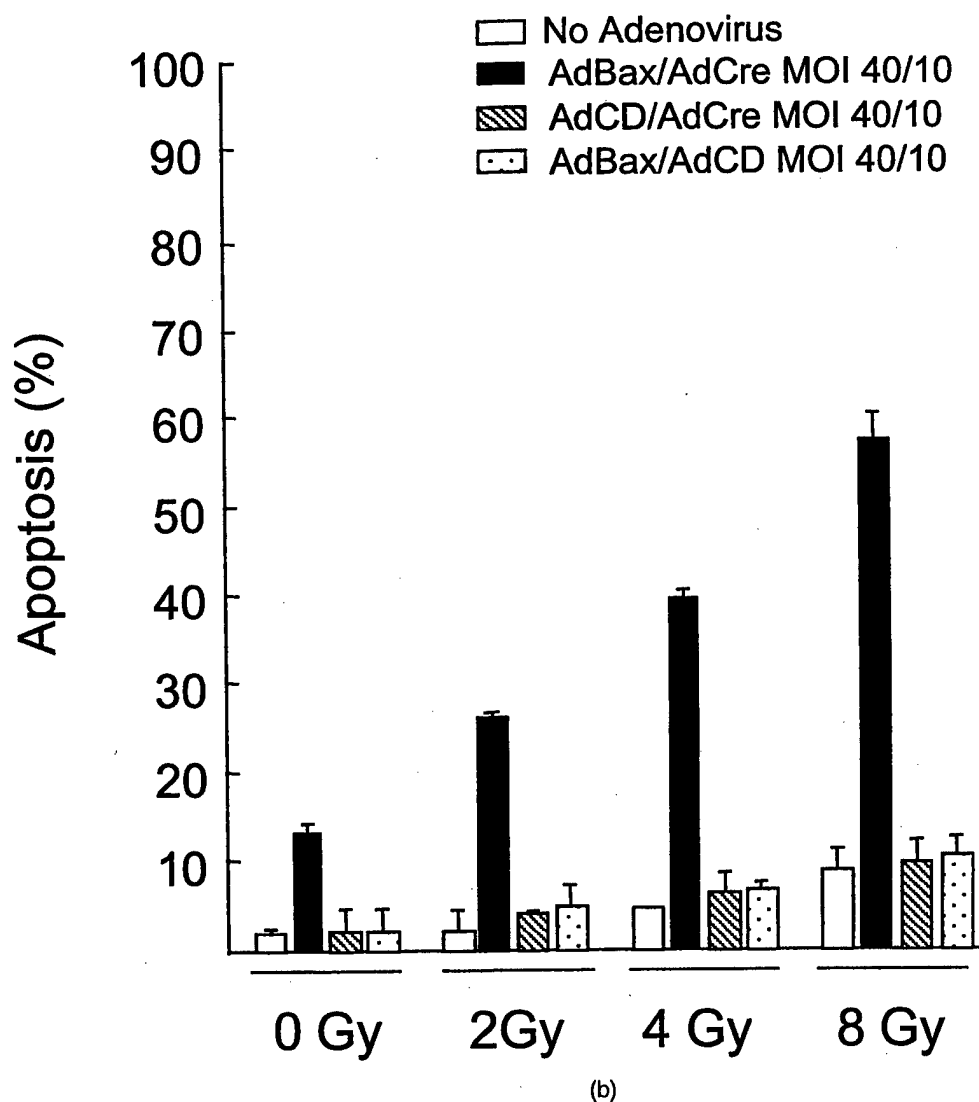


Fig. 3. (Cont'd.)

and phenylmethylsulfonyl fluoride) (Sigma, St. Louis, MO). Total protein (10–50 μ g) was separated on a 12% sodium dodecyl sulfate–polyacrylamide gel electrophoresis (SDS-PAGE) gel and subsequently transferred to a polyvinylidene difluoride membrane (Bio-Rad, Hercules, CA). The membranes were blocked with 2% nonfat dry milk and probed with a hemoagglutinin (HA) monoclonal antibody at a dilution of 1:1000 (Santa Cruz Biotechnology, Santa Cruz, CA). After washing with Tris-buffer saline containing 0.05% Tween-20 (TBST), a secondary antibody conjugated to horseradish peroxidase (Jackson 1:3000 diluted in TBST) was added for a 1-h incubation. Finally, the blot was washed and developed using enhanced chemiluminescence (Renaissance, NEN, Boston, MA) according to the manufacturer's protocol and exposed to a radiographic film (Eastman Kodak, Rochester, NY).

In vivo therapeutic experiment

In this experiment, nude mice 4 to 6 weeks old were used. Mice had been classified into five groups ($n = 5$) according

to treatment as follows: radiation alone, irrelevant virus alone or with radiation (5 Gy \times 4), and Ad/Bax and Ad/Cre with or without radiation (5 Gy \times 4). Mice were injected subcutaneously into lower flanks with 2×10^7 D54 MG cells, and then followed for nodule formation. When nodules reached suitable size (6 \times 5 mm in two largest diameters), mice were irradiated and virus was injected 24 h later intratumorally at a total MOI of 1×10^9 with the same Ad/Bax and Ad/Cre ratio as *in vitro* after each dose of radiation for 4 times. Nodules were monitored up to 6 months for tumor growth. Animal experiments were performed following institutional guidelines and under the supervision of the Animal Resources Program of the University of Alabama at Birmingham.

Statistics

To test the interaction of viral treatment and radiation, two-way analysis of variance (ANOVA) was performed using the SAS System (SAS Institute, Inc., Cary, NC).

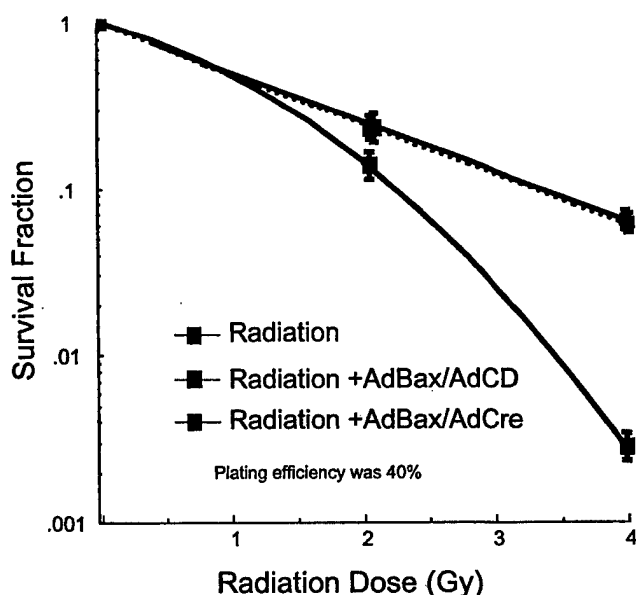


Fig. 4. Colony-formation assay. To evaluate radiosensitization by *bax*, 2×10^5 D54 MG cells were plated 8 h before irradiation in 6-well plates. The cells were irradiated using a ^{60}Co therapy unit at a dose of 80 cGy/min; 24 h later the cells were infected with 80 PFU/cell of Ad/Bax and 20 PFU of Ad/Luc, with 80 PFU/cell of Ad/Bax and 20 PFU/cell of Ad/Cre, or left uninfected. Immediately, 200 to 5000 of the treated cells were plated in T-25 flasks and returned to the incubator for colony formation. Fourteen days later, the colonies were fixed in ethanol and stained with 1% crystal violet. Colonies that contained more than 50 cells were counted. Survival was calculated as the average number of colonies counted divided by the number of cells plated times the plating efficiency (PE), where PE was the fraction of colonies counted divided by cells plated without radiation.

RESULTS

Recombinant adenovirus encoding proapoptotic Bax is highly inducible and tightly controlled in different glioma cell lines

Overexpression of Bax is known to be cytotoxic in many cell lines, which would impede the propagation of a vector encoding it in sensitive packaging cells. To overcome this problem, we have employed the Cre-LoxP system (Fig. 1A) to generate an inducible recombinant *bax* adenoviral vector (Ad/Bax). The HA-tagged *bax* coding sequence was placed under the control of the β -actin promoter and a downstream loxP-neo^r-loxP sequence in the SmaI site of the pDEloxP vector. The loxP-neo^r-loxP cassette is composed of a neo^r gene flanked by two head-to-tail loxP sites, which disrupt the promoter/coding-region structure, required for *bax* expression. In this system, the *bax* gene cannot be expressed until the loxP-neo^r-loxP cassette is excised by Cre recombinase. Expression of Bax protein in infected cells was confirmed by co-delivery of Ad/Bax and Ad/Cre, followed by immunoblotting analysis with an anti-HA monoclonal antibody (Fig. 1B).

Recombinant adenovirus encoding Bax induces apoptosis in the presence of radiotherapy

To determine the effect of Bax on irradiated cells, D54 MG cells were irradiated with 0 or 8 Gy. After 24 h, cells were infected with Ad/Bax and Ad/Cre, Ad/Bax and irrelevant virus, or left uninfected. After 5 days, the cells were stained for viability using crystal violet. Cells treated with bax alone or with radiation alone showed little inhibition of cell growth (Fig. 2A). In contrast, cells treated with Ad/Bax plus Ad/Cre and radiation showed near-complete cell killing. Quantitated analyses of density values showed a significant interaction between these viruses and radiation (63,028 vs. 0) ($p = 0.0001$, two-way ANOVA), indicating a synergistic effect.

To further quantify cell killing, we assayed by flow cytometry for induction of apoptosis. D54 MG cells were treated as in Fig. 2A, and 4 days later the cells were stained with annexin V, which reveals phosphatidylserine, a protein transferred from the inside of the cell membrane to the outside surface in apoptotic cells. As shown in Fig. 2B, 78.5% of cells treated with Ad/Bax plus Ad/Cre and radiation showed induction of apoptosis ($p = 0.003$). The percentage of apoptotic cells after radiation alone, radiation with Ad/Bax + Ad/CD viruses, or infection with Ad/Bax and Ad/Cre without radiation was 23%, 25%, and 27%, respectively. Thus, treatment of glioma cells with induced Ad/Bax significantly enhanced the effect of radiation via augmentation of apoptosis.

To confirm the nature of the death mechanism, we evaluated morphologically the cell and nuclei phenotypes. After staining treated cells with Hoechst 33258, a large number of small apoptotic bodies were observed in the D54 MG cells infected with Ad/Bax + Ad/Cre with radiation, demonstrating that *bax* gene expression combined with ionizing radiation induced apoptosis in D54 MG cells (Fig. 2C, bottom right panel). In contrast, untreated D54 MG cells and those exposed to 8 Gy alone exhibited almost none (Fig. 2C, upper and bottom left panels). As expected, treatment with Ad/Bax and Ad/Cre induced apoptotic changes but in a lower level than when combined with radiation (Fig. 2C, upper right panel). Thus, cell death induced by Bax and radiation had, in these conditions, the typical morphologic features of apoptosis.

Radiosensitization of glioma cells by an adenovirus encoding Bax is radiation- and viral dose-dependent

To further characterize the interaction between Bax and radiation, dose-dependency studies were performed. First, the effect of increasing doses of viral vector was determined. D54 MG glioma cells were treated with either 0 or 8 Gy of radiation and then were infected with MOI of 16/4, 40/10, and 80/20 ratios of Ad/Bax to Ad/Cre, or of irrelevant viruses. The development of apoptosis was confirmed by flow cytometry as before. The magnitude of appearance of apoptosis compared with untreated cells increased at higher MOI in both unirradiated (4.2%, 10.6%, and 32.1%, for Ad/Bax/Ad/Cre MOI doses of 16/4, 40/10, and 80/20,

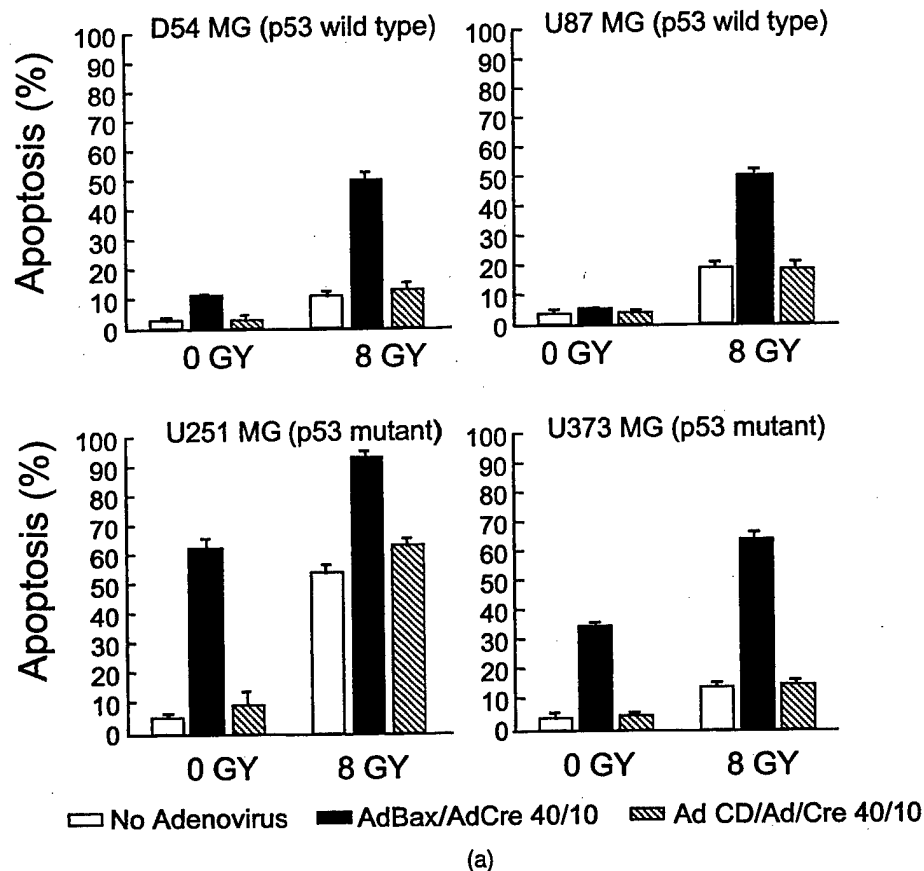


Fig. 5. The induction of apoptosis is independent from the status of p53. (a) Four different glioblastoma cell lines with different functional status of p53 were treated with Ad/Bax + Ad/Cre, and radiation. 2×10^5 cells per well of the four glioblastoma cell lines were plated into 6-well plates. Apoptosis was detected using annexin V as mentioned previously. (b) Cell proliferation assay in the same four cell lines. Cells were treated as above, and 96 h later, cell proliferation was determined by counting cells using trypan blue dye exclusion test.

respectively) and irradiated cells (37.1%, 60.5% and 78.5%, respectively) (Fig. 3A). D54 MG cells infected with Ad/Bax and Ad/Cre were compared with uninfected controls. No increase in apoptosis was observed in D54 MG cells infected with control adenovirus (Ad/CD + Ad/Cre) or (Ad/Bax + Ad/CD) compared with the uninfected controls with or without radiation. Remarkably, the large increase in the levels of apoptosis observed at all MOIs tested in irradiated D54 MG cells suggested a synergistic effect of the combination, which was confirmed statistically ($p = 0.0001$ in two-way ANOVA). Interestingly, while the combination of Ad/Bax plus Ad/Cre at as low an MOI as 16/4 led to a background level of apoptosis in unirradiated D54 MG cells, its association with radiation led to a 3.2-fold increase in apoptosis.

To determine the effect of the dose of radiation on the induction of apoptosis, cells were irradiated with 0, 2, 4, or 8 Gy, and then infected with a constant dose of Ad/Bax + Ad/Cre or Ad/Bax + Ad/CD viruses, or left uninfected. Flow cytometry analysis of annexin V was done 96 h later (Fig. 3B). After infection with Ad/Bax + Ad/Cre at an MOI

of 40/10, the level of apoptosis was 13.3%, 26.2%, 39.6%, and 57.4% ($p = 0.010$, $p < 0.001$, $p = 0.006$ for comparisons with the nonirradiated cells) in cells exposed to 0, 2, 4, and 8 Gy, respectively. Thus, apoptosis increased significantly as the dose of radiation increased.

Radiosensitization of a glioma cell line is confirmed by a colony-formation assay

To confirm the radiosensitization effect of Bax on glioma cells, the gold standard test, i.e., a colony-formation assay, was used. To this end, D54 MG cells were irradiated at 0, 2, and 4 Gy and infected with Ad/Bax + Ad/Cre or irrelevant viruses (Ad/Bax + Ad/CD), or left uninfected. Then, cells were plated for colony formation, which was assayed 14 days later. The survival fraction of cells treated with Ad/Bax + Ad/Cre and 2, 3, or 4 Gy radiation was significantly lower than that observed in cells treated with radiation alone or with radiation and irrelevant viruses. Of note, the plating efficiency of D54 MG was 39%. (Fig. 4). Thus, Bax indeed significantly sensitized glioma cells to radiation.

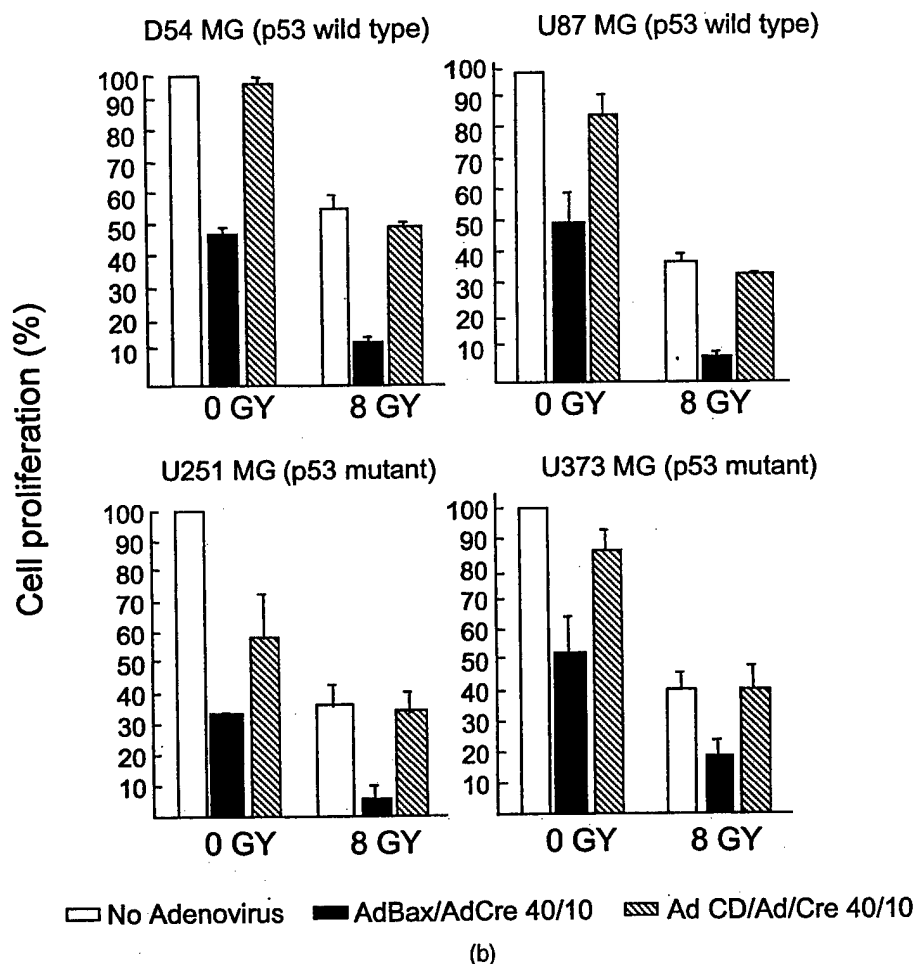


Fig. 5. (Cont'd)

The functional status of p53 does not preclude the radiosensitization effect by a recombinant adenovirus encoding Bax

To determine the effect that the functional status of p53 might have on the radiosensitizing effect of Bax, we compared the induction of apoptosis in glioblastoma cell lines characterized by possessing wild-type or mutant p53 genes. Four glioblastoma cell lines, D54 MG, U87 MG, U251 MG, and U373 MG, were treated with radiation and viruses as described above, then apoptosis was assessed by annexin as described above. The p53 wild-type glioblastoma cell lines (D54 MG and U87 MG) were more resistant to bax-mediated apoptosis induction when no radiation was administered, compared with the p53 mutant cell lines (U251 MG and U373 MG) (Fig. 5A). However, the combination of Bax treatment with 8 Gy of radiation showed a p53-independent response to apoptosis induction. In fact the U373 MG p53 mutant cell line showed a higher level of apoptosis after infection alone, or after combined treatment. Additionally, U251, which is also p53 mutant, showed a relatively high level of apoptosis with virus alone or radiation alone, and this effect was augmented when both treatments were used.

To confirm these results, a cell proliferation assay was performed with the four tumor cell lines. After irradiation and cell infection, the four glioblastoma cell lines were assayed for proliferation by counting of viable cells. All showed a variable degree of inhibition of growth with Ad/Bax infection. However, this inhibition of growth was dramatically increased with the addition of 8 Gy of radiation (Fig. 5B). Thus, a significant induction of apoptosis and growth inhibition was achieved using the combined bax gene delivery and radiation treatment, and this effect was independent of the p53 functional status of the cells.

Combined treatment with radiation and an adenovirus encoding Bax induces complete regression of glioblastoma tumor nodules

To evaluate the capacity of adenovirus to deliver bax *in situ* and to sensitize previously irradiated tumor, we performed an *in vivo* therapeutic experiment. Nude mice ($n = 5/\text{group}$) bearing established D54 MG subcutaneously received either radiation alone, irrelevant virus with radiation, or Ad/Bax + Ad/Cre with or without radiation. Radiation (5 Gy) and viruses were administered every other day, four times. Mice treated with

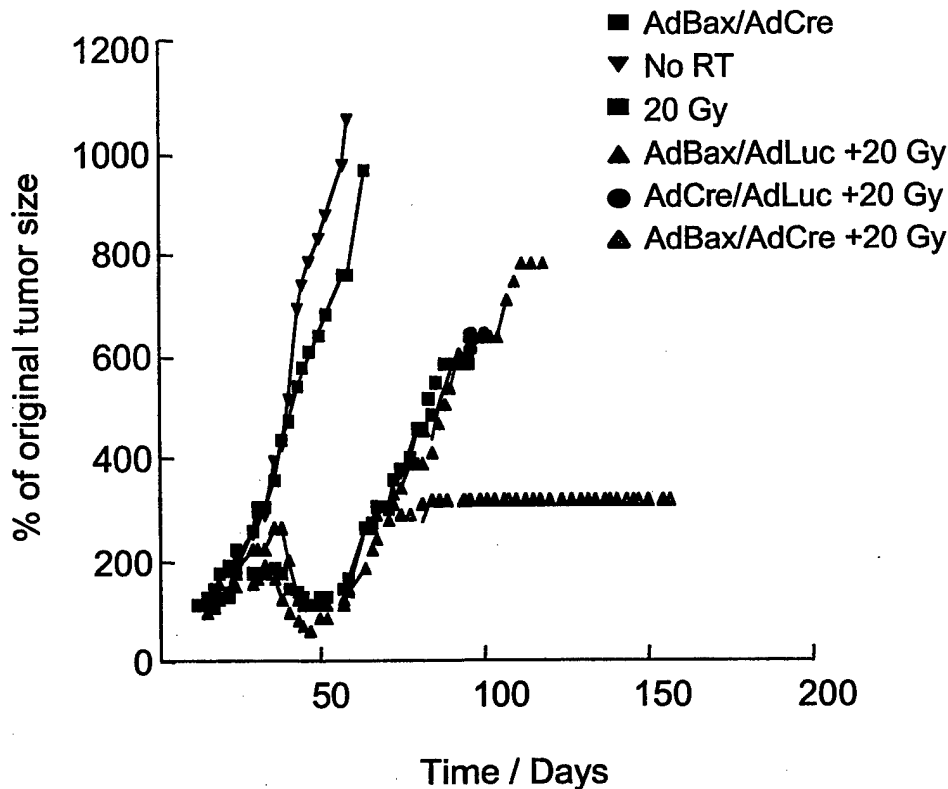


Fig. 6. Subcutaneous nodules of glioma are radiosensitized by intratumoral delivery of Bax. In this experiment, nude mice 4 to 6 weeks old were used. Mice were classified in six groups ($n = 5$), according to treatment as follows: radiation alone, irrelevant virus with or without radiation ($5 \text{ Gy} \times 4$), and Ad/Bax + Ad/Cre with or without radiation ($5 \text{ Gy} \times 4$). Mice were injected subcutaneously into lower flanks with 2×10^7 D54 MG cells, and then followed for nodule formation for 3 weeks. When nodules reached suitable size (5×6), tumors were irradiated and viruses were injected intratumorally at an MOI of 1×10^9 after each administration of radiation, 4 times. Nodules were monitored up to 6 months for tumor size. Representative data from one of two similar experiments are shown.

Ad/Bax + Ad/Cre without radiation, as well as those nontreated, showed rapid tumor growth, and had to be killed after 5 weeks (Fig. 6). On the other hand, mice treated with radiation alone or radiation with irrelevant viruses showed a transient inhibition of their growth although the tumor grew back aggressively, and the mice had to be killed after 8–10 weeks. In contrast, mice treated with Ad/Bax + Ad/Cre and radiation showed significant regression and inhibition of tumor growth over a 6-month time period. Of these mice, 60% had no evidence whatsoever of tumor. Thus, combined treatment with bax and radiation is uniquely able to completely eradicate malignant glioma tumor nodules in this mouse model.

Normal human astrocytes are not radiosensitized by recombinant adenovirus encoding Bax

To test whether Bax induces apoptosis in normal human astrocytes, and to determine if it has sensitizing effects to radiation, astrocytes were exposed to 0 or 8 Gy radiation and infected with 100 PFU of Ad/Bax + Ad/Cre or irrelevant viruses (Ad/CD + Ad/Cre). Four days later, apoptosis was determined. Radiation alone induced apoptosis over that observed in unirradiated controls (18% vs. 10% respec-

tively). Bax also induced some apoptosis over that observed in uninfected controls (24% vs. 10%, respectively); the levels were only slightly higher than those induced by irrelevant control viruses (18%) (Fig. 7A). Most importantly, the addition of radiation provoked a minor and insignificant ($p = 0.267$) increase in apoptosis. This effect was indeed small compared with the much greater increase of apoptosis observed with radiation in all the glioblastoma cell lines tested. To confirm this result, a cell proliferation assay was performed. Astrocytes treated with Ad/Bax and Ad/Cre or irrelevant virus showed no significant inhibition of cell proliferation (Fig. 7B). In addition, cell proliferation of irradiated cells did not differ significantly with or without viral treatment. Thus, Bax does not appear to sensitize normal astrocytes to the effect of radiation.

DISCUSSION

Radiotherapy, alone or combined with surgery, is unable to achieve cures or even a reasonable rate of response in the treatment of glioblastoma (1). Our growing understanding of the mechanisms behind radioresistance in malignant glioma offers the intriguing possibility of modulating radio-

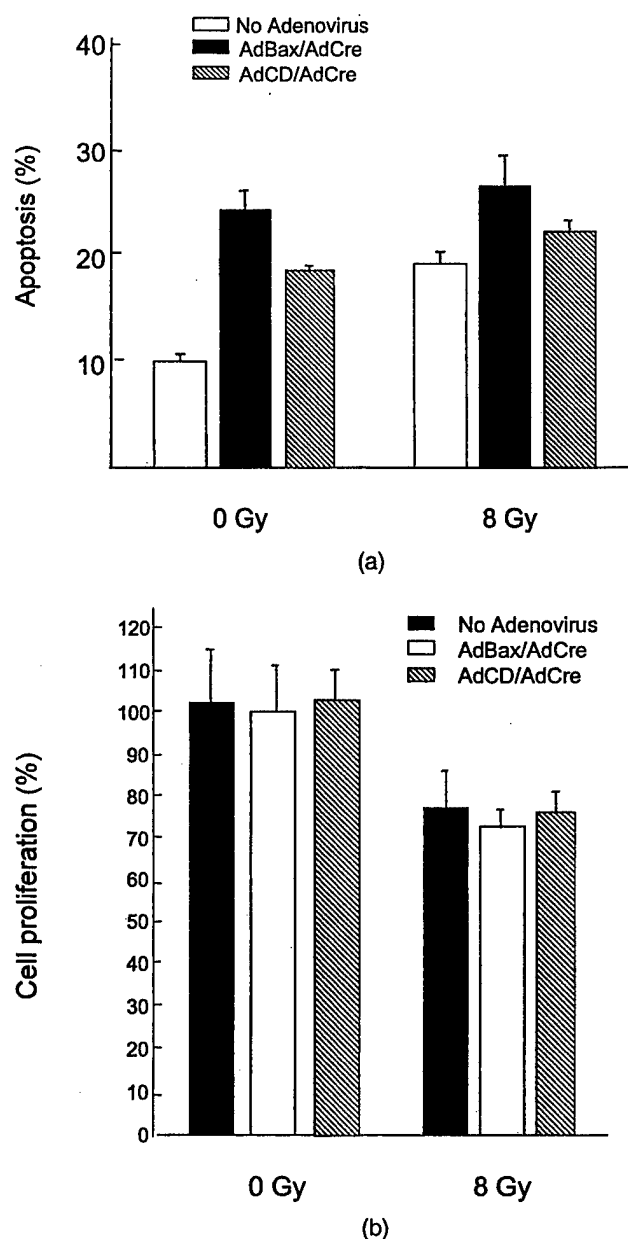


Fig. 7. Bax does not sensitize normal human astrocytes to radiation. (a) Human astrocytes (2×10^5 /well) were plated into 6-well plates and irradiated with 8 Gy of ^{60}Co irradiation or mock irradiated 5 days later. To determine apoptosis, the same experimental design described in Fig. 5A was followed, with harvest of the cells at 6 days after irradiation. As a control, cells were infected with Ad/Bax and Ad/CD. All determinations were done in duplicate. (b) A cell proliferation assay was performed with human astrocytes as described in Fig. 5B.

therapy response using genetically based treatments. In this report, we have described our evaluation of the hypothesis that transient induction of the proapoptotic gene *bax*, via recombinant adenovirus-mediated gene delivery, will sensitize glioma cells and tumors to the cytotoxic effects of radiation.

To this end, an adenovirus encoding the *bax* gene was constructed (25). This vector, based on the cre/Loxp system

(26), induces cellular expression of Bax only upon coinfection with a second inducing adenoviral vector, thus allowing the propagation of the proapoptotic *bax*-encoding virus without inducing undue toxicity in the packaging cells. The results demonstrate that this vector system robustly induced expression of Bax in glioma cell lines. Induction of Bax enhanced synergistically the cytotoxic effect of radiation in several malignant glioma cell lines. In addition, the radiosensitizing effect was confirmed in a murine model of glioblastoma. It is interesting that Bax-induced radiosensitization did not depend on the functional status of p53. Most importantly, it was observed that *bax*-encoding adenovirus does not sensitize normal astrocytes to radiation.

Several attributes of glioblastoma render this tumor an ideal target for the development of gene therapy approaches aimed to revert the resistance to conventional therapies. Specifically, glioblastoma is most often confined to the brain, where it has become readily accessible to stereotactic gene delivery via magnetic resonance imaging and computed tomographic imaging. Additionally, ample experience exists for the treatment of malignant brain tumors with radiotherapy, although durable cures are admittedly rare. Gene transfer into brain tumor cell lines using adenoviral vectors is quite efficient. Lastly, genetic lesions have been identified that are associated with resistance of glioblastomas to radiation, offering targets for gene therapy approaches (13–16, 28, 29).

Abundant evidence exists indicating that radiation induces *in vivo* upregulation of Bax and subsequent apoptosis in radiosensitive tissues (30). Based on this, we explored the ability of Bax to modify the response to chemotherapeutic and radiotherapeutic agents in cancer cells, and found evidence of its sensitizing capacity in both contexts (23, 31). These results are in accord with observations by other authors that, in glioblastomas, radioresistance is associated with the inability of tumor cells to upregulate *bax* (24). Thus, these facts established a compelling rationale for us to explore radiosensitization mediated by *bax* in the context of glioblastoma. Numerous attempts have been made previously to genetically sensitize glioblastomas in the context of radiotherapy. p53 has been extensively evaluated as a modifier of the radiosensitivity of glioblastoma (9–16, 28). Even though there is evidence of the ability of p53 to radiosensitize tumor cells, two facts probably will mitigate its use. First, not all brain tumors are mutant in p53, which is an important factor in determining the sensitizing potential of exogenous p53. Second, it is well established that the inability of p53 to upregulate *bax* contributes to the radioresistance of glioblastoma, as mentioned in this report. In contrast, when four different cell lines characterized by a different functional status of p53 were tested, it was found, as hypothesized, that all became radiosensitive after Bax induction, regardless of p53. More importantly, the radiosensitizing effect of Bax is mediated through the direct induction of apoptosis, which suggests its potential widespread effect in tumors otherwise heterogeneous for upstream or downstream components of the cell death regu-

latory pathways. In this regard, no association between the level of Bax-induced radiosensitization and the status of anti-apoptotic Bcl-2 or the endogenous level of bax was found (data not shown).

Although it has been shown that Bax does induce apoptosis in some glioma cell lines, other genes (for instance, caspase 8) have enhanced this effect (32). This fact suggests that, similar to radiation alone, *bax* itself is not powerful enough to achieve a full apoptotic response and cytotoxic effect. In accord with our goals for clinical translation, we have sought to explore the synergistic capacity of combined *bax* and radiation to treat glioblastoma more robustly. To this end, we were able to demonstrate adenoviral vector-mediated transfer and expression of Bax within cell lines and in an *in vivo* model of glioblastoma. On the other hand, the current configuration of our vector system in two viruses and the suboptimal efficiency of adenoviral vectors found in human patients can be a fundamental limitation toward the clinical application of this gene therapy approach. In this regard, the need for an inducible system is determined by

the toxicity of Bax in the vector packaging cells, as we have discussed previously. To increase the efficiency of the two-vector system, which currently requires infection of target cells by both recombinant adenoviruses, novel viral configurations have been made in our laboratory to allow *bax* gene delivery by a single vector (33). In addition, further modifications of the viral vector and its tropism may provide a substantial improvement in the levels of gene transfer (34). This, together with the favorable therapeutic index suggested by the lack of toxicity of Bax in human primary astrocytes, provides the opportunity for developing a potent radiosensitization strategy for treatment of brain tumors.

In conclusion, this study demonstrates a synergistic radiosensitizing effect of Bax in refractory glioblastoma cell lines after gene delivery via recombinant adenovirus. This result was confirmed in an *in vivo* murine xenograft model of glioblastoma. Toxicity was selectively induced in tumors, and spared normal astrocytes. Thus, the combination of *bax* gene delivery and radiotherapy might have clinical utility for the treatment of malignant brain tumors.

REFERENCES

1. Simpson JR, Horton J, Scott C, *et al.* Influence of location and extent of surgical resection on survival of patients with glioblastoma multiforme: Results of three consecutive Radiation Therapy Oncology Group (RTOG) clinical trials. *Int J Radiat Oncol Biol Phys* 1993;26:239–244.
2. Urtasun R, Feldstein ML, Partington J, *et al.* Radiation and nitroimidazoles in supratentorial high grade gliomas: A second clinical trial. *Br J Cancer* 1982;46:101–108.
3. Wen PY, Alexander E, Black PM, *et al.* Long term results of stereotactic brachytherapy used in the initial treatment of patients with glioblastomas. *Cancer* 1994;73:3029–3036.
4. Stea B, Rossman K, Kittelson J, *et al.* A comparison of survival between radiosurgery and stereotactic implants for malignant astrocytomas. *Acta Neurochir Suppl* 1994;62:47–54.
5. Whartenby KA, Abboud CN, Marrogi AJ, *et al.* The biology of cancer gene therapy. *Lab Invest* 1995;72:131–145.
6. Fueyo J, Gomez-Manzano C, Yung WK, Kyritsis AP. Targeting in gene therapy for gliomas. *Arch Neurol* 1999;56:445–458.
7. Fueyo J, Gomez-Manzano C, Yung WK, *et al.* Overexpression of E2F-1 in glioma triggers apoptosis and suppresses tumor growth in vitro and in vivo. *Nat Med* 1998;4:685–690.
8. Gomez-Navarro J, Arafat W, Xiang J. Gene therapy for carcinoma of the breast: Pro-apoptotic gene therapy. *Breast Cancer Res* 2000;2:32–44.
9. Asai A, Miyagi Y, Sugiyama A, *et al.* Negative effects of wild-type p53 and s-Myc on cellular growth and tumorigenicity of glioma cells: Implication of the tumor suppressor genes for gene therapy. *J Neurooncol* 1994;19:259–268.
10. Badie B, Drazan KE, Kramar MH, *et al.* Adenovirus-mediated p53 gene delivery inhibits 9L glioma growth in rats. *Neurol Res* 1995;17:209–216.
11. Hsiao M, Tse V, Carmel J, *et al.* Intracavitary liposome-mediated p53 gene transfer into glioblastoma with endogenous wild-type p53 in vivo results in tumor suppression and long-term survival. *Biochem Biophys Res Commun* 1997;233:359–364.
12. Badie B, Kramar MH, Lau R, *et al.* Adenovirus-mediated p53 gene delivery potentiates the radiation-induced growth inhibition of experimental brain tumors. *J Neurooncol* 1998;37:217–222.
13. Lang FF, Yung WK, Raju U, *et al.* Enhancement of radiosensitivity of wild-type p53 human glioma cells by adenovirus-mediated delivery of the p53 gene. *J Neurosurg* 1998;89:125–132.
14. Cirielli C, Inyaku K, Capogrossi MC, *et al.* Adenovirus-mediated wild-type p53 expression induces apoptosis and suppresses tumorigenesis of experimental intracranial human malignant glioma. *J Neurooncol* 1999;43:99–108.
15. Lang FF, Yung WK, Sawaya R, Tofilon PJ. Adenovirus-mediated p53 gene therapy for human gliomas. *Neurosurgery* 1999;45:1093–1104.
16. Broadus WC, Liu Y, Steele LL, *et al.* Enhanced radiosensitivity of malignant glioma cells after adenoviral p53 transduction. *J Neurosurg* 1999;91:997–1004.
17. Lang, F, Fuller, G. Preliminary results of a Phase 1 clinical trial of adenovirus-mediated p53 gene therapy for recurrent glioma: Biological studies. 2000. *Proc Am Soc Clin Oncol*, abstract 1785.
18. Oltvai ZN, Millman CL, Korsmeyer SJ. Bcl-2 heterodimerizes in vivo with a conserved homolog, Bax, that accelerates programmed cell death. *Cell* 1993;74:609–619.
19. Korsmeyer SJ, Shutter JR, Veis DJ, *et al.* Bcl-2/Bax: A rheostat that regulates an anti-oxidant pathway and cell death. *Semin Cancer Biol* 1993;4:327–332.
20. Marzo I, Brenner C, Zamzami N, *et al.* Bax and adenine nucleotide translocator cooperate in the mitochondrial control of apoptosis. *Science* 1998;281:2027–2031.
21. Sakakura C, Sweeney EA, Shirahama T, *et al.* Overexpression of bax sensitizes human breast cancer MCF-7 cells to radiation-induced apoptosis. *Int J Cancer* 1996;67:101–105.
22. Sakakura C, Sweeney EA, Shirahama T, *et al.* Overexpression of bax enhances the radiation sensitivity in human breast cancer cells. *Surg Today* 1997;27:90–93.
23. Arafat WO, Gómez-Navarro J, Xiang J, *et al.* An adenovirus encoding proapoptotic bax induces apoptosis and enhances the radiation effect in human ovarian cancer. *Mol Ther* 2000;1:545–554.

24. Shu HK, Kim MM, Chen P, *et al.* The intrinsic radioresistance of glioblastoma-derived cell lines is associated with a failure of p53 to induce p21(BAX) expression. *Proc Natl Acad Sci USA* 1998;95:14453-14458.
25. Xiang J, Piché A, Rancourt C, *et al.* An inducible recombinant adenoviral vector encoding Bax selectively induces apoptosis in ovarian cancer cells. *Tumor Targeting* 1999;4:84-91.
26. Zhang HG, Bilbao G, Zhou T, *et al.* Application of a Fas ligand encoding a recombinant adenovirus vector for prolongation of transgene expression. *J Virol* 1998;72:2483-2490.
27. Rosenfeld ME, Feng M, Michael SI, *et al.* Adenoviral mediated delivery of the herpes simplex virus thymidine kinase gene selectively sensitizes human ovarian carcinoma cells to ganciclovir. *Clin Cancer Res* 1995;1:1571-1580.
28. Li H, Alonso-Vanegas M, Colicos MA, *et al.* Intracerebral adenovirus-mediated p53 tumor suppressor gene therapy for experimental human glioma. *Clin Cancer Res* 1999;5:637-642.
29. Kerr JF, Winterford CM, Harmon BV. Apoptosis: Its significance in cancer and cancer therapy. *Cancer* 1994;73:2013-2026.
30. Kitada S, Krajewski S, Miyashita T, *et al.* Gamma-radiation induces upregulation of Bax protein and apoptosis in radio-sensitive cells in vivo. *Oncogene* 1996;12:187-192.
31. Xiang J, Gomez-Navarro J, Arafat W, *et al.* Pro-apoptotic treatment with an adenovirus encoding Bax enhances the effect of chemotherapy in ovarian cancer. *J Gene Med* 2000;2:97-106.
32. Shinoura N, Saito K, Yoshida Y, *et al.* Adenovirus-mediated transfer of bax with caspase-8 controlled by myelin basic protein promoter exerts an enhanced cytotoxic effect in gliomas. *Cancer Gene Ther* 2000;7:739-748.
33. Kaliberov S, Buchsbaum DJ, Gillespie GY, *et al.* Adenovirus-mediated transfer of Bax driven by the vascular endothelial growth factor promoter induces apoptosis in lung cancer cells. *Mol Ther* 2002;6:190-198.
34. Dmitriev I, Krasnykh V, Miller CR, *et al.* An adenovirus vector with genetically modified fibers demonstrates expanded tropism via utilization of a coxsackievirus and adenovirus receptor-independent cell entry mechanism. *J Virol* 1998;72:9706-9713.

Adenovirus-Mediated Transfer of BAX Driven by the Vascular Endothelial Growth Factor Promoter Induces Apoptosis in Lung Cancer Cells

Sergey A. Kaliberov,¹ Donald J. Buchsbaum,¹ G. Yancey Gillespie,² David T. Curiel,³ Waleed O. Arafat,³ Mark Carpenter,⁴ and Murray A. Stackhouse^{1,*}

Departments of ¹Radiation Oncology, ²Surgery, and ³Medicine, and ⁴Medical Statistics Section, University of Alabama at Birmingham, Birmingham, Alabama 35294, USA

*To whom correspondence and reprint requests should be addressed. Fax: (205) 975-7060. E-mail: mstack@uab.edu.

Apoptosis induction is a promising approach for cancer gene therapy. *Bax* is a death-promoting member of the *Bcl2* family of genes that are intimately involved in apoptosis. Overexpression of BAX protein can accelerate cell death by homodimers that promote apoptosis in a variety of cancer cell lines. The cytotoxic effect of BAX was evaluated *in vitro* by a recombinant adenovirus system expressing the human BAX gene under control of human vascular endothelial growth factor (VEGF) promoter element (AdVEGF_{BAX}). Overexpression of BAX in human lung carcinoma cells resulted in apoptosis induction, caspase activation, and cell growth suppression, none of which were observed in BEAS-2B normal human bronchial epithelial cells that do not overexpress VEGF under normoxic conditions. To examine the hypoxia responsiveness of the VEGF promoter, lung cancer cells were transiently exposed to hypoxia; this treatment increased enhanced green fluorescent protein (EGFP) expression after AdVEGFEGFP infection in both normal and cancer cell lines, and enhanced apoptosis and decreased the number of surviving cancer cells compared with the Ad/BAX plus Ad/Cre binary adenoviral system. These results suggest a possible therapeutic application of cancer-specific expression of the pro-apoptotic *Bax* gene driven by the VEGF promoter.

Key Words: apoptosis, BAX, lung cancer cells, vascular endothelial growth factor

INTRODUCTION

Tumor growth is the result of the deregulation of the balance between cell proliferation and death. This imbalance may play a critical role in the process of tumorigenesis, and inhibition of apoptosis is the main cause of this phenomenon. Apoptosis, or programmed cell death, is a physiological form of cell death that plays a central role in tissue homeostasis and in the regulation of the cell suicide program. Apoptosis is necessary to prevent several diseases, including cancer [1]. Apoptosis induction is a promising approach for cancer gene therapy. Several proteins that control programmed cell death in cancer cells have been identified [1]. The *Bcl2* family of genes is intimately involved in the mitochondria-dependent pathway of apoptosis [2]. The process of homodimerization or heterodimerization of different gene products of the *Bcl2* family forms a complex network that regulates the choice between life and death of a cell [3,4]. *Bax* is a death-promoting member of the *Bcl2* family of genes. Translocation of BAX homodimer to the mitochondria can trigger its dysfunction and activate the caspase pathway, causing

apoptotic death of mammalian cells [4]. Recent studies have shown that alterations of relative ratios of anti- and pro-apoptotic BCL2-family proteins through BCL2 overexpression and/or BAX downregulation have been correlated with poor prognosis of lung cancer patients [5-7].

The antitumor effects of the *Bax* gene have been investigated. Transfection of naked DNA encoding *Bax* to bronchioloalveolar carcinoma cells leads to death of transfected cells. However, this method of gene delivery demonstrated low-level transfection efficiency in lung cancer cell lines [8]. Another strategy employs adenoviral vectors for high-efficiency gene transfer into mammalian cells *in vitro* and *in vivo* [9,10]. Several binary adenoviral recombinant systems for *Bax* gene expression have been generated [11,12]. Potential limitations of this strategy are the requirement for cells to be infected with both adenoviruses and nonspecific expression of the proapoptotic *Bax* gene, which may restrict the clinical potential for this approach. One means by which this limitation can be overcome is to use a single adenoviral vector using *Bax* under control of a tumor-specific and/or metabolically controlled promoter element [13-15].

% EGFP-positive cells

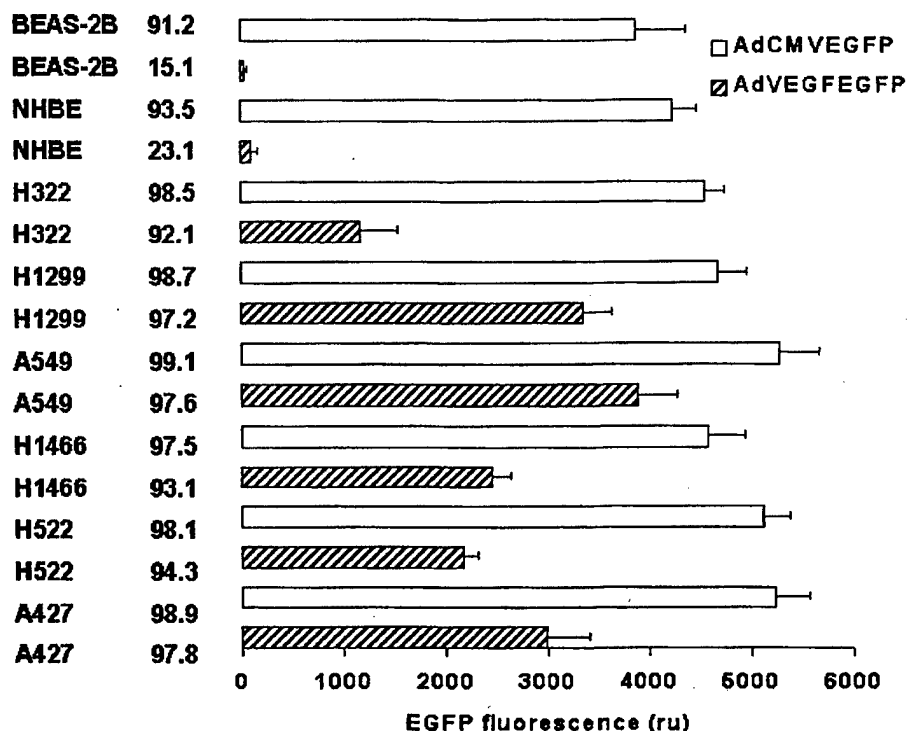


FIG. 1. EGFP expression in lung cell lines analyzed using FACS. Cells were harvested 48 hours after AdVEGFEGFP or AdCMVEGFP (5000 v.p./cell) infection. Samples (10,000 cells) were analyzed by FACSscan. EGFP fluorescence was the mean fluorescence signal in EGFP⁺ cells in ru after subtraction of background fluorescence. Data expressed as percentage of EGFP⁺ cells are the means after subtraction of uninfected control cells. Presented are mean values \pm SD of two to five independent experiments, each carried out in triplicate.

It is now well known that neovascularization, the process leading to the formation of new blood vessels, plays a critical role in the growth of both primary and metastatic tumors [16]. Tumor angiogenesis is induced by the expression of angiogenic factors in tumors that stimulate host vascular endothelial cell mitogenesis and possibly chemotaxis. One such factor, the protein VEGF, is a selective endothelial cell mitogen and angiogenic agent. Expression of VEGF is induced by several growth factors and cytokines, including elevated expression of the *ras* [17], *raf* [18], and *src* [19] oncogenes, mutant *p53* [20], and hypoxia characteristic of rapidly growing solid tumors [21]. Overexpression of VEGF has been demonstrated in cancer cells from lung [22], colon [23], breast [24], glioma [25], ovary [26], and liver [27] cancers. VEGF expression has been reported to be a negative prognostic sign in patients with lung [28], breast [29], and gastric [30] cancer.

In this study, we assessed the specificity and regulatory activity of human VEGF promoter element in human lung cancer cells. We evaluated the cytotoxic activity of a recombinant adenoviral vector encoding human BAX under control of the human VEGF promoter element. This study demonstrates the feasibility of expressing an apoptosis-promoting protein such as BAX through adenoviral gene transfer at levels that are sufficient to result in the selective death of cancer cells.

RESULTS

Induction of EGFP Expression in Human Cell Lines Infected with AdVEGFEGFP

We constructed the recombinant adenoviral vector AdVEGFEGFP, which harbors the EGFP gene under the control of the human VEGF promoter sequence. For initial determination of transduction efficiency and specificity of VEGF promoter-driven EGFP expression, several human lung cell lines were infected with AdVEGFEGFP or AdCMVEGFP recombinant adenoviruses. Cells were harvested 48 hours after infection, and EGFP expression was analyzed by fluorescence-activated cell sorting (FACS). Lung cancer cells demonstrated high levels of EGFP expression after infection with both AdVEGFEGFP and AdCMVEGFP adenoviral vectors (Fig. 1). However, the level of expression was lower by 1.4- to 3.8-fold in cells infected with AdVEGFEGFP. In contrast, NHBE and BEAS-2B normal human bronchial epithelial cells demonstrated elevated levels of EGFP expression and percentage of positive cells following AdCMVEGFP infection in comparison with AdVEGFEGFP. For subsequent experiments, we used BEAS-2B normal cells and A549, H522, H1466, and A427 lung cancer cell lines that demonstrated the highest levels of EGFP expression after AdVEGFEGFP infection.

These data correlated with VEGF expression in the human lung cell lines. The expression of the VEGF protein

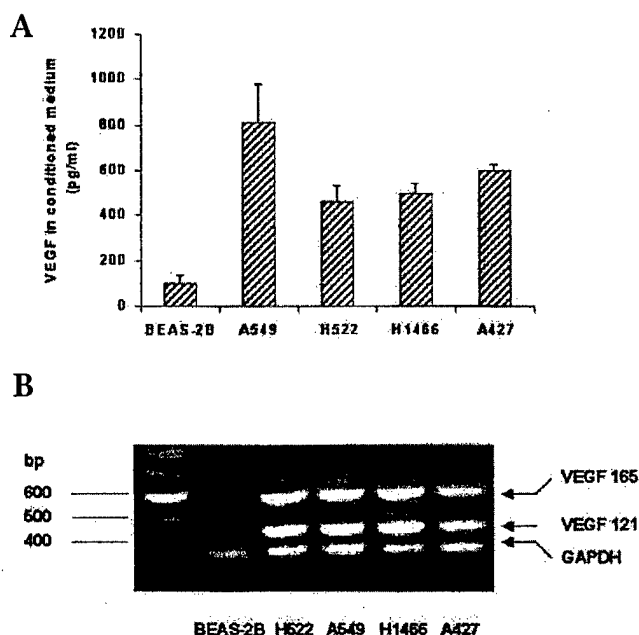


FIG. 2. VEGF protein and mRNA expression in lung cell lines. (A) The level of expression of VEGF protein was examined using ELISA. VEGF concentrations in conditioned media of the indicated cell lines were normalized to number of viable cells. Presented are mean values \pm SD of experiments that were carried out in duplicate cultures in two separate experiments. (B) Analysis of VEGF mRNA transcripts by RT-PCR using primers specific for all known isoforms. The size of the indicated bands of 441 and 573 bp was determined by a 100-bp DNA ladder and correspond to VEGF₁₂₁ and VEGF₁₆₅, respectively. One representative of three different experiments is shown.

was examined using an enzyme-linked immunosorbent assay (ELISA) of conditioned media of cells grown under normoxic conditions (Fig. 2A). Lung cancer cells demonstrated high levels of VEGF secretion in comparison with normal lung cells BEAS-2B. Expression of VEGF protein was associated with detectable levels of VEGF mRNA expression in lung cancer cell lines (Fig. 2B). The human glyceraldehyde 3-phosphate dehydrogenase (GAPDH) cDNA was used as an internal standard for template loading in PCR.

Induction of BAX Protein Expression Causes Cancer Cell Death

For evaluation of the biological activity of recombinant Bax, we infected BEAS-2B, H1466, and A427 cells with the different recombinant adenoviral vectors AdVEGF_{Bax} (expressing BAX under VEGF promoter element control) or Ad/BAX plus Ad/Cre (expressing BAX under inducible control, using the β -actin promoter) for various multiplicities

of infection (Fig. 3A). AdVEGF_{Bax} decreased the number of viable H1466 and A427 lung cancer cells as compared with BEAS-2B, whereas infection of cells using Ad/BAX plus Ad/Cre caused death of both lung cancer and normal cells, as measured by 3-(4,5-dimethylthiazol-2-yl)-5-(3-carboxymethoxyphenyl)-2-(4-sulfophenyl)-2H-tetrazolium, inner salt (MTS) assay (Fig. 3A).

Cell death could be detected as early as 24 hours after AdVEGF_{Bax} infection of H1466 lung cancer cells and affected nearly 90% of cells (for 5000 viral particles (v.p.)/cell) within 48 hours (Fig. 3B). The time course of cell death correlated with the time course of BAX-HA expression, which was detected as early as 12 hours after infection and reached a peak at 24–48 hours (Fig. 3C). Similar results were obtained with H522 cells (data not shown).

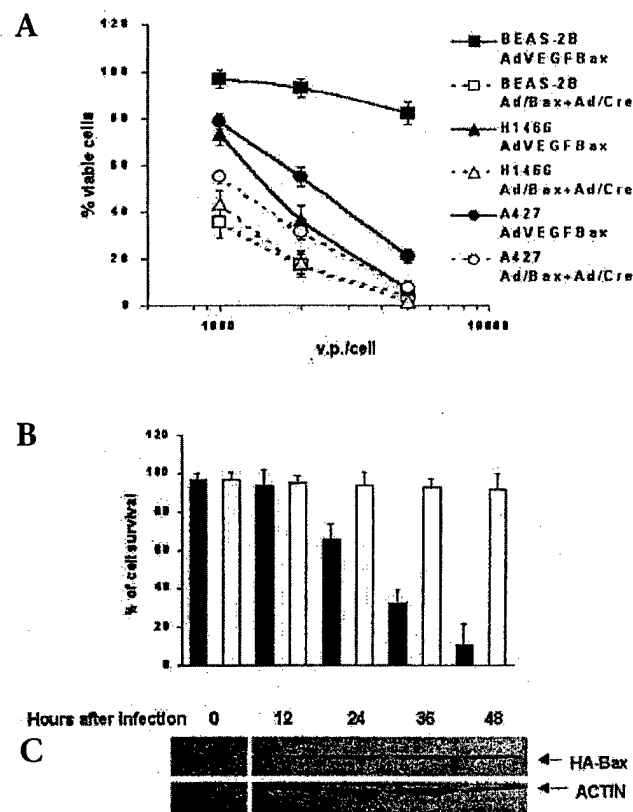


FIG. 3. AdVEGF_{BAX} preferentially induces death in lung cancer cells. (A) Normal human bronchial epithelium cells (BEAS-2B) and lung carcinoma (H1466 and A427) cells were infected with the recombinant adenoviruses as indicated. Cell viability was determined at 96 hours after infection by using the MTS assay. Data shown are mean values \pm SD of three experiments. (B) Induction of BAX protein expression causes lung cancer cell death. Cell viability after infection (5000 v.p./cell) of H1466 cells with AdVEGF_{BAX} (closed columns) or AdVEGF_{GFP} (opened columns) was determined using Trypan Blue exclusion. The data show mean values \pm SD of three experiments. (C) The level of expression of HA-BAX and β -actin was examined using a western blot technique. After AdVEGF_{BAX} infection (5000 v.p./cell), H1466 cells were collected at the times indicated. Equal amounts (50 μ g) of protein were loaded for each sample in all lanes and electrophoretically separated on 12% SDS-PAGE followed by transfer to a PVDF membrane. One representative of three different experiments is shown.

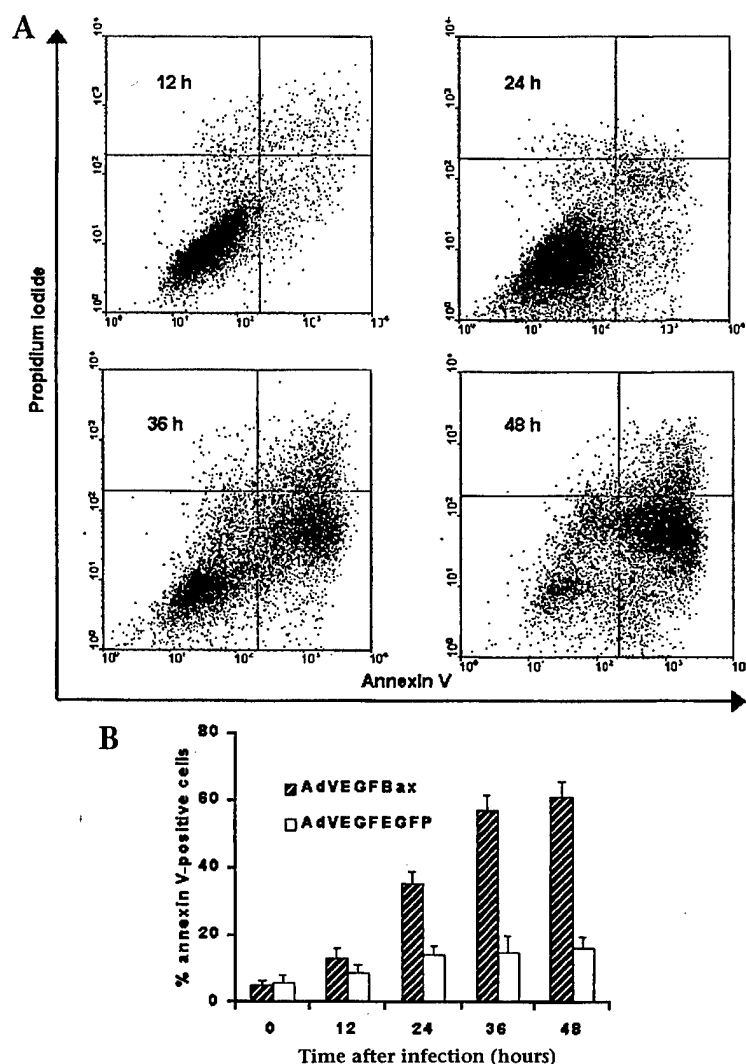


FIG. 4. Apoptosis profile of H1466 cells after AdVEGFBAX infection. (A) For annexin-V binding assay and propidium iodide (PI) uptake evaluation, after AdVEGFBAX or AdVEGFEGFP infection (5000 v.p./cell) cells were collected over time as indicated and double-stained with FITC-conjugated annexin-V and PI. One representative of three different experiments is shown. (B) All cells taking vital dye PI were considered necrotic, annexin V⁺ cells were considered apoptotic, and only cells in the lower right quadrant were used for calculation of percentages from the total number of cells. Samples (10,000 cells) were analyzed by FACScan. Data points are the mean values \pm SD of two or three experiments, each conducted in triplicate.

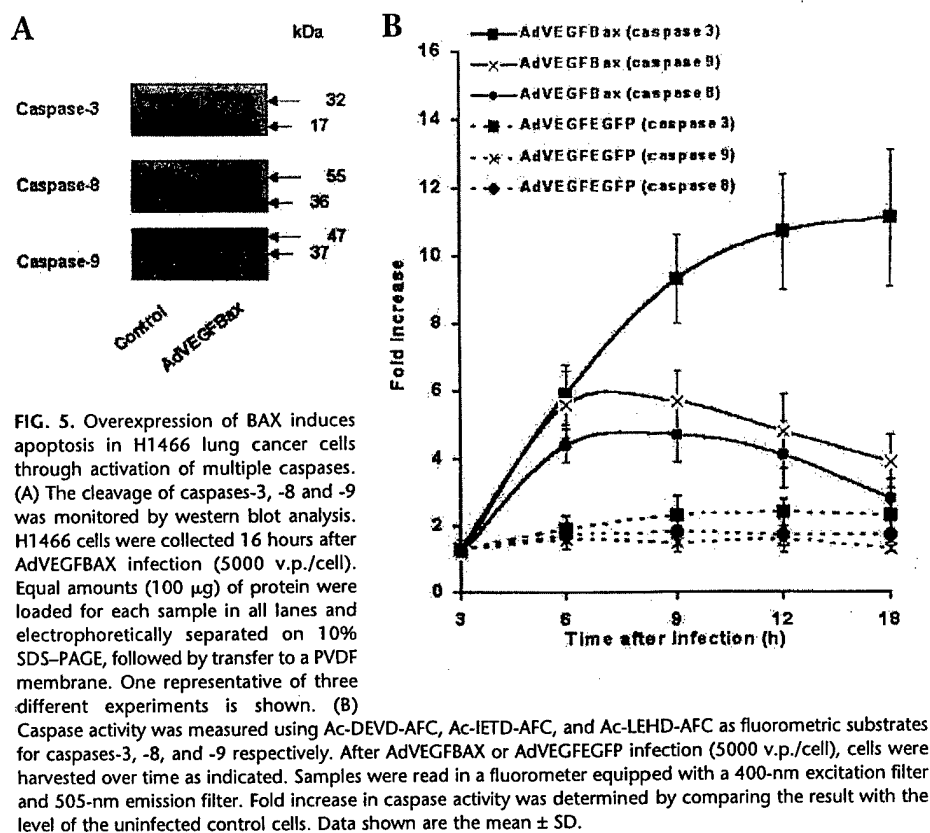
after infection with AdVEGFBAX (Fig. 4B). At 24 hours annexin-V⁻ cells had decreased, and subsequently the two types of positive (annexin-V⁺ and PI⁺) cells had increased. The results indicate that AdVEGFBAX rapidly induced apoptosis and then necrosis at a later time.

Activation of a family of cysteine aspartyl-specific proteases is intimately associated with apoptosis regulation. Enzymatic activation of initiator caspases (that is, caspases-8 and -9) leads to proteolytic activation of effector caspases (that is, caspase-3) and cleavage of a number of proteins in the apoptosis pathway [1]. Caspases are synthesized as inactive proenzymes that are processed in cells undergoing apoptosis by self-proteolysis and/or cleavage by another protease. Western blot analysis of cellular proteins using antibodies against caspases that can detect both unprocessed proenzyme and active forms of caspases demonstrated caspase-3, -8, and -9 activation in H1466 lung cancer cells after AdVEGFBAX infection (Fig. 5A). For each caspase, three independent experiments were carried out in triplicate cultures and normalized for protein. Statistical analyses were conducted on the mean triplicate value from each

experiment. The activation of caspases-3, -8, and -9 was examined after exposure of H1466 lung cancer cells to AdVEGFBAX, using Ac-DEVD-AFC, Ac-IETD-AFC, and Ac-LEHD-AFC as substrates. Figure 5B summarizes the results for caspases-3, -8, and -9. To examine differences across time for each caspase, ANOVA (an analysis of variance) was conducted and summarized herein. There was a time-dependent increase of caspase-3 activity that was evident at 6 hours (Fig. 5B), and increased amounts of caspase-3 were detected at 12–18 hours, in comparison with caspases-8 and -9, which reached a peak of activity at 6–9 hours after AdVEGFBAX infection. For caspase-3, there were significant differences across time for those cells infected with AdVEGFBAX ($P < 0.001$). Multiple comparisons showed that caspase-3 activity at 3 hours was significantly less than at 6, 9, 12, and 18 hours, and there was a significant increase from 6 hours to 12 and 18 hours but no significant difference in caspase-3 activity between 9, 12, and 18 hours. For caspase-8, there were significant

Apoptosis Profile after AdVEGFBAX Treatment

To confirm that AdVEGFBAX induces apoptosis, H1466 cells were stained with both propidium iodide (PI) and fluorescein isothiocyanate (FITC)-labeled annexin-V, which preferentially binds to phosphatidylserine residues. The exposure of phosphatidylserine on the outside of the plasma membrane is an early event characteristic of the apoptotic process, preceding the loss of integrity of the plasma membrane. Combined staining with fluorescein-conjugated annexin-V and PI distinguishes between early (annexin-V⁺ and PI⁻) and late apoptotic cells (annexin-V⁺ and PI⁺) [31]. The cells were analyzed by flow cytometry (Fig. 4A). Cells taking vital dye PI were considered necrotic, while annexin-V⁺ and PI⁻ cells were considered apoptotic, and their percentages were calculated. Nontreated control cells were annexin-V⁻, and annexin-V⁺ cells did not increase at 48 hours after exposure to 2500 v.p./cell of AdVEGFEGFP. In contrast, an increase in annexin-V⁺ cells was observed at 24–48 hours compared with control cells



differences across time for H1466 lung cancer cells infected with AdVEGF_{BAX} ($P = 0.001$), but multiple comparisons demonstrated that this was due to the difference between 3 hours versus all other time points with no significant differences between the 6-, 9-, 12-, and 18-hour time points. Similarly, for caspase-9, there were significant differences across time for cells infected with AdVEGF_{BAX} ($P = 0.001$), but multiple comparisons showed that this was due to the difference between 3 hours versus all other time points, with no significant differences between the 6-, 9-, 12-, and 18-hour time points. There were no AdVEGF_{FEGFP}-induced changes in caspase-3, -8, or -9 activity, in contrast to the case of AdVEGF_{BAX} treatment. Similar results were obtained with H522 cells (data not shown). The data shown in Figs. 4 and 5 demonstrate that apoptosis induced by AdVEGF_{BAX} in lung cancer cells is associated with activation of caspases-3, -8, and -9.

AdVEGF_{BAX} Enhances Lung Cancer Cell Death Under Hypoxic Conditions

Most solid tumors have areas of low oxygen tension. Expression of VEGF is induced in cells exposed to hypoxia [32]. Hypoxia for 16 hours increased levels of secreted VEGF in the conditioned medium (Fig. 6A) of cancer cells (1.8- to 4.5-fold induction), as well as in normal human bronchial epithelial cells (3.2-fold; Fig. 6B). For determination of the

response of the VEGF promoter to hypoxic conditions, we infected BEAS-2B cells with AdVEGF_{FEGFP}. The cells were exposed to hypoxia for 18 hours and, after 4 hours of reoxygenation, were examined for EGFP expression by fluorescent microscopy. After culturing BEAS-2B cells under hypoxic conditions, EGFP expression was increased (Fig. 6C). FACS analysis also confirmed these results for BEAS-2B and A549 cells (Fig. 6D). For the A549 cancer cell line, there was a significantly greater EGFP expression for cells infected with AdVEGF_{FEGFP} under hypoxic versus those under normoxic conditions ($P = 0.05$), but no significant difference between those cells infected with AdCMVEGF_{FEGFP} under normoxic versus hypoxic conditions ($P = 0.2$). For the BEAS-2B lung cell line, there was a significantly greater EGFP expression for cells infected with AdVEGF_{FEGFP} under hypoxic conditions in contrast to those under normoxia ($P = 0.05$), but no significant differences between cells infected with AdCMVEGF_{FEGFP} under

normoxia in contrast to conditions of low oxygen tension ($P = 0.2$). The A549 human lung cancer cells had greater EGFP expression than the BEAS-2B human lung cells under all treatment conditions ($P = 0.05$). Infection with AdVEGF_{FEGFP} at 6000 v.p./cell did not induce EGFP expression in BEAS-2B cells under conditions of normal oxygen tension. These results demonstrate the specificity of VEGF promoter-driven EGFP expression.

To test whether VEGF promoter-regulated BAX expression is able to modulate cell death under hypoxic conditions, A549 and BEAS-2B lung cells after AdVEGF_{BAX} infection were exposed to hypoxia for 72 hours. A two-factor ANOVA with an interaction term was used to analyze these data. As shown in Fig. 7A and confirmed by the analysis, there was a significant reduction in mean cell viability in both cell lines A549 ($P < 0.001$) and BEAS-2B ($P < 0.001$) exposed to hypoxic conditions. In addition, there was a significant reduction in mean cell viability in the A549 lung cancer cells as compared with the BEAS-2B lung cells under both hypoxic and normoxic conditions ($P < 0.001$), and A549 lung cancer cells were more sensitive to AdVEGF_{BAX} treatment after incubation under conditions of low oxygen tension (O_2 , 1%), as measured by MTS assay (interaction $P = 0.005$). To confirm that AdVEGF_{BAX} induces apoptosis under hypoxia, A549 and BEAS-2B cells were stained with both PI and FITC-labeled

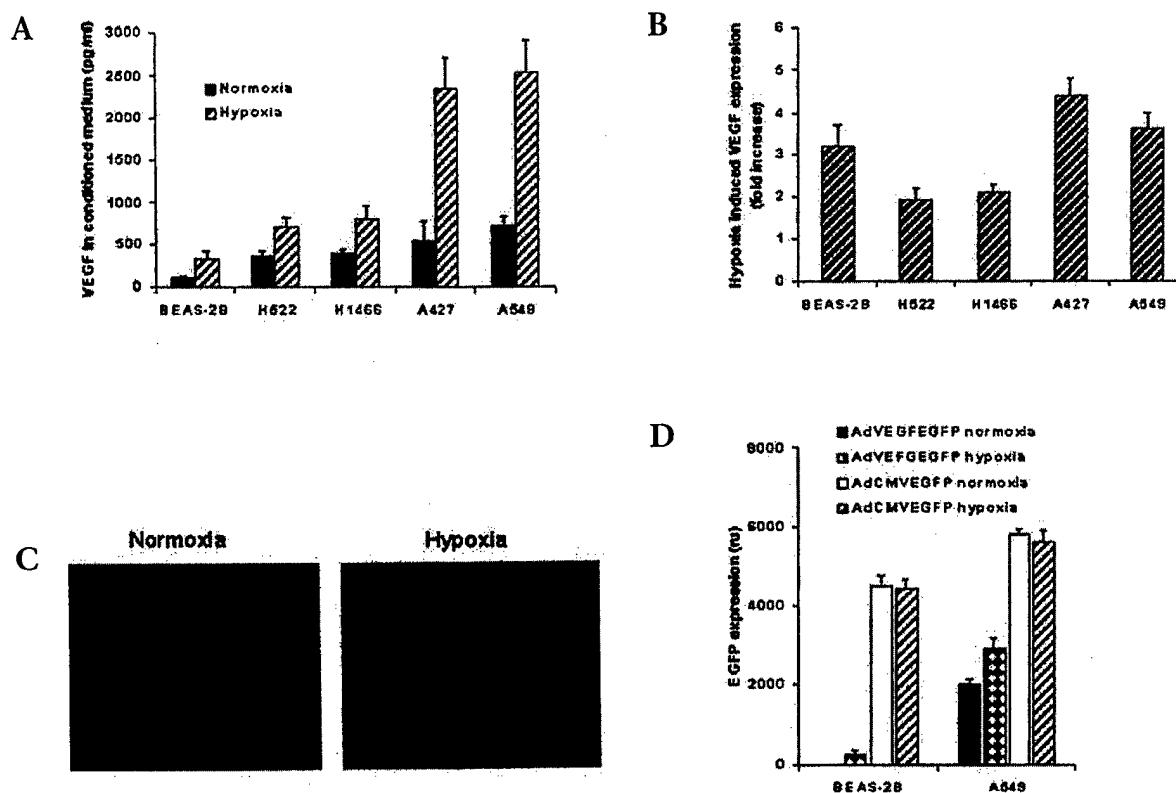


FIG. 6. Effect of hypoxic conditions on VEGF protein expression. (A) VEGF-specific ELISA was used to determine VEGF concentrations in conditioned media of the human lung cell lines incubated under normoxic (O_2 , 21%) or exposed to hypoxic (O_2 , 1%) conditions for 16 hours and normalized to number of viable cells. (B) Fold increase protein concentration was determined by comparing VEGF concentration in conditioned media after incubation under hypoxia with the level of the VEGF protein secretion under normoxic conditions. Data presented are mean values \pm SD of two separate experiments. The VEGF promoter response to hypoxic conditions is determined. (C) For determination of response of VEGF promoter element to hypoxic conditions, following infection with AdVEGFEGFP (6000 v.p./cell), BEAS-2B human lung cells were cultured under normoxic (O_2 , 21%) or exposed to hypoxic (O_2 , 1%) conditions for 18 hours and after reoxygenation for 4 hours examined for EGFP expression by fluorescent microscopy. Original magnification was $\times 100$. (D) At the same time points after AdVEGFEGFP infection, BEAS-2B and A549 cells were harvested and samples (10,000 cells) were analyzed by FACSscan. EGFP fluorescence was the mean fluorescence signal in EGFP⁺ cells in ru after subtraction of background fluorescence. Data presented are mean values \pm SD of three separate experiments.

annexin-V, and the samples were analyzed by flow cytometry (Fig. 7B). A two-factor ANOVA with an interaction term was used to analyze these data. There was significantly greater mean apoptosis for those cells under hypoxic versus normoxic conditions in both cell lines, A549 ($P < 0.001$) and BEAS-2B ($P < 0.001$). In addition, there was significantly greater apoptosis in the A549 cell line than in the BEAS-2B cell line ($P < 0.001$), and the A549 lung cancer cells were more sensitive to AdVEGFBAX treatment after incubation under conditions of low oxygen tension (interaction $P = 0.004$). These data demonstrated that AdVEGFBAX can enhance cancer cell death through increasing apoptosis under hypoxic conditions.

DISCUSSION

Tumor targeting is one of the most important goals of cancer gene therapy. Different approaches have been used to attain selective and regulated expression of therapeutic

genes. For instance, selective gene expression can be achieved through transcriptional regulation using tumor-specific promoter elements. Another regulatory strategy is metabolite-specific responsive gene therapy. In this case, transgene expression is regulated by endogenous mechanisms in such a way that production of a desired protein correlates with a physiological stimulus [33]. Although the use of BAX protein overexpression for apoptosis induction or VEGF promoter for driving therapeutic gene expression in cancer cells has been described, this is the first report of a physiologically regulated single adenoviral vector that can be used to target BAX gene expression to cancer cells. Furthermore, our results demonstrate the potential to regulate this gene expression system through conditions of low oxygen tension. In the present study, the selectivity of EGFP or human BAX expression was achieved through use of the human VEGF promoter element in human lung cancer cells that expressed high levels of VEGF mRNA and protein [28].

For screening VEGF promoter activity, several human

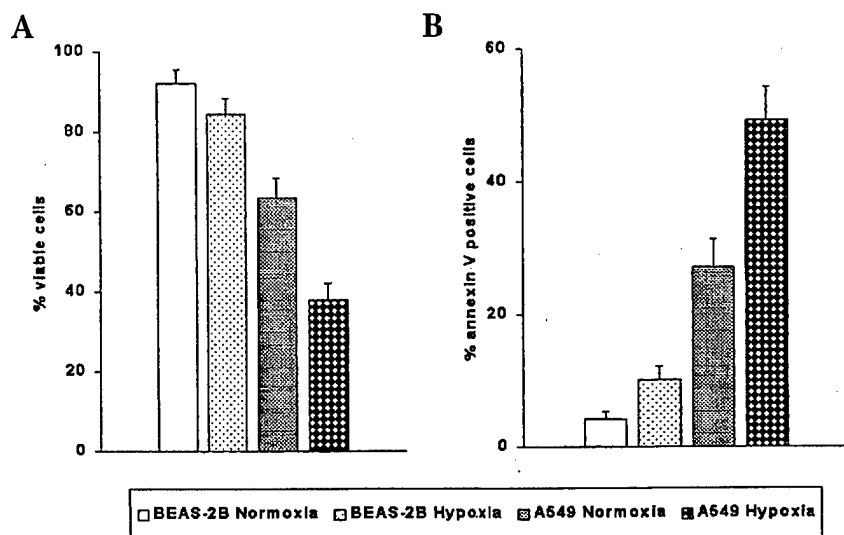


FIG. 7. AdVEGF BAX enhances lung cancer cell death through increasing apoptosis under hypoxic conditions. (A) BEAS-2B and A549 lung cells after AdVEGF BAX (5000 v.p./cell) infection were exposed to hypoxic (O_2 , 1%) or cultured under normoxic (O_2 , 21%) conditions for 72 hours, and cell viability was determined using the MTS assay. Each bar represents the mean values \pm SD of three experiments. (B) After infection with 5000 v.p./cell AdVEGF BAX, A549 and BEAS-2B cells were cultured under normoxic (O_2 , 21%) or exposed to hypoxic (O_2 , 1%) conditions for 48 hours and after reoxygenation for 4 hours were examined for annexin-V binding and PI uptake. Cells were collected and double-stained with FITC-conjugated annexin-V and PI. Cells taking up vital dye PI were considered necrotic; annexin-V⁺ cells were considered apoptotic and their percentages were calculated. Samples (10,000 cells) were analyzed by FACScan. Data expressed as percentage of annexin-V⁺ cells are the means after subtraction of uninfected control. Data presented are the mean values \pm SD of three independent experiments.

lung cell lines were infected with AdVEGFEGFP. Lung cancer cells showed increased levels of EGFP expression in comparison with normal lung cells, which had high levels of EGFP expression driven by the vector with the cytomegalovirus (CMV) promoter. Additionally, lung cancer cells were more sensitive to AdVEGF BAX treatment, because overexpression of BAX induced apoptosis and decreased cell growth in these cells. Thus, specific gene expression under control of the VEGF promoter can be useful for gene therapy of a variety of cancers.

Tumor nodules larger than 1–2 mm ($\sim 10^6$ cells) in diameter have areas of low oxygen tension. These conditions result in the induction of neovascularization by angiogenesis from the surrounding host tissue blood vessels. VEGF expression has been observed in most tumors, especially in hypoxic areas [32,34]. VEGF gene transcription is activated in hypoxic cells through interaction of the hypoxia-inducible factor-1 (HIF-1) with binding sites of the hypoxia-responsive element (HRE) in the 5'-flanking promoter region [35]. In recent studies, a new nonviral, hypoxia-responsive vector encoding luciferase reporter gene and the HRE of human VEGF promoter was developed [36].

We infected cells with AdVEGFEGFP for *in vitro* determination of response of VEGF promoter to hypoxic

conditions. The lung cells demonstrated upregulated levels of EGFP expression under hypoxic conditions after 4 hours of reoxygenation. Infection with AdVEGFEGFP at the highest titer used in these experiments did not induce EGFP expression in BEAS-2B lung cells under conditions of normal oxygen tension. These results demonstrate the specificity of VEGF promoter-driven EGFP expression. On the other hand, hypoxic conditions enhanced apoptosis and lung cancer cell death caused by BAX overexpression following AdVEGF BAX infection.

Koshikawa *et al.* showed the therapeutic effect of a retroviral vector harboring the suicide gene herpes simplex virus thymidine kinase under the control of mouse VEGF promoter in A11 lung cancer carcinoma cells [32]. Hypoxic environment increased cytosine deaminase gene expression driven by a HRE [37].

We used a single adenoviral vector to evaluate the anticancer activity of BAX expression driven by the VEGF promoter element in lung cancer cell lines *in vitro*. Recently, several loss-of-function mutations have been identified in the BAX genes of human tumors [38], and analysis of Bax-

mutant mice indicates that BAX is a tumor suppressor *in vivo* [39]. Transcription of Bax is also directly regulated by p53, thus providing another connection of this important tumor suppressor to apoptosis pathways [40]. Our results demonstrate that overexpression of exogenous BAX protein can induce apoptosis in lung cancer cells, through activation of both caspases-8 and -9, which leads to activation of downstream caspase-3. Several obstacles to adenoviral gene transfer could limit the effectiveness of BAX overexpression controlled by the VEGF promoter element. Although the use of the VEGF promoter has permitted selective expression of BAX in human lung cancer cells, nontargeted adenoviral transport to liver might occur *in vivo*. Several reports have shown that levels of VEGF expression in normal liver are significantly less as compared with hepatocellular carcinoma [41] or cirrhotic liver [42]. However, further studies are required to investigate hepatotoxicity with AdVEGF BAX *in vivo*.

We have shown that overexpression of BAX leads to apoptosis in lung cancer cell lines, but not normal cell lines. Furthermore, the results demonstrated that the regulatory activity of the human VEGF promoter in lung cancer cells led to increased levels of apoptosis and growth suppression under hypoxic conditions.

MATERIALS AND METHODS

Cell cultures. All cell lines, except NHBE 6043NRA cells, were originally obtained from the American Type Culture Collection (ATCC, Rockville, MD). The normal human bronchial epithelial NHBE 6043NRA cells were obtained from Clonetics (San Diego, CA). The normal human bronchial epithelial adenovirus-12-simian virus-40 (SV40) virus hybrid-transformed BEAS-2B and normal human bronchial epithelial NHBE 6043NRA cells were grown in bronchial epithelial growth medium (Clonetics). Human lung cancer A427, A549, H322, H522, and H1466 cells were maintained in RPMI 1640 medium with 10% feline bovine serum (FBS); the human embryonic kidney 293 cells were grown in Dulbecco's modified Eagle's medium (DMEM) with 10% FBS. All cells were maintained at 37°C in a humidified atmosphere with 5% CO₂ (normoxia). For induction of hypoxia, cells were placed in a specially designed chamber (PLASandLABS, Lansing, MI) flushed with a blood gas mixture contain 5% CO₂ and 95% N₂; hypoxic conditions (1% O₂) were confirmed and maintained using a gas oxygen controller PRO:OX-100 (Reming Bioinstruments, Redfield, NY).

Adenoviral vectors. Recombinant adenoviral vectors encoding hemagglutinin (HA)-tagged human BAX- α and enhanced green fluorescent protein (EGFP; Clontech) under the control of the human VEGF promoter element were constructed using a method reported earlier [43]. Briefly, the fragment containing cDNA encoding the EGFP gene with the VEGF promoter was removed from pEGFP/VEGFpro plasmid (a gift from J. A. Forsythe, The Johns Hopkins University, Baltimore, MD) by restriction enzyme digestion, then blunted and cloned into a promoterless plasmid pShuttle to generate the pShuttleVEGFEGFP. To obtain pBax/VEGFpro, plasmid cDNA encoding the HA-BAX gene was isolated from pRc/CMV/Bax plasmid (provided by J. Xiang, University of Alabama at Birmingham, Birmingham, AL), filled in by Klenow fragments, and ligated with blunted VEGFpro segment of pEGFP/VEGFpro plasmid, which was digested and EGFP cDNA removed before cloning. The fragment including HA-BAX cDNA and the VEGF promoter was replaced from the pBax/VEGFpro plasmid, then blunted and cloned into a plasmid pShuttle (Quantum Biotechnologies, Montreal, PQ, Canada) to generate the pShuttleVEGFBAx. The inserts were confirmed by PCR analysis, restriction enzyme mapping, and partial sequencing analysis. The resulting plasmids were linearized and cotransfected with pAdEasy-1 plasmid (Quantum Biotechnologies) into *Escherichia coli* BJ5183 bacteria. Recombinant clones were confirmed by PCR analysis, linearized, and transected into 293 cells using the Effectene lipid-based transfection method (Qiagen, Chatsworth, CA) to generate AdVEGFBAx or AdVEGFEGFP. Each recombinant adenovirus was isolated from a single positive plaque and passed through three rounds of plaque purification and subsequently confirmed by PCR and restriction enzyme analysis as described [44]. AdCMVEGFP was provided by D. L. Della Manna (University of Alabama at Birmingham). The inducible Cre-loxP system, which consists of Ad/BAX and Ad/Cre adenoviruses, was provided J. Xiang (University of Alabama at Birmingham). All viruses were propagated in 293 cells, purified by ultracentrifugation in a cesium chloride gradient, and subjected to dialysis. Viral titer was measured by a standard plaque assay using 293 cells and by absorbance of the dissociated virus at A_{260nm}. Titers for subsequent experiments were viral particles (v.p.) per milliliter determined by A_{260nm}. Viral preparations had ratios of v.p. to plaque-forming units (pfu) between 50:1 and 100:1.

Flow cytometry analysis of apoptosis. Annexin-V binding and propidium iodide (PI) uptake were used for apoptosis evaluation. Cells were collected at different time points and double-stained with FITC-conjugated annexin-V and PI for 15 minutes at room temperature. Annexin-V and PI were added according to the manufacturer's recommendations (BioVision, Palo Alto, CA). Samples were immediately analyzed by FACSscan. Annexin-V and PI emissions were detected in the FL-1 (530/30 nm) and FL-2 (585/40 nm) channels, respectively. For each sample, data from ~10,000 cells were recorded in list mode on logarithmic scales. Analysis was conducted with the Cell Quest software (Becton Dickinson, San Jose, CA) on cells characterized by forward/side scatter (FSC/SSC) parameters. Cell debris characterized by a low FSC/SSC was excluded from analysis. Annexin-V⁺ and PI⁺ cells were considered apoptotic, while cells that were only PI⁺ were considered necrotic. The percentage of apoptotic cells was calculated.

EGFP expression assays. Cellular EGFP expression was quantitatively examined by FACS analysis and visualized using fluorescence microscopy. After AdVEGFEGFP or AdCMVEGFP infection, cells were collected at different time points, and ~10,000 cells were illuminated at 488 nm and fluorescence detected in the FITC (525/20-nm) channel. Nonspecific fluorescence was detected using a 575/30-nm emission filter in the PI channel. EGFP fluorescence is the mean fluorescence signal in EGFP⁺ cells in relative units (ru) after subtraction of background fluorescence. An inverted-system microscope Olympus IX70 (Olympus America, Melville, NY) was used for screening of EGFP expression in cell monolayers. We detected increased levels of EGFP expression after exposure of cells to conditions of low oxygen tension for 18 hours followed by culturing under normoxia for 4 hours.

Cell viability assays. Viability after infection with different adenoviral vectors was determined using the 3-(4,5-dimethylthiazol-2-yl)-5-(3-carboxymethoxyphenyl)-2-(4-sulfophenyl)-2H-tetrazolium, inner salt (MTS) assay according to the manufacturer's instructions (Promega, Madison, WI). Cell viability was also evaluated using Trypan Blue (Life Technologies, Grand Island, NY). Trypan blue⁺ cells were considered dead, and the percentage of dead cells was calculated among the total cell number (at least 200 cells). Cells were counted using a hemacytometer.

Caspase activity assay. Caspase activity was measured using *N*-acetyl-Asp-Glu-Val-Asp-aminofluoro coumarine (Ac-DEVD-AFC), *N*-acetyl-Ile-Glu-Thr-Asp-aminofluoro coumarine (Ac-IETD-AFC) and *N*-acetyl-Leu-Glu-His-Asp-aminofluoro coumarine (Ac-LEHD-AFC) as fluorometric substrates for caspase-3, -8, and -9, respectively (BioVision). Cells were resuspended on ice in cell lysis buffer. The protein concentration in the samples were determined by the Biuret method using the BCA Protein Assay Kit (Pierce, Rockford, IL). A 50- μ g aliquot of cell lysate was added to (1:1 vol/vol) 2 \times reaction buffer containing 10 mM dithiothreitol and AFC-conjugated substrates (50 μ M final concentration) and incubated at 37°C for 2 hours. The optical density was measured in a VersaFluor fluorometer (Bio-Rad, Hercules, CA) equipped with a 400-nm excitation and 505-nm emission filters. Fold increase in caspase activity was determined by comparing the fluorescence of a treated sample with the level of the uninduced control.

Western blot analysis. The level of BAX-HA protein expression and the cleavage of caspases were examined by immunoblotting technique. Briefly, cells were collected, washed in Dulbecco's phosphate buffered saline (PBS), and homogenized in ice-cold lysis buffer (50 mM Tris-HCl, 150 mM NaCl, 2 mM EDTA, 1% IGEPAL CA-630; Sigma, St. Louis, MO). The homogenate was centrifuged at 14,000g for 15 minutes at 4°C. The protein concentration in the supernatant was determined by the Biuret method using the BCA Protein Assay Kit (Pierce). Each sample was denatured for 5 minutes at 100°C in loading buffer. Equal amounts of protein were loaded for each sample in all lanes and electrophoretically separated on SDS-PAGE followed by transfer to a polyvinylidene difluoride (PVDF) membrane (Millipore, Bedford, MA). The membrane was blocked with 2% nonfat milk (Bio-Rad) in TBS (135 mM NaCl, 2.5 mM KCl, 25 mM Tris-HCl, pH 7.5). BAX-HA was detected using specific anti-HA mouse monoclonal antibody (Boehringer Mannheim, Indianapolis, IN) and goat anti-mouse Ig(H+L)-HRP secondary antibody (Southern Biotechnology Associates, Birmingham, AL). Caspases-8 and -9 were detected using specific mouse monoclonal antibodies (BD PharMingen, San Diego, CA) and goat anti-mouse Ig(H+L)-HRP secondary antibody (Southern Biotechnology Associates). Caspase-3 was detected using polyclonal rabbit antiserum (BD PharMingen) and goat anti-rabbit Ig-HRP secondary antibody (Southern Biotechnology Associates). β -Actin protein, expression of which was used as a loading control, was detected using goat anti-actin polyclonal IgG and bovine anti-goat IgG-HRP secondary antibody (Santa Cruz Biotechnology, Santa Cruz, CA). The membrane was processed and treated with HRP color development reagent (Bio-Rad).

Measurement of VEGF protein in cell culture supernatant. For generation of conditioned medium after overnight incubation under normoxic conditions, cells were washed with Dulbecco's PBS, and serum-free medium was added. Cell culture supernatant aliquots were collected after 16 hours of normoxic or hypoxic incubation, centrifuged to remove floating cells, and stored at -20°C. VEGF concentrations were assessed by using

quantitative ELISA (R&D Systems, Minneapolis, MN) following the manufacturer's instructions. The raw VEGF data were normalized according to the number of viable cells in each sample, as determined by using trypan blue (Life Technologies) staining. Cells were counted using a hemacytometer.

RNA preparation and RT-PCR. The levels of VEGF mRNA were determined by RT-PCR. Total RNA was extracted from 10⁷ animal cells using RNeasy Mini Kit (Qiagen, Valencia, CA) following standard protocol, and quantified spectrophotometrically using an MBA 2000 spectrophotometer (Perkin Elmer, Wellesley, MA). cDNA was synthesized by using random hexamer primers and Omniscript RT kit (Qiagen). The first-strand cDNA was used as the template for PCR. For amplification of cDNA encoding VEGF, the following primers were used: VEGF forward, 5'-ATGAACCTTCT-GCTGTCTTGG-3'; VEGF reverse, 5'-TCACCGCCTCGGCTTGT-3'. The human GAPDH cDNA was used as an internal standard for template loading of PCR by using primers 5'-TCCCATCACCATTCTCCA-3' (GAPDH forward) and 5'-CATCAGCCACAGTTTCC-3' (GAPDH reverse). PCR was done under the following conditions: 20 cycles of 95°C for 45 seconds, 60°C for 30 seconds, and 72°C for 1 minute. PCR products were analyzed by 2% agarose electrophoresis with ethidium bromide staining.

Statistical analysis. For experiments in which triplicates were run to reduce measurement error, the statistical analyses were conducted on the mean triplicate value. For all associated two-group comparisons, statistical significance was determined using the nonparametric Wilcoxon-signed rank test with exact computations for *P* value. The differences between groups were considered to be statistically significant when the *P* value was 1 0.05. For multiple-group comparisons (more than two groups), analyses were completed using ANOVA with follow-up multiple comparison in the cases with overall significant differences. All statistical analyses were conducted in SAS [45].

ACKNOWLEDGMENTS

We thank Sally B. Lagan and Soneshia L. M. McMillan (both from University of Alabama at Birmingham) for assistance in preparing the manuscript. This work was supported by Pediatric Brain Tumor Foundation of the United States, Grant 000136268, and Department of Defense Grant DAMD17-01-0012.

RECEIVED FOR PUBLICATION OCTOBER 16, 2001;
ACCEPTED MAY 22, 2002.

REFERENCES

- Reed, J. C. (2000). Mechanisms of apoptosis. *Am. J. Pathol.* 157: 1415-1430.
- Adams, J., and Cory, S. (2001). Life-or-death decisions by the Bcl-2 protein family. *Trends Biochem. Sci.* 26: 61-66.
- Adams, J., and Cory, S. (1998). The Bcl-2 protein family: arbiters of cell survival. *Science* 281: 1322-1326.
- Gross, A., McDonnell, J., and Korsmeyer, S. (1999). BCL-2 family members and the mitochondria in apoptosis. *Genes Dev.* 13: 1899-1911.
- Brambilla, E., et al. (1998). p53 mutant immunophenotype and deregulation of p53 transcription pathway (Bcl2, Bax, and Waf1) in precursor bronchial lesions of lung cancer. *Clin. Cancer Res.* 4: 1609-1618.
- Apolinario, R. M., et al. (1997). Prognostic value of the expression of p53, Bcl-2, and Bax oncoproteins, and neovascularization in patients with radically resected non-small-cell lung cancer. *J. Clin. Oncol.* 15: 2456-2466.
- Chen, Y., et al. (1999). Expression of Bcl-2, Bax, and p53 proteins in carcinogenesis of squamous cell lung cancer. *Anticancer Res.* 19: 1351-1356.
- Coll, J. L., et al. (1998). Antitumor activity of bax and p53 naked gene transfer in lung cancer: *in vitro* and *in vivo* analysis. *Hum. Gene Ther.* 9: 2063-2074.
- Benihoud, K., Yeh, P., and Perricaudet, M. (1999). Adenovirus vectors for gene delivery. *Curr. Opin. Biotechnol.* 10: 440-447.
- Robbins, P. D., Tahara, H., and Ghivizzani, S. C. (1998). Viral vectors for gene therapy. *Trends Biotechnol.* 16: 35-40.
- Kagawa, S., et al. (2000). Antitumor effect of adenovirus-mediated Bax gene transfer on p53-sensitive and p53-resistant cancer lines. *Cancer Res.* 60: 1157-1161.
- Xiang, J., et al. (2000). Pro-apoptotic treatment with an adenovirus encoding Bax enhances the effect of chemotherapy in ovarian cancer. *J. Gene Med.* 2: 97-106.
- Tai, Y. T., Strobel, T., Kufe, D., and Cannistra, S. A. (1999). *In vivo* cytotoxicity of ovarian cancer cells through tumor-selective expression of the BAX gene. *Cancer Res.* 59: 2121-2126.
- Lowe, S. L., et al. (2001). Prostate-specific expression of Bax delivered by an adenoviral vector induces apoptosis in LNCaP prostate cancer cells. *Gene Ther.* 8: 1363-1371.
- Shinoura, N., et al. (2000). Adenovirus-mediated transfer of bax with caspase-8 controlled by myelin basic protein promoter exerts an enhanced cytotoxic effect in gliomas. *Cancer Gene Ther.* 7: 739-748.
- Folkman, J. (1990). What is the evidence that tumors are angiogenesis dependent? *J. Natl. Cancer Inst.* 82: 4-6.
- Arbisher, J. L., et al. (1997). Oncogenic H-ras stimulates tumor angiogenesis by two distinct pathways. *Proc. Natl. Acad. Sci. USA* 94: 861-866.
- Grugel, S., Finkenzeller, G., Weindel, K., Barleon, B., and Marme, D. (1995). Both v-Ha-Ras and v-Raf stimulate expression of the vascular endothelial growth factor in NIH 3T3 cells. *J. Biol. Chem.* 270: 25915-25919.
- Mukhopadhyay, D., Tsiokas, L., and Sukhatme V. P. (1995). Wild-type p53 and v-Src exert opposing influences on human vascular endothelial growth factor gene expression. *Cancer Res.* 55: 6161-6165.
- Kieser, A., Weich, H. A., Brandner, G., Marme, D., and Kolch, W. (1994). Mutant p53 potentiates protein kinase C induction of vascular endothelial growth factor expression. *Oncogene* 9: 963-969.
- Shweiki, D., Itin, A., Soffer, D., and Keshet, E. (1992). Vascular endothelial growth factor induced by hypoxia may mediate hypoxia-initiated angiogenesis. *Nature* 359: 843-845.
- Mattern, J., Koomagi, R., and Volm, M. (1995). Vascular endothelial growth factor expression and angiogenesis in non-small cell lung carcinomas. *Int. J. Oncol.* 6: 1059-1062.
- Andre, T., et al. (2000). Vegf, Vegf-B, Vegf-C and their receptors KDR, FLT-1 and FLT-4 during the neoplastic progression of human colonic mucosa. *Int. J. Cancer* 86: 174-181.
- Brown, L. F., et al. (1995). Expression of vascular permeability factor (vascular endothelial growth factor) and its receptors in breast cancer. *Hum. Pathol.* 26: 86-91.
- Miyagami, M., Tazoe, M., and Nakamura, S. (1998). Expression of vascular endothelial growth factor and p53 protein in association with neovascularization in human malignant gliomas. *Brain Tumor Pathol.* 15: 95-100.
- Orre, M., and Rogers, P. A. (1999). VEGF, VEGFR-1, VEGFR-2, microvessel density and endothelial cell proliferation in tumours of the ovary. *Int. J. Cancer* 84: 101-108.
- Suzuki, K., et al. (1996). Expression of vascular permeability factor/vascular endothelial growth factor in human hepatocellular carcinoma. *Cancer Res.* 56: 3004-3009.
- Yuan, A., et al. (2000). Correlation of total VEGF mRNA and protein expression with histologic type, tumor angiogenesis, patient survival and timing of relapse in non-small-cell lung cancer. *Int. J. Cancer* 89: 475-483.
- Linderholm, B. K., et al. (2001). The expression of vascular endothelial growth factor correlates with mutant p53 and poor prognosis in human breast cancer. *Cancer Res.* 61: 2256-2260.
- Maeda, K., et al. (1996). Prognostic value of vascular endothelial growth factor expression in gastric carcinoma. *Cancer* 77: 858-863.
- Van Engeland, M., Ramaekers, F. C., Schutte, B., and Reutelingsperger, C. P. (1996). A novel assay to measure loss of plasma membrane asymmetry during apoptosis of adherent cells in culture. *Cytometry* 24: 131-139.
- Koshikawa, N., Takenaga, K., Tagawa, M., and Sakiyama, S. (2000). Therapeutic efficacy of the suicide gene driven by the promoter of vascular endothelial growth factor gene against hypoxic tumor cells. *Cancer Res.* 60: 2936-2941.
- Varley, A. W., and Munford, R. S. (1998). Physiologically responsive gene therapy. *Mol. Med. Today* 4: 445-451.
- Rak, J., et al. (1995). Oncogenes as inducers of tumor angiogenesis. *Cancer Metastasis Rev.* 14: 263-277.
- Forsythe, J. A., et al. (1996). Activation of vascular endothelial growth factor gene transcription by hypoxia-inducible factor 1. *Mol. Cell Biol.* 16: 4604-4613.
- Shibata, T., Giaccia, A. J., and Brown, J. M. (2000). Development of a hypoxia-responsive vector for tumor-specific gene therapy. *Gene Ther.* 7: 493-498.
- Dachs, G. U., et al. (1997). Targeting gene expression to hypoxic tumor cells. *Nat. Med.* 3: 515-520.
- Rampino, N., et al. (1997). Somatic frameshift mutations in the BAX gene in colon cancers of the microsatellite mutator phenotype. *Science* 275: 967-969.
- Yin, C., Knudson, C. M., Korsmeyer, S. J., and Van Dyke, T. (1997). Bax suppresses tumorigenesis and stimulates apoptosis *in vivo*. *Nature* 385: 637-640.
- Miyashita, T., and Reed, J. C. (1995). Tumor suppressor p53 is a direct transcriptional activator of human Bax gene. *Cell* 80: 293-299.
- Chow, N. H., et al. (1997). Expression of vascular endothelial growth factor in normal liver and hepatocellular carcinoma: an immunohistochemical study. *Hum. Pathol.* 28: 698-703.
- El-Assal, O. N., et al. (1998). Clinical significance of microvessel density and vascular endothelial growth factor expression in hepatocellular carcinoma and surrounding liver: possible involvement of vascular endothelial growth factor in the angiogenesis of cirrhotic liver. *Hepatology* 6: 1554-1562.
- He, T. C., et al. (1998). A simplified system for generating recombinant adenoviruses. *Proc. Natl. Acad. Sci. USA* 95: 2509-2514.
- Graham, F. L., and van der Eb, A. J. (1973). A new technique for the assay of infectivity of human adenovirus 5 DNA. *Virology* 52: 456-467.
- SAS (1994). *SAS/STAT User's Guide*, version 6. SAS Institute Inc., Cary, N.C.

38 Modulation of DNA Topoisomerase I (TOP1)-Mediated Radiosensitization by DNA-Dependent Protein Kinase

S. Shih,¹ C. Phan,² S. Vijayakumar,¹ A.Y. Chen^{1,2}

¹Radiation Oncology, University of California-Davis Cancer Center, Sacramento, CA, ²Pharmacology & Toxicology Graduate Group, University of California, Davis, CA

Purpose/Objective: Camptothecin (CPT) exerts its biological effects including radiosensitization (RS) by inducing TOP1-mediated DNA damage (T1DD). Extensive genetic and molecular studies have identified the DNA-dependent protein kinase (DNA-PK) complex, consisted of Ku70/Ku80 heterodimer and DNA-PKcs, as an integral component of mammalian DNA non-homologous end joining (NHEJ) double-stranded break repair. Recently, we demonstrated that Ku80 affects TOP1-mediated RS (T1RS) induced by CPT. In the current study, we investigate whether DNA-PK is involved in CPT-induced RS.

Materials/Methods: Clonogenic survival assays using various treatment protocols with combination of drugs and radiation were performed in Chinese hamster ovary V3, V3+human YAC, V3+mouse YAC, SCID/50D, SCID/100E, human glioma M059J and M059K cells. The protein levels of TOP1 and DNA-PK were determined by Western Blot analysis. The DNA-PK kinase activity was determined by using the suggested protocol from Promega (Madison, WI).

Results: Examined by clonogenic survival assays, the DNA-PKcs-deficient V3 cells exhibit a comparable sensitivity to the cytotoxic effect of CPT in comparison to its DNA-PKcs-complemented V3+human YAC and V3+mouse YAC cells. In contrast, the V3 cells exhibit a significantly higher level of CPT-induced RS than both V3+human YAC and V3+mouse YAC cells. To avoid clonal effect, T1RS was further investigated in the DNA-PKcs-deficient SCID/50D and its DNA-PKcs-proficient counterpart SCID/100E cells. Consistently, a comparable sensitivity to the cytotoxic effect of CPT and a reversal of the higher level of CPT-induced RS was observed in the SCID/100E cells, as compared with the SCID/50D cells. Furthermore, a higher level of T1RS was demonstrated in the DNA-PKcs-deficient human glioma M059J cells than their DNA-PKcs-proficient counterpart M059K cells.

Conclusions: Our results demonstrate that DNA-PK modulates the radiosensitizing, but not the cytotoxic effects of CPT. Our findings are consistent with a notion that DNA-PK-dependent NHEJ pathway is involved in repairing a novel type of T1DD that accounts for T1RS.

39 A Novel Radiation/Tissue-Specific Promoter for Gene Therapy of Brain Tumors

W.O. Arafat,¹ D.J. Buchsbaum,² S. Kaliberov,² F. Li,¹ Z.B. Zhu,¹ D.T. Curiel¹

¹Gene Therapy Center, University of Alabama at Birmingham, Birmingham, AL, ²Radiation Oncology, University of Alabama at Birmingham, Birmingham, AL

Purpose/Objective: Radiogenic therapy is a novel approach to treat cancer. It implies using genetic modification to alter sensitivity of tumor or normal tissue to the effect of radiation. Using recombinant adenovirus (Ad) as a vector, heterologous gene delivery with consequent phenotypic change in radiosensitivity has been shown with different therapeutic payloads. Radiation inducible promoters incorporated into Ad vectors have been used to deliver therapeutic genes. However, lack of tumor specificity and moderate levels of gene induction have been a concern. On the other hand, tissue specific promoters (TSP) have been widely developed and show both high selectivity and robust gene expression in transfected tumors. Of note, radiation also induces gene expression by transcriptional regulation of some of these promoters. Herein we hypothesize that radiotherapy may enhance the selectivity and level of expression of TSP.

Materials/Methods: To this end, we have constructed recombinant Ad/Luc, Ad/GFP or Ad/LacZ driven by different promoters; Survivin, inducible Nitric Oxide Synthase (iNOS), Vascular Endothelial Growth Factor (VEGF), Death Receptor 5 (DR5), and Flt-1. Human glioma cell lines were infected with different MOI of the TSP Ad or CMV Ad, then cells were exposed to single fraction ⁶⁰Co radiation (0.5 Gy-16 Gy). Fluorescent microscopy, FACS analysis, luciferase assay and X-gal staining were used to detect level of expression of the various genes. Time course experiments were done to look for effect of time of irradiation on gene expression. Finally quantitative RT-PCR to the corresponding genes was done with RNA isolated from radiation treated cells.

Results: Adenovirus vectors driven by DR5, VEGF, Survivin or Flt-1 were made and showed specificity to glioma cell lines. Radiation increased the level of gene expression by 1.75-fold in DR5, 2-fold in VEGF and 0-fold with Flt-1 at 2 hr after radiation. Most importantly, cells treated with 2 Gy radiation and Ad Luc driven by the Survivin promoter showed a 5-fold increase in expression compared with non-irradiated cells. RNA analysis showed an increase in copy number of corresponding genes from 2-fold for VEGF, 3-fold for iNOS and 30-fold for Survivin. Additionally, elevation of Survivin RNA copy number occurred at 2 hr after radiation and continued to be high 24 hr after radiation.

Conclusions: This novel radiation inducible TSP, Survivin, is a promising tool that could lead to the enhancement of selectivity and specificity of Ad vector transfection in a radiogenic context.

40 Failure Definition-Dependent Differences in Outcome Following Radiation for Localized Prostate Cancer. Can One Size Fit All?

D.A. Kuban,¹ H.D. Thames,¹ L.B. Levy,¹ E.M. Horwitz,² P.A. Kupelian,³ A.A. Martinez,⁴ J.M. Michalski,⁵ T.M. Pisansky,⁶ H.M. Sandler,⁷ W.U. Shipley,⁸ M.J. Zelefsky,⁹ A.L. Zietman⁸

¹UT MD Anderson Cancer Center, Houston, TX, ²Fox Chase Cancer Center, Philadelphia, PA, ³Cleveland Clinic, Cleveland, OH, ⁴William Beaumont Hospital, Detroit, MI, ⁵Mallinckrodt Institute of Radiology, St Louis, MO, ⁶Mayo Clinic, Rochester, MN, ⁷University of Michigan, Ann Arbor, MI, ⁸Massachusetts General Hospital, Boston, MA, ⁹Memorial Sloan-Kettering Cancer Center, New York, NY

Purpose/Objective: To compare long-term outcome using alternative failure definitions after definitive radiation for localized prostate cancer and determine whether one PSA-based definition can be applied across treatment modalities.

Materials/Methods: Data from 4839 patients with stage T1b, T1c and T2 adenocarcinoma of the prostate and a pretreatment PSA were analyzed. Patients were treated to at least 60 Gy without androgen suppression from 1986 to 1995 at nine U.S. institutions. Median follow-up was 6.3 years. The endpoint for outcome analysis was PSA failure, but also included as failures were patients treated with androgen suppression before meeting the PSA failure criteria and those with clinical failure as the first event. Outcome using the following 6 failure definitions was compared: 1) 3 consecutive PSA rises backdated (ASTRO), 2) 2 PSA rises of at least

Approaches to Utilize Mesenchymal Progenitor Cells as Cellular Vehicles

L. PEREBOEVA,^a S. KOMAROVA,^a G. MIKHEEVA,^b V. KRASNYKH,^{a,b} D.T. CURIEL^a

^aDivision of Human Gene Therapy, Departments of Medicine, Pathology, and Surgery, and the Gene Therapy Center, University of Alabama at Birmingham, Birmingham, Alabama, USA;

^bVectorLogics, Inc., Birmingham, Alabama, USA

Key Words. *Mesenchymal progenitor cells · Cellular vehicles · Gene delivery · Adenovirus · Thymidine kinase*

ABSTRACT

Mammalian cells represent a novel vector approach for gene delivery that overcomes major drawbacks of viral and nonviral vectors and couples cell therapy with gene delivery. A variety of cell types have been tested in this regard, confirming that the ideal cellular vector system for ex vivo gene therapy has to comply with stringent criteria and is yet to be found. Several properties of mesenchymal progenitor cells (MPCs), such as easy access and simple isolation and propagation procedures, make these cells attractive candidates as cellular vehicles. In the current work, we evaluated the potential utility of MPCs as cellular vectors with the intent to use them in the cancer therapy context. When conventional adenoviral (Ad) vectors were used for MPC transduction, the highest transduction efficiency of MPCs was 40%. We demonstrated that Ad primary-binding receptors were poorly expressed on MPCs, while the

secondary Ad receptors and integrins presented in sufficient amounts. By employing Ad vectors with incorporated integrin-binding motifs (Ad5lucRGD), MPC transduction was augmented tenfold, achieving efficient genetic loading of MPCs with reporter and anticancer genes. MPCs expressing thymidine kinase were able to exert a bystander killing effect on the cancer cell line SKOV3ip1 in vitro. In addition, we found that MPCs were able to support Ad replication, and thus can be used as cell vectors to deliver oncolytic viruses. Our results show that MPCs can foster expression of suicide genes or support replication of adenoviruses as potential anticancer therapeutic payloads. These findings are consistent with the concept that MPCs possess key properties that ensure their employment as cellular vehicles and can be used to deliver either therapeutic genes or viruses to tumor sites. *Stem Cells* 2003;21:389-404

INTRODUCTION

One of the major requirements for successful gene therapy is efficient delivery of therapeutic genes to the target sites. Among the vector systems that have been used for gene delivery are viruses and plasmids [1]. An optimal gene delivery vector must show a high level of transduction of the desired tissue or cell population, efficient targeting, and the ability to withstand degradation by the immune system

for prolonged periods and after readministration. To date, vectors meeting all three requirements are not available. On this basis, it is apparent that novel vector approaches are required to advance gene therapy.

Mammalian cells have been proposed as gene delivery vehicles with the potential for overcoming the physiological barriers to viral vectors, especially rapid degradation by the immune system and toxicity with escalating doses. The

Correspondence: Larisa Pereboeva, M.D., Ph.D., Division of Human Gene Therapy, Gene Therapy Center, University of Alabama at Birmingham, 901 19th Street South, BMR2-572, Birmingham, Alabama 35294-3300, USA. Telephone: 205-975-8768; Fax: 205-975-2961; e-mail: larisa.pereboeva@ccc.uab.edu Received November 6, 2002; accepted for publication March 18, 2003. ©AlphaMed Press 1066-5099/2003/\$12.00/0

transfer of genetically modified cells into the body constitutes a novel therapeutic paradigm of coupling cell therapy with gene delivery [2, 3]. By virtue of native or introduced tropism, cellular vehicles, after reintroduction, may reside in selective tissues or organs and deliver engineered vectors or genes before they are released from cellular carriers. Therefore, expression or release of these therapeutic payloads can, thus, be achieved at a locoregional level in areas otherwise inaccessible to gene transfer, such as tumor sites. Several somatic cell types, such as fibroblasts [4, 5], hepatocytes [6], mesothelial cells [7], myoblasts [8, 9], neuronal cells [10], and others have been evaluated in a variety of applications as cellular vehicles. Mature endothelial cells have been used to deliver therapeutic genes into areas of angiogenesis [11, 12] as well as to deliver cytotoxic genes to tumors [13]. However, difficult isolation and in vitro expansion present major limitations for the use of mature terminally differentiated cells. Hematopoietic stem cells have also been evaluated as cellular vehicles [14, 15]. However, low levels of transduction also limit their applicability [16]. In the context of cancer treatment, human tumor infiltrating lymphocytes (TILs) were the first immune cells to be genetically modified and applied in a human cancer gene therapy clinical trial [17]. It was suggested that TILs could naturally home to tumor sites; however, in practice, it has been shown that they localize poorly into tumors after reinfusion [18, 19]. Utilization of TILs requires expensive expansion of cells in vitro or in vivo and applying retargeting strategies. Such studies demonstrate both the feasibility of utilizing different cell types as vectors for gene delivery and also the stringent criteria for the ideal cellular vehicle, providing necessities of research into alternative cell populations.

Mesenchymal progenitor cells (MPCs) were identified as a subpopulation of bone marrow stromal cells, which form an essential structural and functional component of the bone marrow microenvironment and are critical in hematopoiesis [20]. MPCs mainly have been employed in cell therapies based on the delivery of the cells themselves, either modified or not, in different models and in the clinical setting to replenish tissue defects or trigger regeneration of various mesenchymal tissues [21-23]. Recent advances in studying MPC biology have shown that this cell population exhibits some properties that suggest the feasibility of their use as a cellular vehicle: A) a simple isolation method [24]; B) the ability to be cultured in vitro in minimal conditions and to expand to quantities required for therapy [25]; C) the ability for ex vivo transduction with viral vectors, although with varying levels of efficiency [26]; D) plasticity, the potential to differentiate under exogenous stimuli [27]; E) the ability to engraft after reintroduction [28]; F) high metabolic activity

and efficient machinery to express therapeutic proteins in secretory form [29], and G) the ability to be delivered systemically or locally [30, 31]. Practical attempts to use MPCs as cellular vehicles, however, have been undertaken mainly for the delivery of therapeutic gene products (interleukin-3, growth hormone, factor IX) into systemic circulation [29, 32]. Research studies exploiting MPCs in the context of cancer are limited. However, recently, one study reported the very important fact that MPCs could selectively proliferate in tumors after systemic delivery and serve as precursors for stromal fibroblasts of solid tumors [33].

Given that the intrinsic properties of MPCs satisfy some of the criteria for the ideal cell vector, this cell population can be considered as an attractive candidate for a cellular vehicle. Our goal in this study was to investigate the utility of MPCs as novel cellular vehicles for gene delivery to tumor sites. Our present data show that MPCs possess key vector properties allowing them to function as cellular vehicles for cancer gene therapy.

MATERIALS AND METHODS

Reagents

Mouse anti-CAR (coxsackievirus and adenovirus receptor) monoclonal antibody (RmcB) prepared as ascites fluid was obtained from Dr. R.L. Crowell (Hahnemann University; Philadelphia, PA). Antibodies to $\alpha_v\beta_3$ (LM609) and $\alpha_v\beta_5$ (PIF6) integrins were purchased from Chemicon International, Inc. (Temecula, CA; <http://www.chemicon.com>).

Cell Lines

The human ovarian carcinoma cell line SKOV3.ip1 was obtained from Dr. Janet Price (University of Texas M.D. Anderson Center; Houston, TX). Cells were maintained in Dulbecco's modified Eagle's medium/F-12, containing 10% fetal bovine serum (FBS) (HyClone Lab; Logan, UT; <http://www.hyclone.com>) and 2 mM glutamine at 37°C in a humidified atmosphere of 5% CO₂. HeLa cells were obtained from the American Type Culture Collection (Manassas, VA; <http://www.atcc.org>) and cultured as recommended.

Isolation and Culture of MPCs

Leftover materials (screen filters with bone marrow cells remaining) were obtained from several individuals undergoing bone marrow harvest for allogeneic transplantation at the University of Alabama Birmingham (UAB) Stem Cell Facility. Mononuclear cells were separated by centrifugation in Ficoll-Hypaque gradients (density = 1.077 g/cm³; Sigma; St. Louis, MO; <http://www.sigmaaldrich.com>), suspended in α -minimum essential medium (MEM) containing 20% FBS and seeded at a concentration of 1×10^6 cells/cm². After

3 days, nonadherent cells were removed by washing with phosphate-buffered saline (PBS), and the monolayer of adherent cells was cultured until confluence. The resultant monolayer of adherent cells was designated as MPC, passage 1. Cells were expanded by consecutive subcultivations in α -MEM with 10% FBS at densities of 5,000-6,000 cells/cm² and used for experiments at passages 2-6. The initial seeding cell number (Ns), harvested cell number (Nh), and days in culture needed to reach 90% confluence (D) were used to calculate doubling time (DT) for each subculture using the formula $DT = 2 \times D \times Ns/Nh$. The mean doubling time was calculated as the average of all DTs for each subculture.

Assay for Cell Differentiation

Mesenchymal progenitor cells were cultured in medium containing either osteogenic (0.1 μ M dexamethasone, 10 mM β -glycerophosphate, 50 μ g/ml ascorbic acid) or adipogenic (1 μ M dexamethasone, 100 μ g/ml 3-isobutyl-1-methylxanthine, 5 μ g/ml insulin, 60 mM indomethacin) supplements (Sigma) for up to 3 weeks. The differentiation potential was defined by the appearance of osteogenic, adipogenic, and chondrogenic phenotypes, which were revealed after Alizarin Red S, Oil Red, and Alcian Blue staining, respectively.

Recombinant Adenoviruses

Replication-incompetent recombinant adenoviral (Ad) vectors having wild-type and genetically modified Ad5 fibers were used for experiments to determine their transduction efficiencies on MPCs. Ad vectors having wild-type Ad5 fibers were: Ad5 expressing either green fluorescent protein (eGFP) (AdCMVGFP; a gift from Corey Goldman; Cleveland Clinic Foundation; Cleveland, OH) or *Escherichia coli* β -galactosidase (AdCMVlacZ; provided by Robert Gerard; The Center for Transgene Technology and Gene Therapy; Leuven, Belgium). Viruses expressing firefly luciferase (AdCMVluc) and herpes virus thymidine kinase (HSV-TK) (AdCMV-TK and AdRGD-TK, see below for arginine-glycine-aspartic acid modification) were constructed through homologous recombination in *E. coli* using the AdEasy system [34] at UAB Gene Therapy Center. All vectors used in these experiments contained transgene cassettes placed in the E1-deleted region of an Ad vector genome.

The luciferase and GFP-encoding Ad vectors, Ad5RGDluc and AdCMVGFP RGD [35], have a genetically modified fiber protein with an integrin-binding motif (CDCRGDCFC) inserted in the HI loop. Ad5/3Luc1 has a chimeric fiber, where the knob of Ad5 fiber is replaced by the Ad3 fiber knob [36]. Ad5luc3 [37] is a replication-competent adenovirus, having the E3 region replaced with the luciferase-expressing cassette (provided by F. Graham;

McMaster University; Hamilton, Canada). Ad5/3luc3 is identical to Ad5luc3 except for a chimeric fiber where the knob of the Ad5 fiber is replaced by the Ad3 fiber knob.

In Vitro Ad-Mediated Gene Transfer

Recombinant Ad vectors were used to transduce cells as described previously [38]. In brief, cells were plated 24 hours before infection. The transduction was performed with the virus diluted in a small volume of appropriate cell-specific medium containing 2% FBS for 2 hours at 37°C. Media were then replaced with complete media containing 10% FBS.

In Vitro Analysis of Gene Expression

Twelve hours after plating (5.0×10^4 cells/well in a 24-well plate), HeLa cells and MPCs were infected with AdCMVlacZ, AdCMVGFP or AdCMVluc, Ad5RGDluc, and Ad5/3luc1 at ratios ranging from 50-5,000 plaque-forming units (pfu) per cell. Gene expression was estimated after 48 hours of incubation in complete media.

X-gal Staining of MPCs

LacZ expression in Ad-transduced cells was evaluated by staining with 5-bromo-4-chloro-3-indolyl- β -D-galactoside (X-gal) at 1 mg/ml followed by cell counting. AdlacZ-transduced MPCs were fixed in freshly prepared 2% formaldehyde/0.2% glutaraldehyde in PBS for 5 minutes at 4°C, washed, and stained in freshly prepared X-gal in 20 mM potassium ferrocyanide and 2 mM MgCl₂ in PBS.

Luciferase Assay

Luciferase expression was determined in cell lysates using a luciferase assay system (Promega; Madison, WI; <http://www.promega.com>) according to protocol. The luciferase activities were measured in a Lumat LB 9501 luminometer (Lumat, Wallac, Inc.; Gaithersburg, MA; <http://www.lifesciences.perkinelmer.com>) for 15 seconds immediately after initiation of the light reaction and normalized by the protein concentration in cell lysates (Bio-Rad DC Protein Assay kit, Bio-Rad; Hercules, CA; <http://www.bio-rad.com>). All experiments were performed in triplicate.

Flow Cytometry

GFP expression and expression of Ad receptors were assessed by flow cytometry. Cultured cells were released with versene, pelleted by centrifugation, and washed with PBS. GFP-expressing cells after Ad-GFP transduction were directly used for flow cytometry. To test the expression of Ad receptor antibodies to CAR (RmcB), integrins $\alpha_v\beta_3$ (LM609) and $\alpha_v\beta_5$ (PIF6) were used. Cells (5×10^5) were incubated with the primary antibody diluted in PBS containing 0.1% bovine serum albumin for 1 hour at 4°C. Concentrations of the primary

antibodies were 10 $\mu\text{g/ml}$, 2.5 $\mu\text{g/ml}$, and 10 $\mu\text{g/ml}$ for RmcB, P1F6, and LM609, respectively. Cells were washed and incubated with fluorescein isothiocyanate (FITC)-conjugated goat anti-mouse IgG for 30 minutes at 4°C in the dark. After washing in PBS, the cells were resuspended in 500 μl of PBS containing 0.1% formaldehyde. Flow cytometry was performed on a FACScan flow cytometer (Becton Dickinson; Erembodegem, Belgium; <http://www.bd.com>).

Toxin Gene-Killing Experiments

In Vitro Analysis of the Cytocidal Effect of HSV-TK Expression

HSV-TK expression by MPCs and SKOV3.ip1 cells after exerting ganciclovir (GCV) was estimated by measuring tetrazolium salt (MTS) 3-(4,5-dimethylthiazol-2-yl)-5-(3-carboxymethoxyphenyl)-2-(4-sulfophenyl)-2H-tetrazolium cell-killing assay. Briefly, MPCs or SKOV3.ip1 cells were plated on 96-well plates at 2×10^4 cells/well. Cells were transduced with AdCMV-TK or AdCMV RGD-TK at the multiplicity of infection (MOI) of 5, 50, 100, and 500 viral particles (vp)/cell. After 24 hours, plates were treated with increasing concentrations of GCV. Four days later, the number of surviving cells was analyzed by MTS assay according to the manufacturer's protocol (Cell Titer 96 Aqueous Non-Radioactive Cell Proliferation Assay, Promega; Madison, WI; <http://www.promega.com>). The plates were processed in an automated E-max spectrophotometer plate reader (Molecular Device Corp.; Sunnyvale, CA; <http://www.moleculardevices.com>). All experiments were carried out in triplicate.

In Vitro Analysis of Cytotoxic Bystander Effect

Cell-mixing experiments were performed on MPCs or SKOV3.ip1 cells to assess the bystander effect as described elsewhere [38]. Briefly, MPCs were transduced with AdCMV-TK or AdCMV RGD-TK and then mixed with untransduced cells (MPCs or SKOV3.ip1 cells). The ratios of TK-expressing cells to untransduced cells were as follows: 0:100, 10:90, 50:50, 90:10, and 100:0. Cell mixtures were plated in 96-well plates at total cell densities of 2×10^4 cells/well. Twenty-four hours later, half the samples were treated with GCV (20 μM). Five days later, the number of surviving cells was analyzed by MTS assay. All experiments were carried out in triplicate.

Assays for Ad Replication in MPCs

Crystal Violet Cell Viability Assay

The cytopathic effect (CPE) of replication-competent Ad was estimated by crystal violet staining. Ad-permissive HeLa cells were used as a positive control for Ad replication and virus-induced cytopathic effect. HeLa cells and MPCs were

plated on 6-well plates at 2×10^5 cells/well and infected with Ad5luc3 for 2 hours at 37°C at the indicated MOI, followed by PBS washes. Plates were incubated at 37°C until a prominent CPE developed. Cells were carefully washed with PBS, fixed with 10% buffered formalin, and stained with 0.2% crystal violet in 10% ethanol for 1 hour. The plates were washed with tap water, dried, and photographed with a Kodak DC260 digital camera. All experiments were done in triplicate.

Cytopathic Effect of Produced Adenovirus on Permissive Cell Line

MPCs or HeLa cells were infected with a replication-competent virus (Ad5luc3) at the designated MOI. After 1 hour of infection, all wells were washed twice with PBS, and complete medium was added, and cultures were incubated for 3 days. Cells were pooled at the end of the incubation period and freeze-thawed three times. The lysates were diluted in 10-fold steps and used for secondary infection of HeLa cells. The cytopathic effect of cell lysates was detected after 4 days with crystal violet staining. All experiments were done in triplicate.

Quantitative Polymerase Chain Reaction Analysis of Ad DNA

MPCs and HeLa cells were plated on 6-well plates at a density of 2×10^5 cells/well 24 hours before infection. Cells were infected with nonreplicative (Ad5luc) or replication-competent (Ad5luc3 and Ad5/3luc3) viruses at an MOI of 1. The infected cells and virus-containing supernatants were harvested 1, 3, 5, 7, and 9 days after infection and used for viral DNA and viral protein quantitation. Culture media and cells from three wells corresponding to each time point were collected, pooled, and used for viral and total cell DNA isolation. Total DNA from cells was purified using the QIAamp DNA, Blood kit (QIAGEN; Valencia, CA; <http://www.qiagen.com>) according to the kit instructions. Total cell DNA was used for quantitative polymerase chain reaction (PCR) with E1 primers, to determine copy numbers of vDNA, and actin primers, to determine number of actin cDNA copies. To isolate only encapsidated viral DNA from culture media and to destroy naked viral DNA present in the supernatant, DNase I treatment was performed. Then, EDTA, SDS, and proteinase K were added (final concentrations: 20 mM, 0.5%, 0.2 mg/ml, respectively) and samples were incubated at 56°C for 1 hour followed by phenol/chloroform extraction and ethanol precipitation. The purified viral DNA was dissolved in Tris-EDTA buffer, pH 8.0.

Real-time PCR (LightCycler; Roche; Indianapolis, IN; <http://www.roche.com>) analysis was used for quantitative evaluation of Ad DNA copy number. Oligonucleotides corresponding to the sense strand of the Ad E1 region (5'-AAC CAGTTGCCGT GAGAGTTG-3': 1433-1453), the antisense strand of the E1 region (5'-CTCGTTAAGCAAGTCTCG

ATACA-3': 1500-1476), and TaqMan fluorogenic probe (5'-CACAGCCTGGCGACGCCCA-3': 1473-1455) were synthesized and used as primers and probe for real-time PCR analysis. To correct for differences in total DNA concentration for each sample, Ad E1A copy numbers were normalized by actin DNA copy number. Primer sequences to detect transcripts of actin DNA were as follows: sense strand 5'-CAGCAGATGTGGATCAGCAAG-3'; antisense strand 5'-CTAGAAGCATTTCGGGTGGAC-3'; and TaqMan probe 5'-AGGAGTATGACGAGTCCGGCCCCCTC-3'.

Evaluation of Presence of Viral Protein in Culture Media

The presence of viral hexon in culture media was estimated with enzyme immunoassay for the detection of Ad in infected cell cultures (IDEA kit; DAKO; Carpinteria, CA; <http://www.dako.dk>) in accordance with kit instructions. OD450 was determined on an automated E-max spectrophotometer plate reader. Samples giving OD450 in the range of 2.0 were diluted, and the correct QD450 was obtained by multiplying by the dilution factor.

RESULTS

Characterization of Isolated Human MPCs

The practical realization of cells as vehicles for gene therapy requires a favorable combination of native properties of a chosen cell type, as well as the ability to be effectively loaded by genes, or other therapeutics, and to deliver such a payload to target sites. The theoretical considerations of utilizing MPCs as such a cellular vector were predicated primarily by their availability, propagating properties, and simple culturing conditions. Our goal was to test several vector properties of MPCs related to their potential application as delivery vehicles for gene therapy. First, we tested the ability of human MPCs to be maintained in culture and to be propagated in quantities required for in vivo applications. Human MPCs were isolated according to the protocol described elsewhere [39, 40] and plated at densities of $6-7 \times 10^3$ cells/cm² in media supplemented with 10% FBS. Human MPC cultures, after two passages in vitro, represented a mainly homogeneous population of cells as assessed by cell

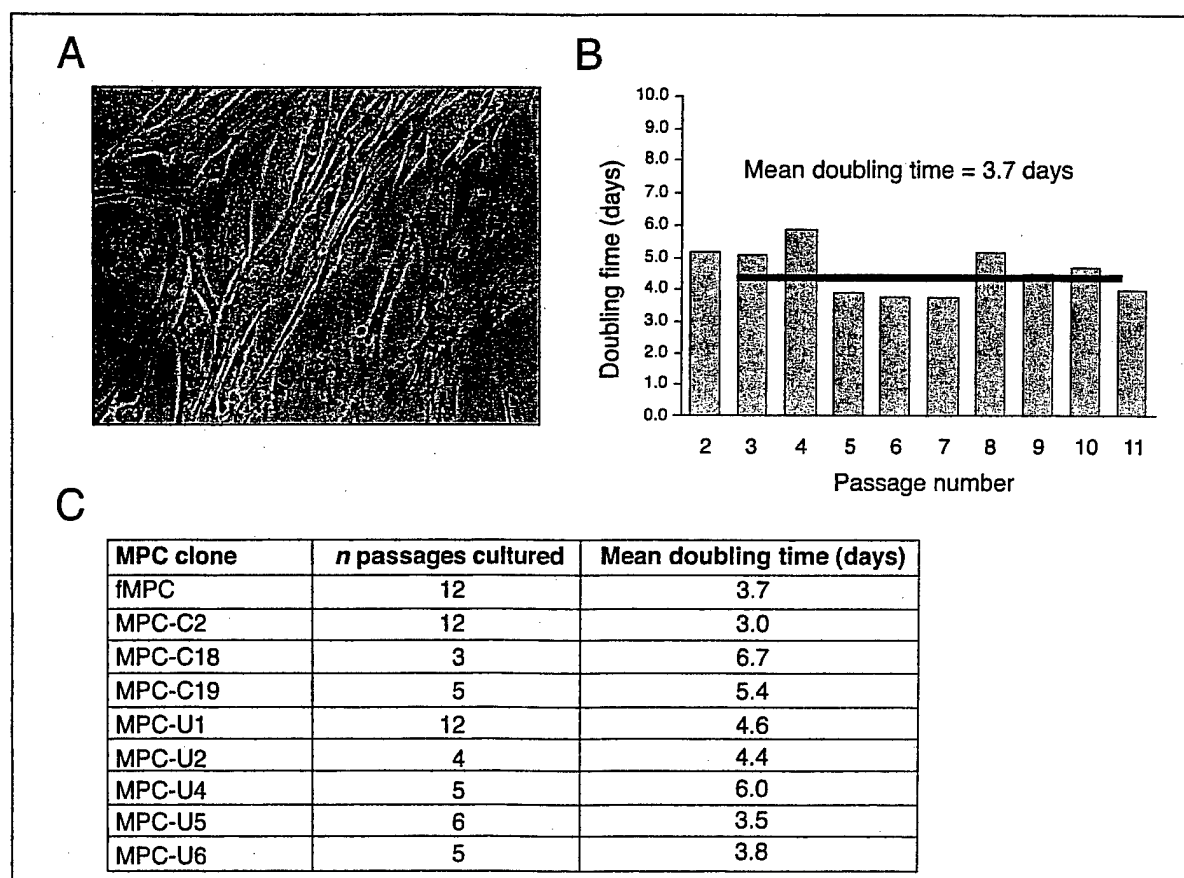


Figure 1. A) Representative phase-contrast photomicrograph of a human MPC culture. Typical cell phenotypes were observed: most cells were spindle shaped, whereas large flat cells and star-shaped cells were present at lower numbers. B) Expansion of MPCs in culture. The primary culture from a single bone marrow donor was followed for up to 12 passages; the doubling time for each passage and the mean doubling time for all passages in observation were calculated as described in Materials and Methods. C) Mean doubling times for different MPC cultures.

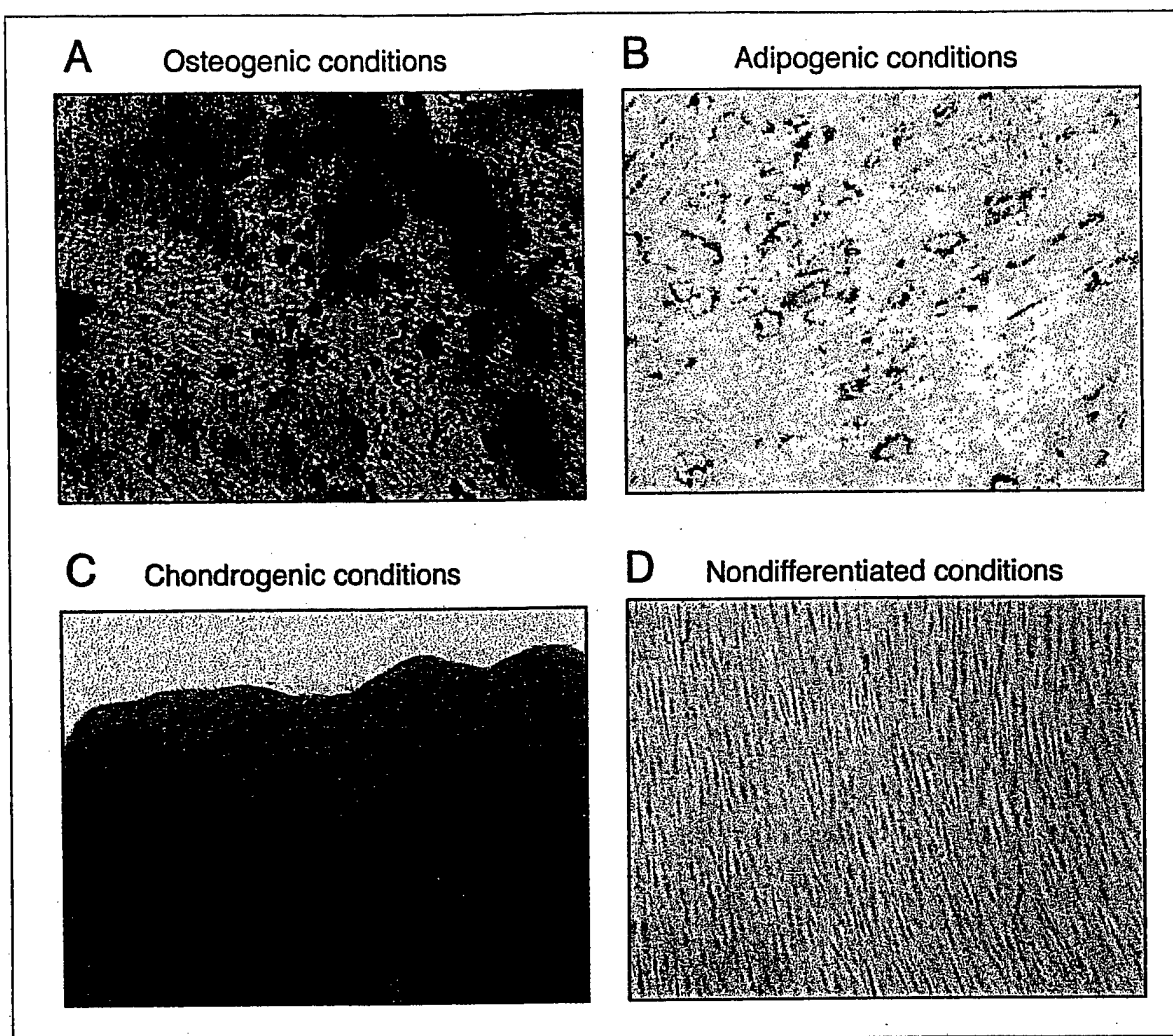


Figure 2. Assay for differentiation abilities of MPCs. Primary MPC cultures at passage 2-5 were subjected *in vitro* to conditions stimulating osteogenic, adipogenic, and chondrogenic differentiation followed by the appropriate staining. A) MPCs cultured in osteogenic media for 21 days. The accumulation of mineral deposits was detected by staining with Alizarin Red. B) MPC culture incubated in adipogenic media for 7 days. Fat droplets in the cells were stained with Oil Red. C) MPC culture incubated under chondrogenic conditions for 14 days. Cells formed a pellet, which stained blue with Alcian Blue. D) MPC culture incubated in nondifferentiating medium, stained with Alizarin Red. No mineral deposits were observed.

morphology, with predominant fibroblast-shaped cells and large flat and star-shaped cells at various percentages (Fig. 1A). Several isolations of MPCs were accomplished according to the described protocol, and primary cultures were monitored for a number of passages (Fig. 1C). The doubling time was calculated for each passage of an individual culture under the described culture conditions and varied from 3 to 6 days. Some MPC cultures were monitored for as long as 12 passages with no noticeable significant changes in propagating properties (Fig. 1B). To confirm that the population of isolated human bone marrow cells contained MPCs or stem cells, we tested the abilities of primary cultures on passage 2-3 to undergo osteogenic, adipogenic, and chondrogenic differentiation after applying the corresponding conditioned

media (Fig. 2A-D). The differentiation potentials of the individual cultures varied from having all three tested lineages being represented to being predominantly skewed toward osteogenic or adipogenic differentiation. Nevertheless, most of the tested cultures demonstrated good propagation and differentiation abilities, confirming the concept that this adherent cell population in fact contains progenitor cells and has sufficient propagation properties to be exploited for application as a cell vehicle.

Accessibility of MPCs to Ad Vector Infection

Our next step was to test the ability of MPCs to be efficiently transduced by Ad vectors and then express the genetic payload. Previous studies have documented that

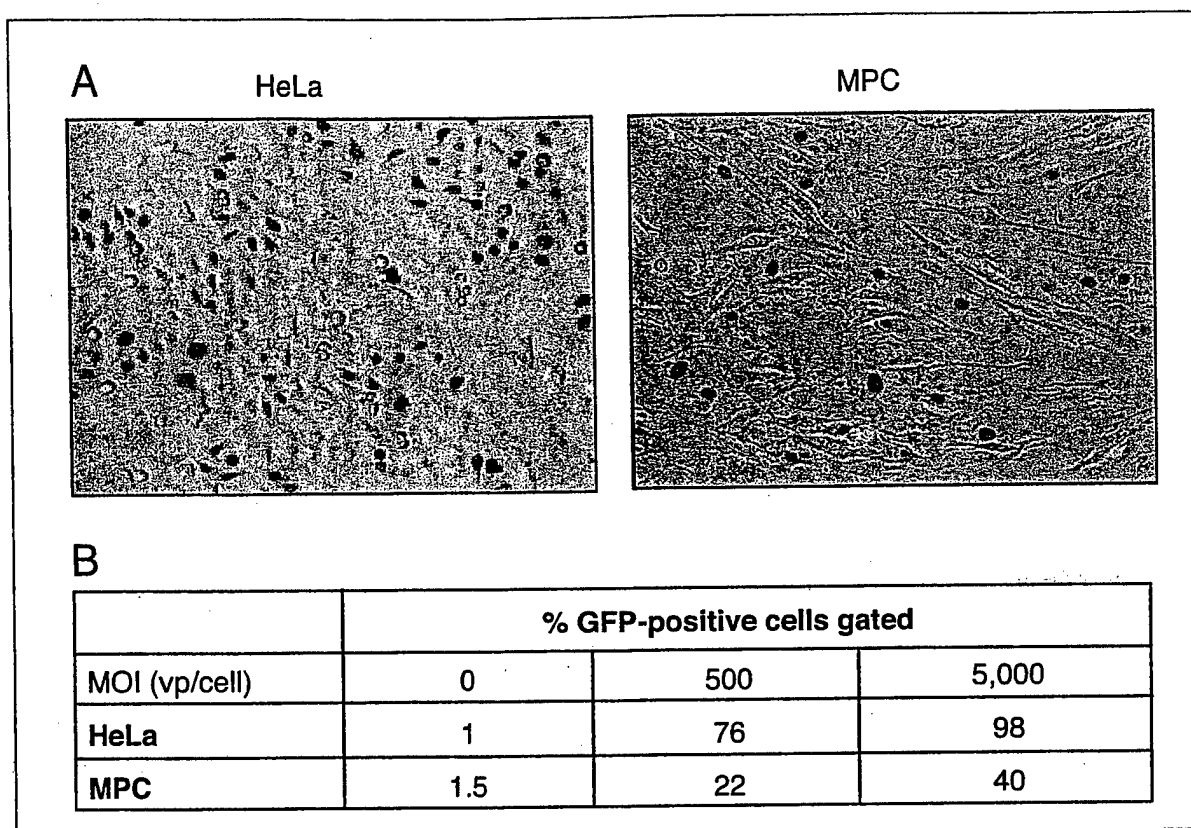


Figure 3. Transduction of MPCs with recombinant Ad5 vectors. A) MPCs and HeLa cells (4×10^5) were transduced with an Ad vector encoding the *E. coli* LacZ gene at an MOI of 500 vp/cell. Forty-eight hours postinfection, cells were fixed and stained with X-gal. B) MPCs and HeLa cells were transduced with an Ad vector encoding GFP reporter at an MOI of 500 or 5,000 vp/cell. Forty-eight hours postinfection, cells were treated with versene and the percentage of GFP-positive cells was determined by flow cytometry. Data are shown as the percent of gated (GFP-positive) cells at the corresponding MOI.

MPCs could be transduced in vitro by Ad vectors, although in any conditions used, the efficiency of transduction did not exceed 20% [41]. For our studies, Ad vectors containing reporter genes (*E. coli* LacZ or eGFP) were used for transduction of MPCs at escalating MOI. Forty-eight hours post infection, MPCs and HeLa cells expressing LacZ were stained with X-gal, and transduction efficiency was assessed by microscopic scoring. Cells expressing eGFP were detected by flow cytometry. Infected with an Ad vector at an MOI of 500 vp/cell, MPC cultures consistently demonstrated a lower efficiency of transduction than did HeLa cells; transduced MPCs represented only 10%-20% of cells in MPC cultures (Fig. 3A). As detected by flow cytometry at the highest MOI tested (5,000 vp/cell), when almost 100% of HeLa cells were transduced, MPC transduction was only 40% (Fig. 3B). These results are consistent with previous observations by others [41, 42] reporting that MPCs are relatively refractive to Ad vector transduction.

The observed relative resistance of MPC cultures to Ad vector transduction could be due to low expression of Ad attachment (CAR) and/or internalization receptors ($\alpha_v\beta$

integrins). By flow cytometry, we compared the expression profiles of Ad receptors on MPCs, HeLa (high CAR, relatively low integrins) cells, and RD (low CAR, high integrins) cells. As shown in Figure 4, MPCs showed very low, if any, expression of CAR but high expression levels of both of the integrins tested. Thus, the pattern of expression of Ad receptors on MPCs resembles that of RD cells and corresponds to a low CAR, high-integrin phenotype. These data suggest that CAR-independent transfer is required to improve the level of Ad-mediated transgene expression by MPC cultures. These considerations prompted our evaluation of the genetically modified adenoviruses for genetic transfer to MPCs.

Increase in Gene Expression by MPCs Transduced with Modified Ad Vectors

It has been shown that significant augmentation of transduction efficiency can be successfully achieved by exploiting Ad vectors with genetically modified tropism. We have designed and characterized an Ad vector with the RGD-4C peptide incorporated in the HI loop of the fiber knob (AdRGD) as well as a vector having the Ad5 knob replaced

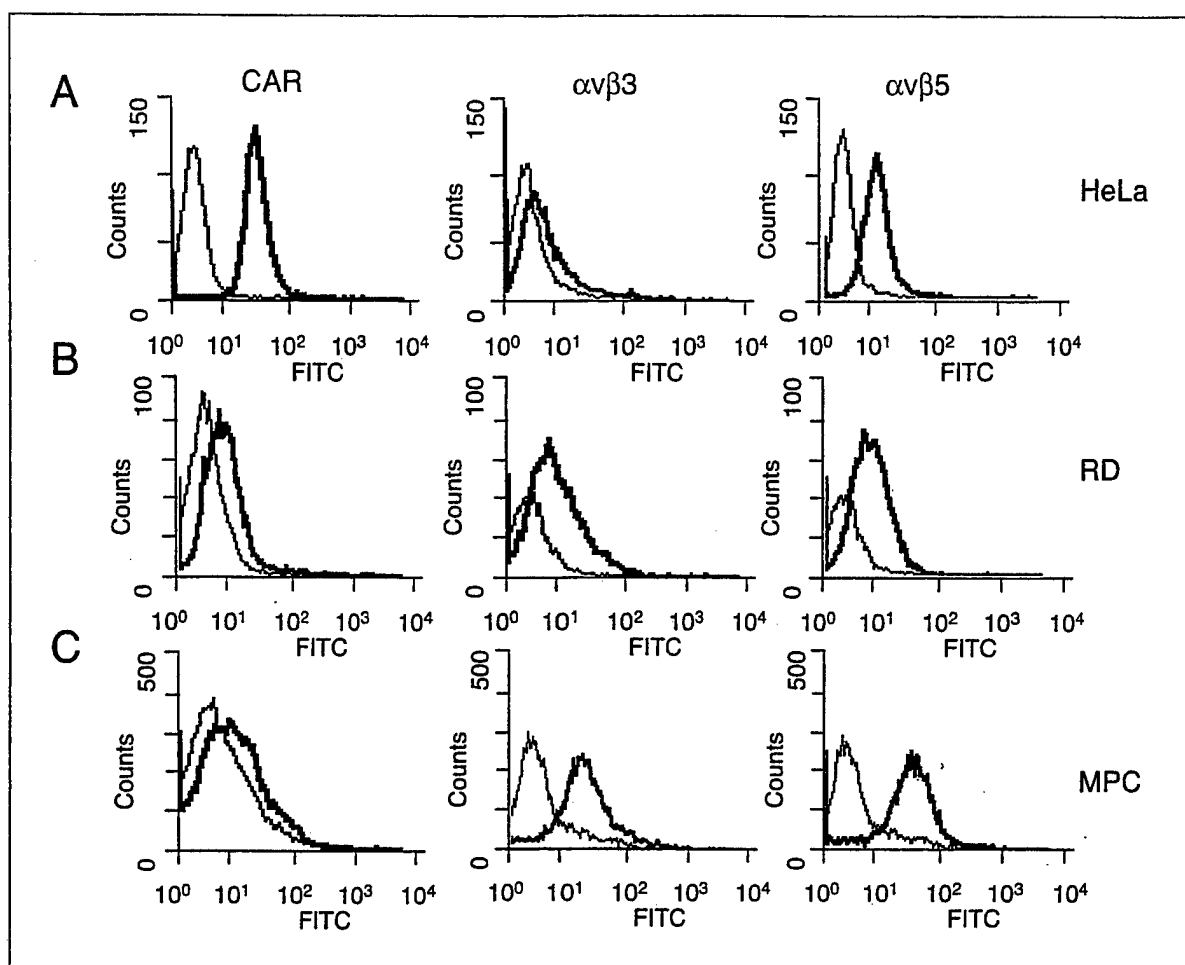


Figure 4. Cell surface expression of Ad attachment (CAR) and internalization ($\alpha_v\beta_3$, $\alpha_v\beta_5$) receptors. After treatment with the indicated primary antibody and FITC-conjugated secondary antibody, cells were analyzed by flow cytometry. Histograms show fluorescence intensity data for HeLa (A), RD (B), and MPC (C) cells. HeLa and RD cultures were taken as a positive control for CAR and integrin expression, respectively.

with the knob of Ad3 (Ad5/3) [35, 36]. These structural modifications confer expanded tropism to the adenoviruses, enabling CAR-independent mechanisms of infection via binding to either cellular integrins or still unknown Ad3 receptors. In addition, these vectors have shown a remarkable improvement in gene transfer efficiency in cell lines normally refractory to CAR-dependent infection [43, 44].

We used genetically modified Ad vectors encoding the luciferase gene, Ad5RGDLuc, and Ad5/3luc1, in which the expression of luciferase is driven by the CMV promoter, to evaluate the transduction of several primary MPC cultures. Improvement in transduction efficiency was evaluated by direct comparison with an unmodified control Ad5 vector, AdCMVluc. The application of AdRGDLuc to MPCs repeatedly resulted in a tenfold augmentation of gene transfer compared with AdCMVluc (Fig. 5A). Ad5/3luc1 also showed an improvement in gene transfer, although with varied results on different primary MPC cultures (data not shown). Considering

that an elevated level of luciferase expression in MPC cultures could result in either a greater number of transduced cells or enhanced protein expression by selective MPC subpopulations, we also tested MPC transduction efficiency with Ad vectors encoding GFP as the reporter gene. Transduction with CMVAd GFP RGD resulted in greater numbers of GFP-expressing cells detected by flow cytometry (Fig. 5B) and microscopy (Fig. 5C). These data indicate overall enhancement of MPC gene transduction by RGD-modified Ad vectors. Thus, these results indicate that an Ad vector retargeted to cellular integrins provides a means to overcome the CAR deficiency in MPCs and allows for an enhanced gene transfer to these cells.

MPC Expression of Prodrug-Converting HSV-TK Results in the Cytotoxic Effect of GCV

Next, we proceeded to confirm the ability of MPCs to express a therapeutic anticancer gene. For this study, we

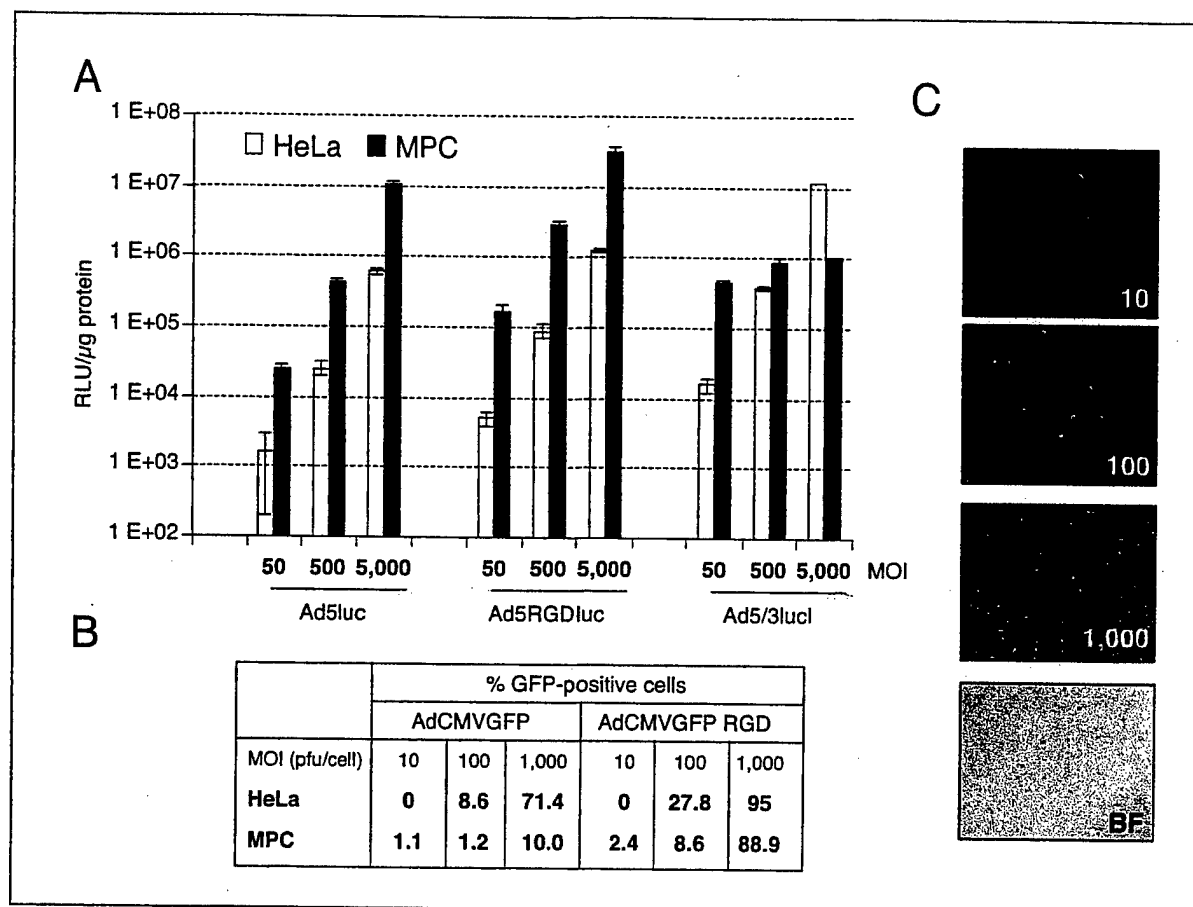


Figure 5. Enhanced transduction efficiency of MPCs with Ad vectors having genetically modified fibers. Comparison of the gene transfer efficiencies was performed employing nonreplicative Ad5 vectors: Ad5luc, Ad5RGDluc, and Ad5/3luc encoding the luciferase gene (A) or AdCMVGFP and AdCMVGFP RGD (B, C). Human MPCs and HeLa cells were infected at the designated MOI (pfu/cell) and analyzed for luciferase expression after 48 hours (A). Data are shown as relative light units (RLU)/μg of total cellular protein. All experiments were done in triplicate. Error bars show standard deviations. MPCs transduced with GFP-encoding vectors were analyzed for GFP expression by flow cytometry (B) and by microscope (C). Microphotographs represent MPC cultures transduced with AdCMVGFP RGD at the MOI designated on each picture (10, 100, or 1,000 pfu/cell). A bright-field microphotograph of a corresponding MPC culture is labeled BF.

utilized the HSV-TK gene, whose product causes cell killing by activating GCV. HSV-TK was chosen with the intent to subsequently employ MPCs as vehicles delivering cytotoxicity to tumor sites in an animal model relevant to ovarian cancer. In this study, MPCs and SKOV3.ip1 cells, a human ovarian cancer cell line taken as a parallel control, were transduced with AdCMV-TK and AdRGD-TK at different MOIs (5, 50, 100, or 500 pfu/cell). Forty-eight hours postinfection, GCV was added to the media at different concentrations (0, 10, 100, or 1,000 μM), and 5 days later, the number of remaining viable cells was determined by an MTS assay. A similar killing effect on MPCs and SKOV3.ip1 cells was observed after AdCMV-TK transduction (Fig. 6A and C). For example, infection at an MOI of 50 pfu/cell resulted in 50% of cells of both types being killed in wells with 10 μM GCV added to the culture medium. In contrast, a dramatic enhancement of the toxic effect exerted by the prodrug was

observed when AdRGD-TK was used for MPC transduction (Fig. 6B and D). Compared with AdCMV-TK, AdRGD-TK caused a killing effect at a lower MOI and a lower GCV concentration (Fig. 6B). This finding validated the aforementioned advantage of RGD-containing Ad vectors in introducing genes into MPCs. Results of this experiment also suggest that transient expression of the HSV-TK delivered by Ad vectors will allow achievement of sufficient levels of suicide gene expression suitable for a cellular vehicle strategy.

Bystander Effect of AdCMV-TK-Transduced MPCs on SKOV3.ip1 Cells

A key advantage embodied in the molecular chemotherapy strategy to kill cancer cells is based on the bystander effect, whereby the killing of untransduced neighboring cells can be induced by a toxic drug metabolite present in a transduced cell. We, therefore, investigated

whether HSV-TK-expressing MPCs could accomplish such a bystander effect on the SKOV3.ip1 tumor cells *in vitro*. AdCMV-TK- or AdRGD-TK-transduced MPCs were mixed in various ratios with untransduced MPCs or SKOV3.ip1

cells. An MOI of 50 pfu/cell, for the transduction of cell populations, and a GCV concentration of 10 μ M were chosen as the lowest viral and prodrug doses showing a killing effect in the previous experiment (Fig. 6). Our mixing experiment

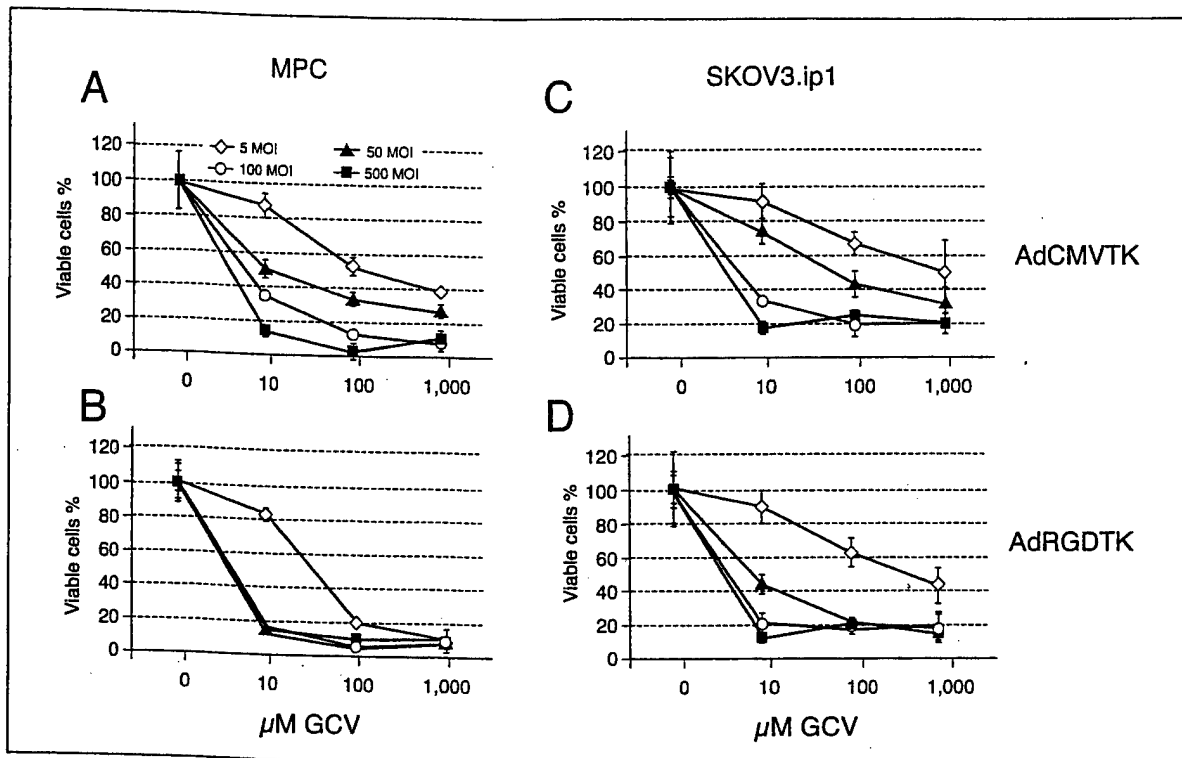


Figure 6. Viability of MPCs transduced with AdCMV-TK or AdRGD-TK after GCV treatment. MPCs or SKOV3.ip1 cells were plated on 96-well plates at a density of 3,000 cell/well and transduced with AdCMV-TK or AdRGD-TK at an MOI of 5, 50, 100, or 500 pfu/cell for 2 hours. After infection, GCV was added at a final concentration of 0, 10, 100, or 1,000 μ M. Cell viability was determined by MTS assay after 5 days of incubation. Data are expressed as percent of viable cells at corresponding GCV concentrations. All experiments were done in triplicate. Error bars represent standard deviations.

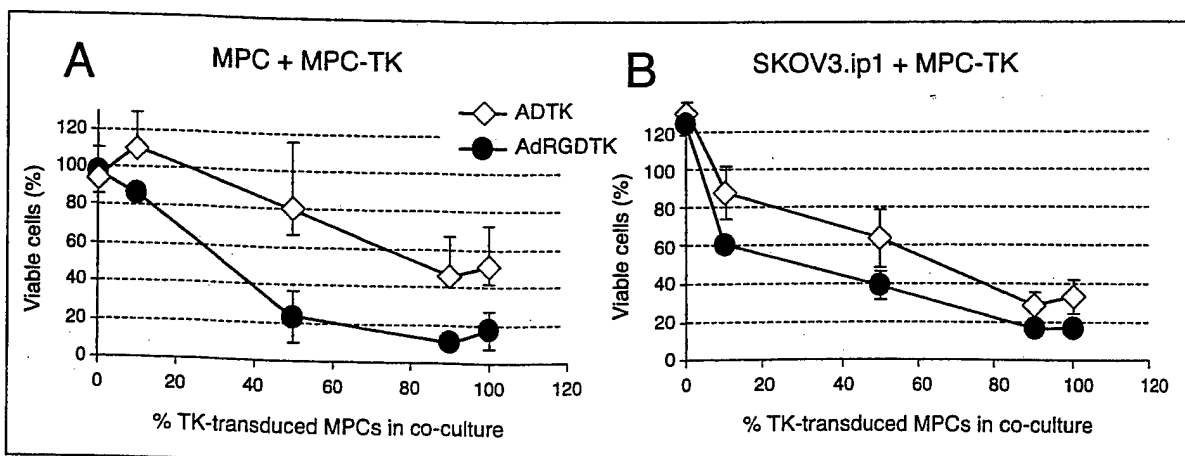


Figure 7. Bystander effect exhibited *in vitro* by AdCMV-TK- and AdRGD-TK-transduced MPCs when mixed at various ratios with uninfected MPCs (A) and SKOV3.ip1 cells (B). MPCs were first transduced with AdCMV-TK or AdRGD-TK. Twenty-four hours after transduction, MPC-TK were mixed in different ratios with untransduced cells (MPCs or SKOV3ip1 cells) and plated on 96-well plates. Twenty-four hours after plating cell mixtures, half the cells were treated with 10 μ M GCV. Five days later, cell killing was measured by MTS assay. Data are presented as a percent of viable cells in GCV-treated wells. All experiments were done in triplicate. Error bars represent standard deviations.

demonstrated that AdRGD-TK-transduced MPCs had a greater killing effect on nontransduced MPC populations (Fig. 7A) and on SKOV3.ip1 cell populations than AdCMV-TK-transduced MPCs (Fig. 7B). Moreover, an appreciable bystander effect was documented for AdRGD-TK-transduced MPCs, as the addition of only 10% of TK-expressing MPCs resulted in a total cell viability of 50%. AdCMV-TK-transduced MPCs did not show a noticeable bystander effect in these conditions, likely due to inefficient transduction of MPCs by the unmodified Ad vector, resulting in an insufficient number of TK-producer cells in the mixture. These mixing experiments establish that MPCs possess a capacity to accomplish a bystander effect using the HSV-TK/GCV enzyme/prodrug approach.

MPCs as Cellular Vehicles Delivering Replication-Competent Ad Vectors

We also considered the possibility of using MPCs to deliver an oncolytic virus as a therapeutic payload. For this approach to be successful, MPCs must be able to support Ad replication and produce viral particles after viral infection. We first determined if replication-competent Ad vectors could cause a cytopathic effect in MPC cultures, an indication of the ability of MPCs to support a productive Ad infection. For this study, MPCs and HeLa cells, used as a highly permissive cell line, were infected with replication-competent Ad5luc3 at an escalating MOI; the cytopathic effect was evaluated by crystal violet staining. Three days postinfection HeLa cells were completely killed in wells infected at MOIs of 100 and 10 vp/cell, and early cytopathic effects were observed at an MOI of 1 vp/cell. At this time, MPCs remained viable at all viral doses. However, 7 days postinfection, MPCs showed a cytopathic effect at the highest MOI tested (Fig. 8), which indicates that the cycle of Ad replication in MPCs is not inhibited completely, but may have different kinetics.

To investigate the kinetics of Ad replication in MPCs, we infected the cells with Ad5luc3 and Ad5/3luc3 at an MOI of 1 pfu/cell and monitored the infection for 11 days. Real-time PCR was used to measure the amount of viral DNA in cells and culture media over time (Fig. 9B and 9C). We also used the detection of the

viral hexon protein in culture media as an indication of viral replication (Fig. 9A). HeLa cells were included in the experiment as a cell line supporting a high level of Ad replication.

In all MPC cultures tested (two of four shown), we observed an increase of viral DNA copy number over time in cell lysates as well as in medium samples. Quantitatively, copy numbers of viral DNA produced by MPCs were 10-100 times lower than with HeLa cells. Ad5/3 did not have an infectivity advantage over Ad5 in HeLa cells as judged by quantitation of viral DNA and viral protein production, while two of the four MPC cultures showed greater amounts of viral DNA and viral protein after infection with Ad5/3. This effect of replication-competent Ad5/3 on MPC cultures corroborates our earlier observation with Ad5/3 nonreplicative viruses resulting in differential efficiencies of gene transfer on different primary MPC cultures. Testing the culture media of infected cultures for the presence of viral hexons confirmed the data obtained with viral DNA. The amount of viral protein increased with progression of infection for all cell cultures. In HeLa cells, the hexon concentration in media increased 14-fold and peaked 5 days after infection. Hexon measurement in infected MPC cultures found an increase of only two- to threefold after 7 days postinfection. Elevation of viral DNA and viral protein during infection, as well as virus-induced cytolysis, clearly indicated viral replication in MPCs.

To prove that MPCs are able to complete the whole cycle of viral replication and produce the next generation of viral particles, we took cell lysates of MPC cultures infected with escalated doses of Ad5luc3 and applied tenfold dilutions of those lysates to the Ad-permissive cell line, HeLa. As shown in Figure 10, the positive control representing lysates of infected HeLa cells resulted in a second round of

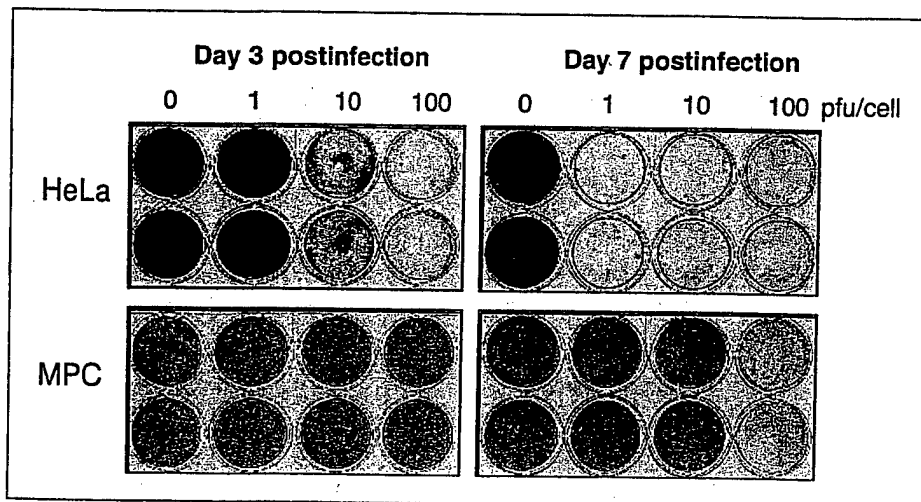


Figure 8. Cytopathic effect of replication-competent adenovirus (Ad5luc3) on MPCs and HeLa cells. HeLa cells and MPCs were plated on 6-well plates with a plating density of 5×10^5 cells/well and infected in duplicate with Ad5luc3 at the designated MOI. The viral cytopathic effect was estimated by crystal violet staining on day 3 and day 7 after infection.

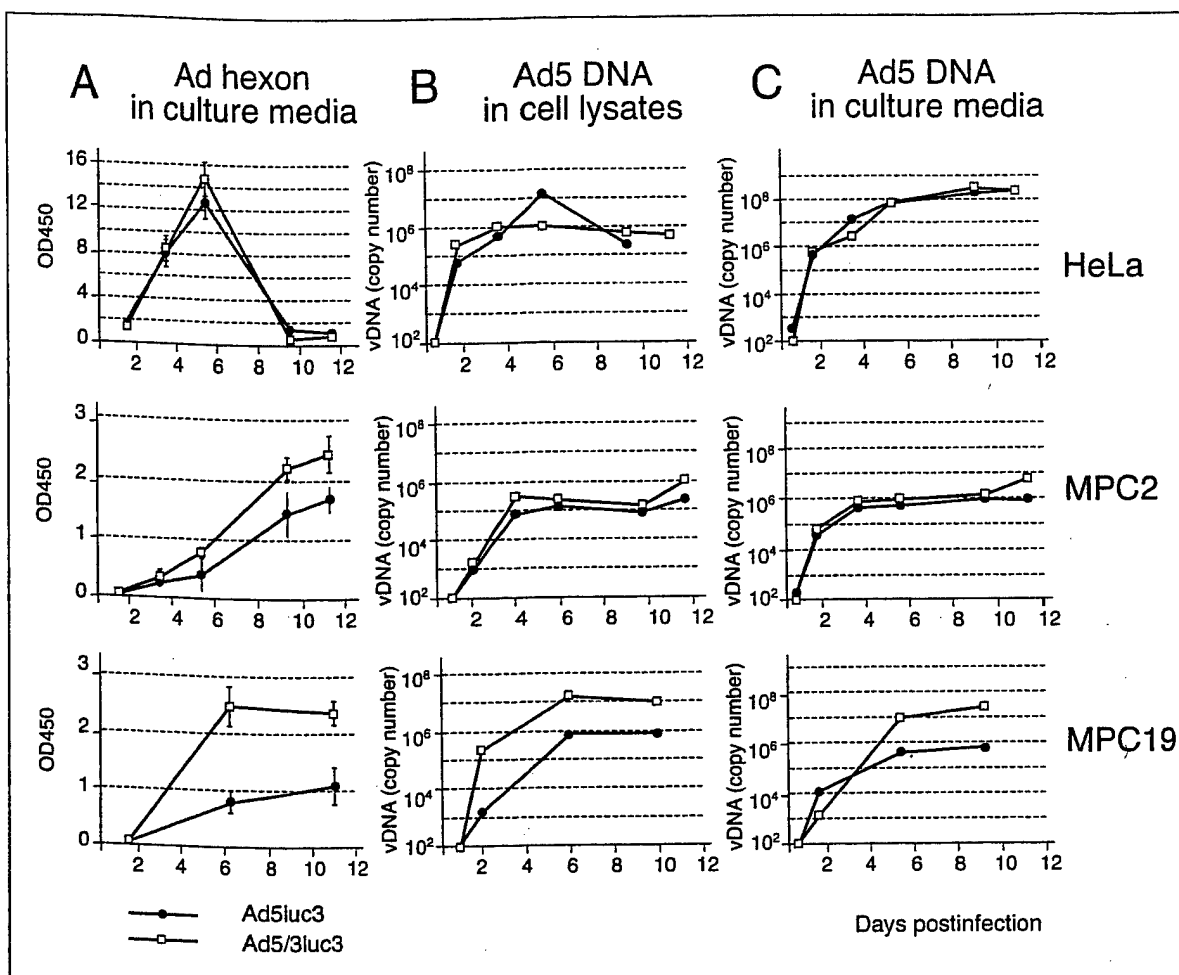


Figure 9. Kinetics of Ad production by MPCs. HeLa cells and two primary cultures of MPC (MPC2 and MPC19) were infected with replication-competent Ad5luc3 and Ad5/3luc3 viruses at an MOI of 1 pfu/cell. Virus-containing media were collected at 1, 3, 5, 7, and 9 days after infection. Viral production was estimated as A) accumulation of viral protein in culture media by immunoenzyme assay with detection of Ad hexons. Data are presented as OD450 of 100 μ l of culture media. B) Accumulation of viral DNA in Ad-infected cells. C) Accumulation of viral DNA in culture media measured by quantitative PCR. Data are presented as Ad vDNA copy number relative to actin DNA copy number.

infection of HeLa cells. Lysates of infected MPCs also caused a cytopathic effect on HeLa cells, confirming the presence of viable Ad virions in the samples. Thus, these data prove that MPCs are able to support Ad replication and can, therefore, potentially serve as vehicles to deliver not only gene products but also viruses *in vivo*.

DISCUSSION

There is a continuous intensive search for the optimal delivery vector for different gene therapy protocols. Studies employing mammalian differentiated cells, such as fibroblasts, endothelial cells, mesothelial cells, and others, revealed the feasibility of an *ex vivo* strategy in general. The progenitors (stem cells) have also been tested in this regard [45, 46], although only a few attempts have been undertaken to address their full potentials as cellular vehicles. This study was

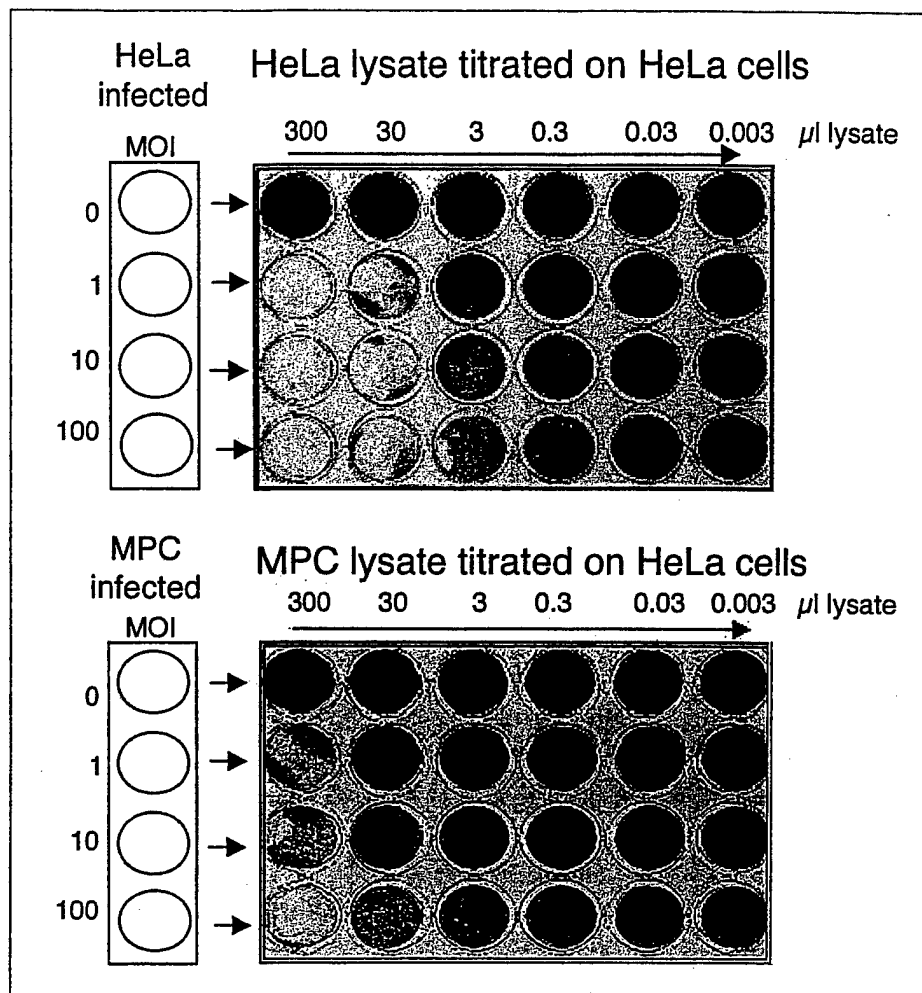
undertaken to establish key concepts of an MPC-based cellular vehicle strategy, with the intent to develop an autologous cellular vehicle to deliver therapeutic agents to tumor sites.

We demonstrated that isolation of adherent cells from bone marrow resulted in a cell population with the morphologic and functional characteristics of multipotential MPCs. Overall, isolated MPC cultures had sufficient proliferative and differentiation potentials and retained a multipotential phenotype in culture during several passages. Recently, the high proliferative potential of MPCs has been challenged even further after plating the cells at a low density [25]. In optimized culturing conditions, extensive and rapid cell expansion has been achieved, which will be of great importance for future cell and gene therapy applications.

In addition to intrinsic properties, several characteristics of delivery vehicles must be investigated to consider the

Figure 10. Production of Ad particles by MPCs. HeLa cells (A) and MPCs (B) were plated on 6-well plates with a plating density of 5×10^5 cells/well and infected with Ad5luc3 at an MOI of 1, 10, or 100 pfu/cell. After 3 days, cells in individual wells were lysed, and serial dilutions of lysates were applied onto HeLa cells. The cytopathic effect of produced virus on HeLa cells is shown by crystal violet staining on day 3.

MPC as a candidate for a cell-based strategy. First, it is prerequisite that these cells can be efficiently loaded with a gene of choice. In an attempt to achieve this, both retroviral and Ad vectors have been evaluated for gene transfer to human and nonhuman MPCs; however, the transduction had a relatively low efficiency in both cases [42, 45]. Our strategy is based on the short-term expression of a therapeutic gene; therefore, we considered Ad vectors as the vector of choice for ex vivo MPC loading. In our experiments, the efficiency of ex vivo transduction of MPCs with Ad vectors encoding two reporter genes, LacZ and GFP, did not exceed 40% at the highest MOI tested. It is widely understood that the main reason for Ad refractivity, especially in vitro, is the low level of expression of primary Ad receptors. The absence of CAR and the presence of α_v -integrins on the surfaces of MPCs were confirmed by flow cytometry, providing a plausible explanation for Ad resistance. As a means to circumvent CAR deficiency, we used Ad vectors retargeted to alternative receptors. Ad5lucRGD, having an integrin-binding motif in the fiber protein, introduces an alternative Ad entry pathway, allowing viral binding directly to cell-surface integrins. Ad5/3luc1 also represents an Ad vector redirected to an, as yet, unidentified Ad3 receptor. We previously demonstrated that such retargeted vectors often augment gene transfer to a variety of primary cell types and cancer cell lines that are otherwise relatively refractory to Ad5 infection [35, 43, 44]. In agreement with previous observations, all primary MPC cultures showed substantial enhancement of gene transfer with Ad5lucRGD. Thus, we demonstrated that MPC genetic loading can be increased tenfold by ex vivo transduction with integrin-retargeted Ad vectors.



Transduction with Ad5/3luc1 on several primary MPC cultures resulted in variable levels of luciferase expression. It is possible that the Ad3 receptor is expressed only within certain subpopulations of MPCs, representing variable fractions in different primary cultures. Of note, MPCs infected with luciferase-encoding Ad vectors produced higher levels of luciferase than HeLa cells in the same experimental setting. One possible explanation for this observation is that each individual transduced MPC might produce more luciferase than each transduced HeLa cell. The ability of MPCs to produce large amounts of protein may represent a quality that could also be useful in the context of a cell-based strategy.

Selective and effective killing of tumor cells remains a major strategy for any of the cancer gene therapy applications. Suicide therapy employs transfer of genes responsible for converting nontoxic products to toxic drugs or genes sensitizing tumor cells to irradiation. To be applicable in the cancer context, our proposed cellular system was tested for the ability of MPCs to express an anticancer gene and to exert cytotoxicity on neighboring tumor cells, thereby providing a local bystander killing effect. We found that MPCs could effectively express a suicide gene and that modified MPCs

themselves were sensitive to the toxic effect of GCV. We also explored the ability of MPC-TK to induce a bystander cytotoxic effect on the ovarian tumor cell line SKOV3.ip1 in vitro as a molecular chemotherapy approach on a model system of ovarian carcinoma. This approach was tested previously using human endothelial cells and was shown to accomplish an anti-tumor effect comparable with viral vector-mediated toxin delivery [13].

Here, we report that the efficiency of MPC gene loading can be substantially increased and the expression of payload genes reaches relevant levels, thereby meeting conditions for applications requiring a relatively short-term intervention. An enhanced bystander effect might potentially overcome the requirement to achieve quantitative transduction of the majority of tumor cells within tumor foci, a major challenge for gene therapy for cancer. Thus, we demonstrated that two important requirements for the use of MPCs as cellular vectors can be met: efficient gene transfer to the cells and high levels of desired protein production, which serve to achieve the biological effect.

We also hypothesized that cellular vehicles can potentially be exploited to deliver oncolytic viruses, which can be considered as promising suicidal tumor agents. For treating neoplastic diseases, conditionally replicative adenoviruses (CRADs) represent a novel and promising approach, employing the intrinsic cytopathic effect of the virus with additional specificity against tumor cells [47]. However, delivery of such a virus to tumor sites faces the same problems as nonreplicative Ad vectors. In this study, we explored the possibility of using MPCs as a means of delivering CRADs. To this end, the ability of MPCs to maintain Ad infection, which includes viral DNA replication and formation of new infectious viral particles, has to be examined. Nothing is known about the ability of MPCs to support Ad infection. Susceptibility of several committed hematopoietic cell lines to different Ad serotypes has been studied, and very low or no Ad5 production has been documented for the cell lines tested [48]. Nevertheless, low levels of virus production have been demonstrated for Ad11 and Ad35, which also showed enhanced binding to those cells. We proved, by several methods, that MPCs were able to support Ad5 replication, although the kinetics of viral production were different from those in a cell line highly permissive to Ad replication. We showed that Ad5 infection of MPCs developed at a slower rate and resulted in the production of a significantly lower number of viral particles than did HeLa cells. Nevertheless, there is no immediate obstacle to utilizing these cells as carriers for oncolytic viruses, and this strategy may have therapeutic applications. Further improvement of CRADs, in terms of

oncolytic potency and tumor selectivity, will offer new promising anticancer agents, and the development of appropriate cell carriers for such viruses would represent an attractive line of investigation.

Tumor-specific trafficking of infused cells remains the major question of investigation for cell-based strategies. Apparently, it can be mediated either by biological properties of the tumor itself or by native tumor-related tropism of the chosen cell population. Although the use of circulating cellular vehicles was first proposed a decade ago, only a few cell types have been exploited in the context of tumors. Human TILs were considered as an enriched source of tumor-specific cytotoxic T lymphocytes, and based on their putative preferential localization to tumor sites, were used as vehicles for retroviral-mediated gene transfer [49]. In a recently proposed complex targeting strategy, T lymphocytes were recruited to both produce and deliver a retrovirus to the tumors in an animal model [50]. This approach showed that inefficient T-cell targeting could be overcome by introducing a complex regulatory mechanism. It also demonstrated, for the first time, that cells can be turned into a source of viral production and that those progeny viruses can serve as the delivery cargo. Several lines of investigation utilized the process of angiogenesis, which is highly activated in tumors, as an attractant of cellular vehicles naturally endowed with angiogenic tropisms [11].

Tumor-specific targeting of MPC as one of the essential vector characteristics for our cell-based strategy has not been included in this study but will represent a subject of our future investigations. Although native homing of MPCs after systemic or local infusion has been tested on different animal models in a variety of experimental settings [28, 31], there is still insufficient information about in vivo distribution and survival of infused MPCs. The possibility of MPCs homing to tumor sites could be theoretically envisioned. However, there are only a few very restricted studies investigating the relation of MPCs to tumor formation or growth. It has been confirmed that infused MPCs may reach tumor sites, selectively proliferate there, and participate in the formation of tumor stroma [33]. It has also been demonstrated that MPCs tend to home to sites of injury or damaged tissue irrespective of the damaged tissue type. This ability of MPCs has been demonstrated in experiments with brain injuries [51], wound healing, and tissue regeneration sites [52]. Apparently, signals from the site of damage are required for MPCs to travel and fill this niche by engrafting and proliferating. Fibroblasts have demonstrated a similar effect of accumulating at the site of injury [4]. Theoretically, a tumor can be considered as a site of "damage" or at least a site of production of cytokines and chemokines of a different nature. It remains to be tested, at least in a model system, which conditions are required for

MPCs to see a tumor as an attractant. Another attractive approach that may seem relevant is to introduce an engineered affinity or tropism to MPCs, making them artificially attracted to a tumor.

SUMMARY

The current study demonstrated the ability of MPCs to foster expression of a suicide gene and to support replication of an adenovirus as potential anticancer therapeutic payloads. The potential of MPCs as cell-based vectors for delivery of therapeutic genes and viruses certainly warrants further investigation. Our observations to date establish some of the key properties of this cell population that allow

them to function as cellular vectors and thus represent a rational strategy for cancer gene therapy.

ACKNOWLEDGMENTS

We thank *Ming Wang* for performing quantitative PCR and *Joel Glasgow* for proofreading of the manuscript and helpful advice. We give special acknowledgment to the Department of Pathology, UAB Core Center for Musculoskeletal Disorders (NIH RCC grant P30AR46031) for obtaining MPCs and for their useful advice. This work was supported in part by grants from the National Institutes of Health (R01 CA94084, P50 CA83591, R01 CA83821) and from the Lustgarten Foundation and Susan B. Komen Foundation.

REFERENCES

- 1 Blaese M, Blankenstein T, Brenner M et al. Vectors in cancer therapy: how will they deliver? *Cancer Gene Ther* 1995;2:291-297.
- 2 Bordignon C, Carlo-Stella C, Colombo MP et al. Cell therapy: achievements and perspectives. *Haematologica* 1999;84:1110-1149.
- 3 Kaji EH, Leiden JM. Gene and stem cell therapies. *JAMA* 2001;285:545-550.
- 4 Yang W, Arai S, Mori A et al. Sflt-1 gene-transfected fibroblasts: a wound-specific gene therapy inhibits local cancer recurrence. *Cancer Res* 2001;61:7840-7845.
- 5 Naffakh N, Henri A, Villeval JL et al. Sustained delivery of erythropoietin in mice by genetically modified skin fibroblasts. *Proc Natl Acad Sci USA* 1995;92:3194-3198.
- 6 Overturf K, Al-Dhalimy M, Finegold M et al. The repopulation potential of hepatocyte populations differing in size and prior mitotic expansion. *Am J Pathol* 1999;155:2135-2143.
- 7 Nagy JA, Shockley TR, Masse EM et al. Mesothelial cell-mediated gene therapy: feasibility of an ex vivo strategy. *Gene Ther* 1995;2:393-401.
- 8 Rinsch C, Quinodoz P, Pittet B et al. Delivery of FGF-2 but not VEGF by encapsulated genetically engineered myoblasts improves survival and vascularization in a model of acute skin flap ischemia. *Gene Ther* 2001;8:523-533.
- 9 Rando TA, Blau HM. Primary mouse myoblast purification, characterization, and transplantation for cell-mediated gene therapy. *J Cell Biol* 1994;125:1275-1287.
- 10 Taylor R. Cell vehicles for gene transfer to the brain. *Neuromuscul Disord* 1997;7:343-351.
- 11 Ojefo JO, Lee HR, Rezza P et al. Endothelial cell-based systemic gene therapy of metastatic melanoma. *Cancer Gene Ther* 2001;8:636-648.
- 12 Ojefo JO, Forough R, Paik S et al. Angiogenesis-directed implantation of genetically modified endothelial cells in mice. *Cancer Res* 1995;55:2240-2244.
- 13 Rancourt C, Robertson MW 3rd, Wang M et al. Endothelial cell vehicles for delivery of cytotoxic genes as a gene therapy approach for carcinoma of the ovary. *Clin Cancer Res* 1998;4:265-270.
- 14 Van Tendeloo VF, Van Broeckhoven C, Berneman ZN. Gene therapy: principles and applications to hematopoietic cells. *Leukemia* 2001;15:523-544.
- 15 Smith C, Storms B. Hematopoietic stem cells. *Clin Orthop* 2000; (suppl 379):91-97.
- 16 Halene S, Kohn DB. Gene therapy using hematopoietic stem cells: Sisyphus approaches the crest. *Hum Gene Ther* 2000;11:1259-1267.
- 17 Rosenberg SA, Anderson WF, Blaese M et al. The development of gene therapy for the treatment of cancer. *Ann Surg* 1993;218:455-464.
- 18 Pockaj BA, Sherry RM, Wei JP et al. Localization of 111indium-labeled tumor infiltrating lymphocytes to tumor in patients receiving adoptive immunotherapy. Augmentation with cyclophosphamide and correlation with response. *Cancer* 1994;73:1731-1737.
- 19 Chin Y, Janssens J, Bleus J et al. In vivo distribution of radio-labeled tumor infiltrating lymphocytes in cancer patients. *In Vivo* 1993;7:27-30.
- 20 Prockop DJ. Marrow stromal cells as stem cells for non-hematopoietic tissues. *Science* 1997;276:71-74.
- 21 Bruder SP, Fink DJ, Caplan AI. Mesenchymal stem cells in bone development, bone repair, and skeletal regeneration therapy. *J Cell Biochem* 1994;56:283-294.
- 22 Horwitz EM, Prockop DJ, Gordon PL et al. Clinical responses to bone marrow transplantation in children with severe osteogenesis imperfecta. *Blood* 2001;97:1227-1231.
- 23 Wakitani S, Goto T, Pineda SJ et al. Mesenchymal cell-based repair of large, full-thickness defects of articular cartilage. *J Bone Joint Surg Am* 1994;76:579-592.
- 24 Minguell JJ, Conget P, Erices A. Biology and clinical utilization of mesenchymal progenitor cells. *Braz J Med Biol Res* 2000;33:881-887.

- 25 Colter DC, Class R, DiGirolamo CM et al. Rapid expansion of recycling stem cells in cultures of plastic-adherent cells from human bone marrow. *Proc Natl Acad Sci USA* 2000;97:3213-3218.
- 26 Conget PA, Allers C, Minguell JJ. Identification of a discrete population of human bone marrow-derived mesenchymal cells exhibiting properties of uncommitted progenitors. *J Hematother Stem Cell Res* 2001;10:749-758.
- 27 Pittenger MF, Mackay AM, Beck SC et al. Multilineage potential of adult human mesenchymal stem cells. *Science* 1999;284:143-147.
- 28 Pereira RF, Halford KW, O'Hara MD et al. Cultured adherent cells from marrow can serve as long-lasting precursor cells for bone, cartilage, and lung in irradiated mice. *Proc Natl Acad Sci USA* 1995;92:4857-4861.
- 29 Hurwitz DR, Kirchgesser M, Merrill W et al. Systemic delivery of human growth hormone or human factor IX in dogs by reintroduced genetically modified autologous bone marrow stromal cells. *Hum Gene Ther* 1997;8:137-156.
- 30 Chuah MK, Van Damme A, Zwinnen H et al. Long-term persistence of human bone marrow stromal cells transduced with factor VIII-retroviral vectors and transient production of therapeutic levels of human factor VIII in nonmyeloablated immunodeficient mice. *Hum Gene Ther* 2000;11:729-738.
- 31 Gao J, Dennis JE, Muzic RF et al. The dynamic in vivo distribution of bone marrow-derived mesenchymal stem cells after infusion. *Cells Tissues Organs* 2001;169:12-20.
- 32 Allay JA, Dennis JE, Haynesworth SE et al. LacZ and interleukin-3 expression in vivo after retroviral transduction of marrow-derived human osteogenic mesenchymal progenitors. *Hum Gene Ther* 1997;8:1417-1427.
- 33 Studeny M, Marini FC, Champlin RE et al. Bone marrow-derived mesenchymal stem cells as vehicles for interferon-beta delivery into tumors. *Cancer Res* 2002;62:3603-3608.
- 34 He TC, Zhou S, da Costa LT et al. A simplified system for generating recombinant adenoviruses. *Proc Natl Acad Sci USA* 1998;95:2509-2514.
- 35 Dmitriev I, Krasnykh V, Miller CR et al. An adenovirus vector with genetically modified fibers demonstrates expanded tropism via utilization of a coxsackievirus and adenovirus receptor-independent cell entry mechanism. *J Virol* 1998;72:9706-9713.
- 36 Krasnykh VN, Mikheeva GV, Douglas JT et al. Generation of recombinant adenovirus vectors with modified fibers for altering viral tropism. *J Virol* 1996;70:6839-6846.
- 37 Mittal SK, McDermott MR, Johnson DC et al. Monitoring foreign gene expression by a human adenovirus-based vector using the firefly luciferase gene as a reporter. *Virus Res* 1993;28:67-90.
- 38 Rosenfeld ME, Wang M, Siegal GP et al. Adenoviral-mediated delivery of herpes simplex virus thymidine kinase results in tumor reduction and prolonged survival in a SCID mouse model of human ovarian carcinoma. *J Mol Med* 1996;74:455-462.
- 39 Bruder SP, Jaiswal N, Haynesworth SE. Growth kinetics, self-renewal, and the osteogenic potential of purified human mesenchymal stem cells during extensive subcultivation and following cryopreservation. *J Cell Biochem* 1997;64:278-294.
- 40 Conget PA, Minguell JJ. Phenotypical and functional properties of human bone marrow mesenchymal progenitor cells. *J Cell Physiol* 1999;181:67-73.
- 41 Conget PA, Minguell JJ. Adenoviral-mediated gene transfer into ex vivo expanded human bone marrow mesenchymal progenitor cells. *Exp Hematol* 2000;28:382-390.
- 42 Olmsted EA, Blum JS, Rill D et al. Adenovirus-mediated BMP2 expression in human bone marrow stromal cells. *J Cell Biochem* 2001;82:11-21.
- 43 Kasono K, Blackwell JL, Douglas JT et al. Selective gene delivery to head and neck cancer cells via an integrin targeted adenoviral vector. *Clin Cancer Res* 1999;5:2571-2579.
- 44 Kanerva A, Mikheeva GV, Krasnykh V et al. Targeting adenovirus to the serotype 3 receptor increases gene transfer efficiency to ovarian cancer cells. *Clin Cancer Res* 2002;8:275-280.
- 45 Ding L, Lu S, Batchu R et al. Bone marrow stromal cells as a vehicle for gene transfer. *Gene Ther* 1999;6:1611-1616.
- 46 Gomez-Navarro J, Contreras JL, Arafat W et al. Genetically modified CD34⁺ cells as cellular vehicles for gene delivery into areas of angiogenesis in a rhesus model. *Gene Ther* 2000;7:43-52.
- 47 Krut FA, Curiel DT. Toward a new generation of conditionally replicating adenoviruses: pairing tumor selectivity with maximal oncolysis. *Hum Gene Ther* 2002;13:485-495.
- 48 Segerman A, Mei YF, Wadell G. Adenovirus types 11p and 35p show high binding efficiencies for committed hematopoietic cell lines and are infective to these cell lines. *J Virol* 2000;74:1457-1467.
- 49 Kasid A, Morecki S, Aebersold P et al. Human gene transfer: characterization of human tumor-infiltrating lymphocytes as vehicles for retroviral-mediated gene transfer in man. *Proc Natl Acad Sci USA* 1990;87:473-477.
- 50 Chester J, Ruchatz A, Gough M et al. Tumor antigen-specific induction of transcriptionally targeted retroviral vectors from chimeric immune receptor-modified T cells. *Nat Biotechnol* 2002;20:256-263.
- 51 Mahmood A, Lu D, Wang L et al. Treatment of traumatic brain injury in female rats with intravenous administration of bone marrow stromal cells. *Neurosurgery* 2001;49:1196-1204.
- 52 Mackenzie TC, Flake AW. Human mesenchymal stem cells persist, demonstrate site-specific multipotential differentiation, and are present in sites of wound healing and tissue regeneration after transplantation into fetal sheep. *Blood Cells Mol Dis* 2001;27:601-604.